Virginia Commonwealth University
VCU Scholars Compass

Theses and Dissertations | Graduate School

2008

Interneuron Subtypes are Differentially Altered in Malformed, Epileptogenic Cortex

Amanda George
Virginia Commonwealth University

Follow this and additional works at: https://scholarscompass.vcu.edu/etd

 Part of the Nervous System Commons

© The Author

Downloaded from
https://scholarscompass.vcu.edu/etd/1618

This Dissertation is brought to you for free and open access by the Graduate School at VCU Scholars Compass. It has been accepted for inclusion in Theses and Dissertations by an authorized administrator of VCU Scholars Compass. For more information, please contact libcompass@vcu.edu.

www.manaraa.com

© Amanda L. George 2008
All Rights Reserved

www.manaraa.com

INTERNEURON SUBTYPES ARE DIFFERENTIALLY ALTERED IN MALFORMED, EPILEPTOGENIC CORTEX

A dissertation submitted in partial fulfillment of the requirements for the degree of Doctor of Philosophy in Anatomy and Neurobiology at Virginia Commonwealth University.

by

Amanda L. George
B.A. Duke University, 2001

Director: Kimberle Jacobs, Ph.D.
Associate Professor
Department of Anatomy and Neurobiology

Virginia Commonwealth University
Richmond, Virginia
September 15, 2008

www.manaraa.com

Acknowledgment

I would like to extend my thanks to those who have supported me during the completion of my graduate studies and the writing of this dissertation. They include my advisor, Dr. Kimberle Jacobs, my graduate committee members, Drs. Richard Costanzo, Gordon Archer, Babette Fuss, John Povlishock and Leslie Satin, fellow members of the Jacobs lab, members of the Povlishock lab, my friends and family.

www.manaraa.com

Table of Contents

www.manaraa.com

www.manaraa.com

List of Tables

www.manaraa.com

List of Figures

www.manaraa.com

www.manaraa.com

List of Abbreviations

°C	degrees Celsius
AHP	afterhyperpolarization
AIDA	1-amino-2,3-dihydro-1H-indene-1,5-dicarboxylic acid
AMPA	alpha-amino-3-hydroxy-5-methyl-4-isoxazolepropionic acid
APV	D,L-2-amino-5-phosphonopentanoic acid
ATP	adenosine 5'-triphosphate
BCNU	1,2-bis-chloroethyl-nitrosourea
BDNF	brain derived neurotrophic factor
BSA	bovine serum albumin
CB	calbindin
CCK	cholecystokinin
CGE	caudal ganglionic eminence
CNS	central nervous system
CO	cytochrome oxidase
CO_2	carbon dioxide
CR	calretinin
DHPG	S-3,5-dihydroxyphenylglycine hydrate
DIC	differential interference contrast

www.manaraa.com

DNQX	dinitroquinoxaline [(6,7)],2,3(1H,4H)-dione
e-	evoked
EC_{50}	half maximal effective concentration
EGTA	ethylene glycol tetra-acetic acid
EPSC	excitatory postsynaptic current
FS	fast-spiking
GABA	γ-aminobutyric acid
GTP	guanosine 5'-triphosphate
Hz	hertz
IL	interleukin
IPSC	inhibitory postsynaptic current
LGE	lateral ganglionic eminence
LTP	long term potentiation
LTS	low threshold-spiking
m-	miniature
MAM	methylazoxymethanol
MGE	medial ganglionic eminence
mGluR	metabotropic glutamate receptor
MGN	medial geniculate nucleus
mM	millimolar
mOsm	milliosmolar
MPEP	6-methyl-2-(phenylethynyl) pyridine hydrochloride

www.manaraa.com

mRNA	messenger ribonucleic acid
msec	millisecond
mV	millivolt
nA	nanoampere
NGS	normal goat serum
NMDA	N-methyl-D-aspartate
NPY	neuropeptide Y
O_2	oxygen
P	postnatal day
PMG	paramicrogyral
PV	parvalbumin
Ra	access resistance
s-	spontaneous
SS	somatostatin
TBS	tris-buffered saline
TTX	tetrodotoxin
VIP	vasoactive intestinal peptide
µm	micrometer
µM	micromolar

www.manaraa.com

Abstract

INTERNEURON SUBTYPES ARE DIFFERENTIALLY ALTERED IN MALFORMED, EPILEPTOGENIC CORTEX

by Amanda L. George

A dissertation submitted in partial fulfillment of the requirements for the degree of Doctor of Philosophy at Virginia Commonwealth University.

Virginia Commonwealth University, 2008

Director: Kimberle Jacobs, Ph.D.
Associate Professor, Department of Anatomy and Neurobiology

The propensity for seizures in patients with epilepsy is due to underlying cortical hyperexcitability, the mechanisms for which are poorly understood. Particularly difficult to treat are patients with developmental malformations of cortex. Using the freeze-lesion rat model of one such malformation, polymicrogyria, we identified, in lesioned cortex, alterations in specific interneuron subpopulations that may promote hyperexcitability. Previous studies demonstrate increased excitatory input to the paramicrogyral region. An increase in the frequency of spontaneous excitatory postsynaptic currents (sEPSCs) recorded from pyramidal cells has also been shown. We report an increase in sEPSCs recorded from one subtype of interneuron, the low threshold-spiking interneuron (LTS), while sEPSCs in the fast-spiking (FS) interneuron remain unchanged. Distributed equally to pyramidal cells and interneurons, extra excitatory afferents should simply

www.manaraa.com

increase overall activity level but maintain the balance of excitation and inhibition. Selective changes in one or more interneuron subpopulations could allow inhibition to appear unchanged, while permitting problematic alterations in inhibitory circuitry.

In what appears to be a morphological division of labor, interneurons with intralaminar orientations are typically characterized as FS, while intracolumnar orientations are associated with LTS cells. These cells are clearly distinguished by a combination of visual identification and electrophysiological and intrinsic properties. We report that these characteristics are unchanged in lesioned cortex, indicating that the malformation is not responsible for intrinsic alteration of the cell types. However, some firing properties demonstrate slight differences that may, in cooperation with the altered level of input, amplify the pro-epileptogenic changes in circuitry. Finally, we also report that there is anomalous expression of metabotropic glutamate receptors (mGluR) in malformed cortex. Our data show that the expression of mGluR5, normally causing no functional response in control cortex, contributes to the activation of interneurons in paramicrogyral (PMG) cortex. These findings provide new insight to the mechanisms of cortical hyperexcitability and identify a possible target for future pharmacological intervention.

www.manaraa.com

Chapter 1

Introduction to Epilepsy and Interneurons

1.1 Epilepsy

The earliest known documentation of epilepsy is found in an ancient Babylonian medical text, the *Sakikku*, where it is referred to as the "falling disease" (101). Throughout history, similar phrases have been used to describe epilepsy, from ancient Chinese and Indian texts to writings from Medieval Europe and the Renaissance. The term "epilepsy" derives from the Greek επιλαμβανειν, or epilamvanein, meaning "to take hold of, to seize." In the age of Hippocrates and still in some cultures today, people have alternately viewed seizures as episodes of demon possession or divine religious experience. Certain that a physiological explanation would unravel the mystery of this condition, Hippocrates himself is credited with saying that discovery of the underlying cause of epilepsy would eliminate its "sacred" quality (101). However, it was not until the mid-1800s that Hughlings Jackson took the first substantial steps in that direction. He, along with Jean-Martin Charcot, Wilder Penfield, Herbert Jasper and Hans Berger made significant contributions to the body of knowledge we currently have regarding epilepsy. At this writing, there are explanations for a number of different epilepsies, specifically those with genetic or acquired etiologies (39; 120; 147; 248; 309). Even so, there are many patients whose epilepsy is poorly understood and managed (306). Despite

www.manaraa.com

advances in both diagnosis and treatment, there is still much to be learned about epilepsy and its underlying mechanisms.

The syndrome of epilepsy consists of multiple, recurrent seizures that have no other medical explanation. The behavioral manifestations of seizures can vary, but the clinical symptoms are all representative of excessive, synchronous neuronal firing. The Commission on Classification and Terminology of the International League Against Epilepsy identifies two general seizure categories, partial and generalized (2). Partial seizures are comprised of focal symptoms and are due to abnormal neuronal activity in a restricted region of the brain. Patients with this type of seizure may exhibit characteristic motor behaviors or have a specific sensory experience in the absence of the appropriate stimulus. Alternatively, generalized seizures involve both hemispheres and may have a more severe presentation, including loss of consciousness and postural muscle tone, often resulting in collapse.

It is difficult to accurately assess the number of patients with epilepsy worldwide, particularly in developing countries. However, the estimated global prevalence of epilepsy is 8.2 per 1,000 of the general population (144). This translates into approximately 50 million people worldwide (World Health Organization Website, www.who.int/en/). Extrapolating data from a study in Minnesota, epilepsy affects one to three percent of the U.S. population, with ten percent experiencing a seizure at some point during their lifetime (145). The highest incidence of seizures tends to occur at the extremes of life, first during the neonatal period and then again after seventy years of age (144). Most studies reveal that males have a higher incidence of unprovoked seizures

www.manaraa.com

(144). There are numerous etiologies for seizures, including tumor, genetic predisposition, traumatic brain injury, congenital disease, dysplasia and infectious disease of the CNS (34; 39; 161; 194; 227). However, one study from the early eighties labeled two-thirds of epilepsy cases as idiopathic or cryptogenic, as clear identification of an underlying cause was not possible (144). With the development of modern imaging techniques, it is now increasingly possible for physicians to recognize that previously unrecognized anatomical lesions underlie seizures in a number of these patients (18; 146; 195; 334).

1.2 Cortical malformations

Malformation of the cerebral cortex during development is one of the most common causes of intractable epilepsy, especially in children (114; 366). There are many different malformations that span a wide range of severities, dependent on how and when the malformation arises. The next two sections review several malformations of cortical development and the animal models used to study them.

1.2.1 Clinical aspects and etiologies of cortical malformations

Errors that occur early in central nervous system (CNS) development may result in the generation of too few cells or, with a similar effect, cause too many cells to die. When this happens, there are not enough neurons and glia to populate the developing cortex. The result is an underdeveloped brain, along with microcephaly, a condition in which the head circumference is smaller than average by more than two standard

www.manaraa.com

deviations (20; 140). Factors that may inhibit brain growth and cause this type of lesion include vascular insult, intrauterine infection (cytomegalovirus, rubella, and toxoplasmosis), maternal alcohol consumption and other teratogens (3). Conversely, increased proliferation or apoptotic failure can produce a neoplastic lesion, cortical dysplasia or hemimegalencephaly (20; 140). Patients with hemimegalencephaly in particular suffer from intractable seizures that start at birth, as well as hemiparesis and developmental delay (194).

Malformations that can be attributed to improper migration rather than faulty neuron generation include lissencephaly and heterotopia. Lissencephaly, or "smooth brain" is a condition in which the normal gyri of the cortical surface are absent or dramatically decreased in number. Individuals with lissencephaly exhibit an array of neurological deficits, including mental retardation, hypotonia, difficulty feeding and epileptic seizures (94; 115). Intellectual disability in some of these patients may occur, secondary to intractable seizure activity (194). Several genetic mutations are associated with lissencephaly, the most well-recognized being those in the DCX (or XLIS) and LIS1 (or PAFAH1B1) genes (137; 307). LIS1 encodes a protein subunit associated with platelet activating factor acetylhydrolase (151; 275), while DCX encodes a protein that may be involved in microtubule assembly and/or function. The functional correlation between abnormalities in these gene products and their respective malformation phenotypes is unknown. Heterotopia, on the other hand, refers to the presence of one or more deposits of inappropriately located gray matter, usually within white matter tracts of the brain (138; 317). The major clinical presentation associated with heterotopia includes

www.manaraa.com

mild-to-moderate intellectual disability and some form of epilepsy (98; 136). One study showed that eighty percent of patients with periventricular nodular heterotopia presented with seizures, the majority of them being intractable (23). Another variation of this malformation, subcortical laminar heterotopia, is associated with the lissencephaly gene DCX, but in the more common familial X-linked bilateral periventricular nodular heterotopia, mutations in the FLN1 gene are responsible nearly one hundred percent of the time (117). FLN1 encodes a protein important for cell morphology and migration (117), so this may provide a logical correlation between protein deficiency and cortical malformation. Heterotopia is one of the malformations more frequently observed in the animal models described in the next section.

Also due to dysfunction of post-neurogenesis development, schizencephaly refers to a cleft in the brain that allows aCSF to flow directly from the ventricles through two cortical "lips," into the subarachnoid space (20; 138; 140). If the "lips" are closed, the patient often exhibits hemiparesis or motor delay. "Open-lipped" schizencephaly more commonly results in hydrocephalus or seizures (194). *De novo* mutations of the EMX2 gene have been associated with several cases of schizencephaly, particularly those with severe clinical presentation (48). Almost always, the schizencephalic cleft is bordered by one or more areas of polymicrogyria. Polymicrogyria is a malformation defined by an abundance of abnormally small gyri, and as it is the malformation most closely related to the experiments described here, it will be discussed in detail in the next section of this chapter.

www.manaraa.com

1.2.2 Animal models of cortical malformation

A number of techniques can be used to model in rats the cortical malformations described above. These include, but are not limited to: genetic mutation (192), irradiation (282), exposure to methamphetamine or other chemicals *in utero* (32; 84; 297), injection of a toxin (211), direct mechanical damage to the cortex (109), and, as is used in these studies, ischemia secondary to freeze probe application (99). Similar to human patients, the type and severity of malformation that occurs during development depends on both the timing and nature of the insult (132). While some models involve a loss of cells throughout the cortex due to global damage, the model employed for the studies in this body of work involves specific elimination of deep layer neurons in somatosensory cortex (99). Some of the models described here produce spontaneous seizures, and all of them demonstrate *in vitro* hyperexcitability (232). While they each have unique mechanisms that underlie the hyperexcitability, there are shared characteristics between them, and it is instructive to compare the mechanisms contributing to epileptogenesis from one model to another.

Three methods of inducing cortical malformation *in utero* are: irradiation (282), 1,2-bis-chloroethyl-nitrosourea (BCNU) injection (32), and methylazoxymethanol (MAM) exposure (17). Each of these reduces cortical thickness and is usually accompanied by some type of heterotopia (232). X-irradiation of embryonic rat pups *in utero* has been used for a number of years to model cortical dysplasia. These rats have an abnormally thin cortex, as well as disruption of the radial glia (282; 283). The γ-aminobutyric (GABA)ergic neuronal population is reduced in these animals (284), and

www.manaraa.com

reduced excitatory drive onto the existing GABAergic cells in the malformed cortex is observed (367). This suggests that reduced inhibition is a major contributor to the hyperexcitability observed in this model. Injection of MAM also results in a thinning of the cortex, and when the injections are given early enough (E24 in ferret), disorganization of radial glia is observed (240). Pyramidal cells located within cortical heterotopias in these rats demonstrate excessive bursting behavior and excitability, characteristics that promote epileptiform activity (297). The histological characteristics of the cortex in BCNU-exposed pups are similar to those in the MAM model, including disruption of radial glia (32).

Another animal that is used specifically to model heterotopia is the telencephalic internal structural heterotopia (TISH) rat. This malformation is due to a genetic mutation and has similarities with the human conditions of double cortex and subcortical band heterotopia (192). Decreased inhibitory synaptic transmission is observed in this model and occurs two weeks prior to the onset of seizures (352). This appears to be due to a decreased number of inhibitory afferents, as increasing the probability of release with a low Mg^{2+}/high Ca^{2+} solution fails to "rescue" the lost inhibitory function (352). A concomitant decrease in one specific GABAergic cell population is also seen in this model (352). It is likely that the decreased inhibition promotes epileptogenesis, although due to the intervening two week period prior to the onset of seizures, there are likely other contributing factors.

Lastly, microgyria can be modeled in a number of ways. A light mechanical disturbance of the exposed pial surface can cause a microgyral malformation (109), as

www.manaraa.com

can exposure to methamphetamine in utero (84). Two of the more commonly used methods of inducing microgyria are the ibotenate injection (211) model and the freeze-lesion model (99; 156; 157). Injection of the glutamatergic agonist ibotenic acid shortly after birth causes the death of cells in layer V-VI of the developing rodent cortex (211). This manipulation produces a small sulcus in the brain, mimicking the human condition of polymicrogyria (133; 211). Hyperexcitability similar to that seen in the human condition is observed in cortical areas surrounding the lesion (274). The freeze-lesion model creates a similar malformation and will be considered at length in the next section.

1.3 Polymicrogyria

1.3.1 Clinical aspects and etiologies of polymicrogyria

The name "polymicrogyria" describes a malformation that comprises many abnormally small gyri on the surface of the brain, giving it an irregular, bumpy appearance. Seizures and mental retardation are observed in most patients with this type of malformation (137). The etiologies of polymicrogyria are varied and include *in utero* ischemic insult (108) or infection (21; 85), as well as a number of genetic mutations (137). Current advances in medical imaging have helped to identify this malformation as one of the causative factors for epilepsies previously classified as idiopathic (18; 195; 334). However, the epileptogenic zone of this malformation is not always confined to the area of the visible anatomical lesion. Hyperexcitable portions of cortex surround the lesion as well, making it difficult to definitively assign boundaries to the "damaged"

www.manaraa.com

tissue (70). The extent of polymicrogyria and the amount of cortex involved can vary greatly between individuals, but there is usually a correlation between the size of the lesion and the severity of clinical signs and EEG findings (340).

Some of the more common forms of polymicrogyria have stereotyped anatomical presentations, clinical symptoms and known genetic causes. Bilateral frontal polymicrogyria, for example, encompasses practically the entire frontal lobe and causes epilepsy, hypotonia, mental retardation and developmental delay in children (135). Expanding to the parietal lobe, bilateral frontoparietal polymicrogyria is associated with developmental delay, seizures and motor deficits (66; 257). It has a demonstrated association with mutations of GPR56, a G-protein coupled receptor that is important for protein trafficking (258; 259). Often, microgyria is observed around the sylvian fissure, frequently in both hemispheres. Bilateral perisylvian polymicrogyria (BPP) causes dysarthria, facial diplegia, mental retardation and seizures (134). Epilepsy of variable severity is associated with about sixty percent of these cases (134). The combination of BPP, seizures and oro-motor dysfunction has been termed "congenital bilateral perisylvian syndrome," and clinical data has been collected from patients with this condition for over a century (194). Finally, bilateral generalized polymicrogyria affects multiple lobes of the bran, resulting in a severe manifestation of symptoms (67). Most patients with the generalized form suffer from seizures, and virtually all of them have some type of cognitive or motor delay (67). Some patients with seizures secondary to polymicrogyria can be treated with currently available anticonvulsants, but others suffer intractable seizures, requiring surgical intervention (199).

www.manaraa.com

1.3.2 The freeze-lesion model of microgyria

The freeze-lesion model of microgyria was first developed by Dvorak and Feit in the late seventies and recapitulates the histopathology of human four-layered polymicrogyria (99; 100; 100). To reproduce this, a freezing probe (-50^{o}C) is placed on the skull of a neonatal rat pup, creating an ischemic lesion that kills the neurons present in the cortical plate at that time, those comprising layers IV-VI. After subsequent development of the superficial layers is complete, a focal (~1 x 4 mm) microgyral region of laminated cortex containing four, instead of six, cortical layers is produced (99; 100). The superficial layers of the malformed region are similar to normal neocortical layers I and II/III (82; 85; 99). The third layer of the microgyrus is thin and contains a few cells with small somata that are most likely glia (99). Typically, this cell-sparse third layer terminates abruptly at the point of contact between the microgyrus proper and the adjacent six-layered cortex (82; 85). The fourth layer is similar to and often contiguous with layer IVb of normal cortex (82; 85; 100).

Consistent and reproducible evidence of epileptiform activity associated with the formation of the induced microgyrus has been demonstrated after postnatal day (P)12 in rats (156; 157; 202). The area of cortex adjacent to the induced malformation has a normal, six-layered histological appearance, but that is where hyperexcitability is observed, in the form of evoked interictal-like activity (156). This region is identified as the paramicrogyral zone (PMG). Epileptiform activity in rats that are lesioned in this manner is similar in incidence to that of humans with polymicrogyria, about eighty percent (19; 157).

www.manaraa.com

1.3.2.1 Behavioral effects of the freeze-lesion model, including seizure susceptibility

Rats with freeze-lesion-induced microgyria do not exhibit spontaneous seizures, but they have demonstrated increased susceptibility to seizures caused by hyperthermia (300). Freeze-lesioned rats require a shorter latency to attain the most severe seizure stage (generalized convulsions) induced by an episode of hyperthermia at P10, and they do so at a lower threshold temperature than in control (300). Additionally, freeze-lesioned rats develop spontaneous seizures several weeks after a hyperthermia-induced seizure at P10, while unlesioned rats subjected to the same hyperthermia paradigm do not (299). This model, therefore, is helpful to evaluate the propensity for seizure in the hyperexcitable brain. This is useful because it reduces the likelihood of confusing cortical alterations that occur in response to seizures with those that may promote them. However, in contrast to these findings, Kellinghaus et al. found no difference in the amount of cortical excitability in adult lesioned rats compared to control (176). This study used an *in vivo* recording technique and injection of bicuculline to antagonize inhibitory transmission and promote epileptiform activity (176). This presents a conflict between the *in vitro* and *in vivo* studies, but it may be attributed, at least partially, to age differences with regard to both the day of lesion induction and the day the experiments were performed. For the hyperthermia study, lesions were performed on P1, and hyperthermia was induced at P10, while the rats were still immature (299; 300). In contrast, the *in vivo* recordings were taken from animals older than P60 that were given lesions on P0 (176). Jacobs et al. previously showed that in the freeze lesion model,

www.manaraa.com

animals lesioned on P1 exhibit hyperexcitability well into adulthood, while animals lesioned on P0 have a decreased incidence of epileptiform responses after P40 (157).

The physiological evaluation of seizure activity is particularly relevant to the experiments in the following chapters, but behavioral studies have demonstrated other deficits in this model as well. Because polymicrogyria and altered migration are also associated with dyslexia (123; 285), behavioral studies using methods that test the auditory processing in rat have been performed (111; 252; 287). In these studies, the rats were tested on their ability to distinguish small silent gaps in a background of white noise. Interestingly, it is through these studies that sex differences in have been demonstrated in this model. For example, lesioned male rats do not perform as well as sham animals at tasks requiring rapid auditory discrimination, but the lesioned females show no deficit (111). There is no baseline bias, as male and female sham rats perform the task equally well (111). To determine whether a hormonal influence provided the female rats with an advantage, the stage of estrous was used as an independent variable, but still no difference was detected (252; 287). Interestingly, testosterone does appear to contribute to differential cellular effects (287), as discussed below. In general, lesioned animals also show mild cognitive deficits compared to unlesioned rats, as demonstrated by their performance in the Morris Water Maze (299). One behavioral study employing this lesion in mouse somatosensory cortex revealed a post-lesional increase in contralateral thigmotaxis, or increased scanning with the whiskers represented in the lesioned barrel field (200). The authors suggest that this may be indicative of increased excitation in the damaged cortex or a compensatory response to decreased cortical

www.manaraa.com

activity. This behavior resolved within one week, and other assays, such as locomotion and exploration of a novel environment, showed no difference (200).

1.3.2.2 Cellular characteristics of the freeze-lesion model

A number of studies have explored the origin, morphology, and functional changes that occur in the neuronal populations of the freeze-lesion model. One birth-dating study shows that the cell-dense second layer of the microgyrus contains neurons generated on embryonic day (E) 20, as well as those generated on E17 that would normally be found in layers III/IV in un-lesioned cortex (291). Cells that populate the superficial layers are the last to migrate into place after the lesion is made, so the fact that they are labeled with bromodeoxyuridine injected prior to lesion formation suggests two things. Firstly, it suggests that new neurons are not generated in response to the lesion. Secondly, the prenatally generated neurons must migrate through or around the damaged area to arrive at their final position in the cortex. Additionally, neurons born at an earlier time point (E15) are not found in the lesion at all (291). Neurons generated on E15 would typically populate the deep layers of cortex, and the fact that they are absent is consistent with the mechanism of selective cell death of deep-layer neurons in this model (99; 291). There does appear to be some proliferative response to the injury, but the newly generated cells also stain for glial fibrillary acidic protein and are likely reactive astrocytes (316). The presence of these cells in the microgyrus is especially dense at the base, but they are located in the region immediately adjacent to microgyrus as well (44). The proliferative cells show signs of having an altered potassium buffering capacity that

www.manaraa.com

may contribute to abnormal electrical behavior in and around the gyrus (44). The concept of altered potassium buffering has also been demonstrated in astrocytes associated with epilepsy-related tuberous sclerosis, as modeled in the mouse (162). In this paradigm, astrocytes have a decreased K_{ir} current, suggesting poor potassium uptake that is likely secondary to a reduction in mRNA and K_{ir} channel subunit protein (162). The resulting presence of excess extracellular potassium may contribute to hyperexcitability and epileptiform activity. Interestingly, activated microglia have also been observed in cases of intractable epilepsy in humans (9; 42), although this has not been explicitly described in the freeze-lesion model. Recruitment of these cells may occur in response to lesion formation, but microglia may also have a pro-epileptogenic role in the form of inflammatory cytokine secretion (356). In fact, injections of interleukin (IL) β-1 have been shown to increase seizure activity and duration in a model of temporal lobe epilepsy (357), and increased cytokine production has been demonstrated following status epilepticus (86). Further, blockade of the IL β-1 receptor reduced behavioral seizures in both cases (86; 357). There are a number of potential ways that non-neuronal cells may contribute to the mechanism of epileptogenesis, and they have yet to be fully explored.

Several alterations in cellular components suggest that a developmental delay occurs in the freeze-lesion model. For example, fibers that resemble radial glia have been observed within the lesioned cortex up to the fifth postnatal week (290). As no such fibers are found in control cortex at that time, their presence in the PMG may represent the persistence of an immature state. Also, the normally transient Cajal-Retzius cells are

www.manaraa.com

still present in PMG cortex at P12 (331). For these reasons and others, delayed maturity has emerged as a theme in the lesion model, as well as for cortical dysplasia in humans. In fact, what is known as the "dysmature hypothesis" of cerebral development in suggests that the abnormal characteristics of dysplastic cortex should bear some similarity to a normal prenatal time point, providing some idea of when appropriate development deviated from the typical timeline (62). One prominent characteristic of dysplastic human cortex is the presence of morphologically abnormal cells, the large, aspiny balloon cells and cytomegalic neurons (62). Their similarity to neurons that populate the preplate suggests that incomplete development has allowed them to persist, even in mature cortex. These particular cell types are not observed in the rat model of polymicrogyria, although some subtle alterations in cell structure are seen. Within the layers of the microgyrus and in surrounding tissue, pyramidal cells in layer II/III have simpler basal dendrites than those in control animals (129). In contrast to this, the apical dendrites of layer V pyramidal cells around the lesion are longer than those in control cortex (92).

1.3.2.3 Subcellular alterations of the freeze-lesion model

On the subcellular level, some receptor subunits also have atypical or immature expression patterns in the freeze-lesion model. In one study, Redecker et al. analyzed the optical density of immunohistochemical staining for individual $GABA_A$ receptor subunits, revealing a decrease in all subunits in the freeze lesion model, except for α3 (273). Typically, both the α3 and α2 subunits decrease their expression by the second postnatal week and are replaced by the α1 or α4 subunit (190). Consistent with

www.manaraa.com

Redecker's observation, Defazio et al. suggested that there is a persistent expression of the α2 or α3 subunit in lesioned cortex, at the expense of α1 expression (89). This was determined indirectly with application of zolpidem, a benzodiazepine receptor type 1-specific agonist. The type 1 receptor is present on the α1 subunit of the $GABA_A$ receptor, so the fact that zolpidem insensitivity is observed suggests that the α2 or α3, but not the α1 subunit was present in the recorded cells (89). Again, this would suggest the prolonged expression of some subunits and a delay in the expression of others. Autoradiography has also demonstrated decreased binding to GABA receptors in the peri-lesional area, with normal binding levels in the surrounding cortex (374). This means that in addition to altered subtype expression, there may also be an overall decrease in the number of GABA receptors.

Glutamate receptors appear to be altered in this model as well, as an increase in AMPA and kainite receptor binding has been demonstrated (374), along with enhanced function of NR2B-containing NMDA receptors (90). The NR2B subunit is typically expressed in the embryonic brain and joined by NR2A and NR2C by the end of the first postnatal week (218). Augmented function of receptors with the NR2B subunit provides further support for persistent immaturity. Similarly, when freeze-lesions are performed *in utero*, there is a selective increase in NR2B immunoreactivity (335). Some of the lesioned animals that were also exposed to electrical stimulation demonstrated further enhancement of the NR2B expression (335). Both of these results are consistent with increased NR2B levels in tissue taken from humans with epilepsy secondary to focal cortical dysplasia (110). In contrast, NR2B is actually downregulated in tissue from

www.manaraa.com

patients with periventricular nodular heterotopia and subcortical band heterotopia (110). Whether or not alterations to certain receptor subtypes occur and/or contribute to hyperexcitability appears to be specific to the underlying type of cortical malformation. Lastly, chloride transporters KCCl and $NKCC_2$ also have delayed expression patterns in a portion of the PMG cortex (316).

1.3.2.4 Altered anatomical connectivity

There are some alterations to the anatomical connectivity in PMG cortex, as has been demonstrated through the use of neuronal tracers injected into the microgyrus, homotopic regions of control cortex and the thalamus (129; 130). Thalamocortical fibers, commissural fibers and afferents from local pyramidal cells demonstrate abnormal organization in and around the microgyrus. Retrograde labeling initiated by dye injection at the site of the lesion in adult rats was visible in cell bodies of the contralateral infragranular cortex (129). Injections to homotopic areas in control produced retrograde labeling that was more prevalent in the supragranular contralateral cortex (129). Interestingly, when dye was injected in the unlesioned hemisphere of a lesioned animal, retrograde labeling indicated that more of the afferent fibers also had cell bodies of origin in the lower layers of the lesioned hemisphere (130). This suggests a shift towards the deeper layers of cortex for both the origin and targets of commissural fibers. Callosal efferents from the lesioned area also showed an increase in the density of their projection to heterotopic areas of cortex, concomitant with the absence of some homotopic projections (286). Rosen et al. suggest that this increase could be due to the presence of

www.manaraa.com

neurotrophic growth factors released in response to cortical injury that prevent the axonal pruning that would typically occur during this developmental time point (286). In rats with bilateral lesions, the volume of the corpus callosum is also reduced, suggesting that fewer connections between the cortical hemispheres are present (346). The extent of this decrease is largest when the lesions are made on P1, and less when lesions are performed on P3 and P5 (346). This suggests that at early lesion dates, a number of interhemispheric connections may be eliminated entirely.

Some thalamic nuclei, as well as the fibers that form connections between the thalamus and lesioned cortex, are altered in this model. Although the ventrobasilar complex is not directly affected by the freeze-lesion itself, it has fewer neurons in the lesioned animals, and this is particularly the case for males (289). The ventrobasilar complex normally has direct connections to somatosensory cortex; however, it loses those reciprocal connections with the lesioned area, its afferents instead forming a dense collection of fibers adjacent to the microgyrus itself (286). This suggests that thalamocortical afferents originally targeting the lesioned area are rerouted to neighboring cortex, resulting in anatomical hyperinnervation. A separate study within lesioned barrel cortex also revealed disrupted architecture and an apparent reorganization of afferent fibers to the PMG cortex (159). Decreased cytochrome oxidase (CO) staining within the lesion itself and increased CO staining in the surrounding cortex supports the idea of thalamocortical afferent reorganization (159). Additionally, within the medial geniculate nucleus (MGN), the distribution of neuronal size is altered in male rats, resulting in more small neurons and fewer large neurons (148). This is not observed in

www.manaraa.com

the female rat population, but this may be due to the fact that the cells are smaller to begin with and a change would be less noticeable (148). This appears to be at least partially affected by gonadal hormones, as females who received testosterone from E16 to P5 exhibited altered MGN neuronal size, similar to the male population (287).

1.3.2.5 Altered functional connectivity

Some of the anatomical changes described in the preceding section relate to the observed functional alterations in this model. For example, cytoarchitectural disturbances may underlie alterations in plasticity. While electrical stimulation in layer IV of neocortex can successfully induce long term potentiation (LTP) in control, the same procedure fails to do so in the disorganized PMG cortex (255). This is interesting because stimulation of layer VI immediately elicits an NMDA-dependent LTP response in PMG. In control, LTP is only produced by layer VI stimulation when bicuculline is also present to provide disinhibition (255). Afferent reorganization, particularly if it provides extra excitatory fibers to the deep layers may play a role in the altered plasticity.

At the cellular level, increased miniature excitatory postsynaptic current (mEPSC) activity in PMG cortex compared to control also indicates that excitatory afferents are functionally increased (160). When compared by age, PMG cells demonstrate a gradual increase in spontaneous (s)EPSC frequency from P7 to P11 (375). This is prior to the time point when epileptiform activity can be evoked (157), suggesting that this increase may contribute to the onset of epileptogenesis. The mEPSCs increase in frequency as well, further suggesting that an increased number of excitatory afferents may be present,

www.manaraa.com

although increased release probability is also possible (375). Finally, evoked (e)EPSCs are multipeaked and have larger amplitude and greater area in PMG, providing additional support to the idea of increased excitatory input to this area of cortex (375). In the field potential preparation, stimulation of the cortex near the lesion (~0.5-2.5 mm from the lesion itself but not within it) results in evoked epileptiform activity that can spread through the cortex over several millimeters (203). However, stimulating at a point distant to the microgyrus (approximately 3 mm away or more) does not evoke an epileptiform response (157). This indicates that there is a specific region of cortex adjacent to the lesion that contains the mechanism for hyperexcitability. Even when mechanically separated from the actual lesion, epileptiform activity can be evoked form this portion of cortex (157). Interestingly, this area of excitability coincides with the area of increased CO staining, supporting the idea that the functional excitability is due to an increased number of afferent fibers (159).

Inhibitory circuitry is also altered in the freeze-lesion model, and there is evidence for both impaired and enhanced GABAergic function. A decrease in $GABA_A$ receptor-mediated inhibitory transmission has been observed in PMG cortex, possibly due, in part, to weaker excitatory input onto the GABAergic cells (201). For a subset of pyramidal cells in layer V of lesioned cortex, though, evoked inhibitory postsynaptic currents (eIPSCs) were actually enhanced (160). In the presence of APV/DNQX, these eIPSCs were restored to control values, indicating that the enhanced pyramidal cell eIPSC is likely due to increased excitatory input to the inhibitory cells causing that response (160). Also, mIPSC frequency in the PMG cortex is not altered, suggesting that if release

www.manaraa.com

probability at those terminals is maintained, there is not an alteration in the overall number of inhibitory synapses (160).

1.3.2.6 Potential involvement of interneurons in the mechanism of hyperexcitability associated with polymicrogyria

The conventional and logical explanation for the presence of hyperexcitability and epilepsy in malformed cortex is increased excitatory activity. Accordingly, a functional increase in excitation has been demonstrated in the freeze-lesion model of polymicrogyria (160; 375), and it is supported by anatomical evidence (159). However, as discussed above, there is evidence for the alteration of both excitatory and inhibitory synaptic transmission (158). The delay between the increase in excitatory input to cortical PMG pyramidal cells (375) and the onset of epileptiform activity (157) also suggest that increased excitation alone does not account for the hyperexcitability seen in this model. Furthermore, increased excitatory input to at least some inhibitory postsynaptic targets has also been shown (160). Finally, recent observations support the intriguing possibility that enhanced, not diminished inhibitory function may play a role in the pathophysiology of epilepsy (183; 206; 268). In order to clarify the potential role for altered inhibition in the freeze-lesion model of polymicrogyria, the experiments described here focus on the interneurons of the neocortex.

www.manaraa.com

1.4 Interneurons in neocortex

The fundamental role of the neocortical GABAergic neuron is to modulate excitatory output. In addition to doing this on a cell-by-cell basis, interneurons are also able to shape the activity of larger areas of cortex due to coordinated actions as members of chemically and electrically coupled networks. In particular, inhibitory cells are able to "reset" the pattern of pyramidal cell firing by exerting a rhythmic hyperpolarizing influence (74). A single interneuron has the capability to simultaneously affect several pyramidal cells in this manner, causing a number of pyramidal cells to fire at regular intervals, in unison (74). This type of patterned activity is referred to as "synchrony," and it is important for a number of cortical functions. Under physiological conditions, these include, but are not limited to: sensory perception, the formation of sensory representation maps, information processing, motor activity, states of consciousness, and attention (121; 319).

Interneurons make up about twenty-five percent of the neuronal population in neocortex and exhibit a variety of morphologies, electrophysiological properties and molecular characteristics (153; 209). Despite this diversity, interneurons share some common properties that differentiate them from the excitatory cells. Most definitively, these non-pyramidal inhibitory cells use γ-aminobutyric acid (GABA) as their primary neurotransmitter, instead of glutamate. Interneurons typically do not have an apical dendrite, and almost all of them lack dendritic spines (209). Because their axons do not project, as pyramidal cells do, to contralateral cortex, thalamus, or spinal cord, interneurons are considered to be 'local circuit neurons.' The extent of axonal

www.manaraa.com

arborization in these cells is usually several hundred micrometers. Beyond these similarities, the variety of interneuron characteristics enables separation of interneuron subtypes based on distinguishing intrinsic qualities. Furthermore, the difference in axonal projection and synapse target domains suggests that these interneuron groups may have distinct functional roles within the neocortex. No single attribute can fully define any one of these neurons, but a combination of characteristics can be used to classify interneurons and begin to elucidate the functional relationships they have both with each other and with the excitatory cells of the brain.

1.4.1 Morphology of interneuron subtypes

Nearly a century ago, Santiago Ramón y Cajal noted that interneurons, or 'cells with the short axon,' did not all have the same appearance (271). Since then, these cells have been classified based on the differences in the shape of the soma and dendritic tree, the extent of axonal arborization, and in some cases, laminar position (1). The different morphologies can be divided into two main groups; those with vertical or intracolumnar orientation, and those with horizontal or intralaminar orientation. There are a number of different cell types that are considered to be vertically-oriented. Martinotti cells, found mainly in the deep layers of cortex, but also in layer II/III, have a clear vertical bias (105). From the cell body of origin, Martinotti cell axons ascend to layer I where they branch and may extend over a significant horizontal distance (105; 209). Bitufted cells, located mainly in layers II-V, have ovoid cell bodies and vertically oriented axonal arbors. Bipolar and double-bouquet cells have columnar axons whose distribution lies

www.manaraa.com

within narrow, radially-oriented columns of tissue (105). Their names, however, refer to the two groups of dendritic branches that originate from opposite ends of the soma, giving these neurons their characteristic appearance. Double-bouquet cells are largely found in the supragranular layers and have descending axons (105). Bipolar cell axons may originate from the cell body or a proximal dendrite and contact only a few cells (209). Two primary classes of horizontally-oriented interneurons are the chandelier cells and basket cells. Chandelier cells, present in all cortical layers, are named for their distinctive morphology. Their horizontal axons have many short, vertical branches with a number of boutons that selectively form synapses on the initial segments of pyramidal cell axons (323). Basket cells also have intralaminar orientation. Larger cells send axons into neighboring columns, while smaller cells have dense arborizations that form multiple connections on neighboring cell bodies and their associated proximal dendrites (209; 360). The fact that interneurons can be divided into these two categories has functional relevance, as different cell types may perform different roles. The vertically-oriented cells that span the layers of cortex have the potential to provide simultaneous inhibitory input to the neurons within a column. In contrast, the horizontally-oriented cells that synapse on neighboring cell bodies within the same layer may provide inhibition between columns.

1.4.2 Electrophysiological characteristics of interneuron subtypes

With regard to action potential firing patterns, interneurons may fire at a consistent rate, have an irregular pattern, or show clear adaptation (209). Onset of action

www.manaraa.com

potential firing may be immediate, delayed, or occur in bursts (209). Of the numerous existing firing patterns, the majority of this discussion will focus on the fast-spiking (FS) and low threshold-spiking (LTS), as they describe the two interneuron populations that were evaluated for these studies. Interneurons that fire a rapid train of action potentials showing little accommodation are classified as FS cells (219). These cells also have exceptionally short action potential half-widths of <1ms (169), and their maximum firing frequency is approximately 330 Hz (172). Frequently they are basket cells with dense horizontal axonal arborizations that target the somata or dendrites, or they may be chandelier cells (172). The LTS interneurons tend to have bipolar or bitufted morphology. LTS cells respond to depolarizing current with an initial group of temporally close action potentials, followed by an attenuating train of action potentials (169). LTS interneurons are also capable of firing rebound action potentials when returned to resting membrane potential following application of a hyperpolarizing current (169). The action potential itself is slightly longer in LTS cells (> 1ms) than in FS cells (169), and maximum firing frequency approaches 250 Hz (172). Input resistance for LTS interneurons (>350 MΩ) is typically higher than in FS interneurons (<350 MΩ), and LTS resting membrane potentials tend to be more depolarized (169). The action potential afterhyperpolarization (AHP) time to peak is shorter in FS interneurons, compared to LTS (169). Inhibitory postsynaptic currents (IPSCs) recorded from FS cells are more frequent, have a larger amplitude and show faster kinetics than those seen in LTS cells (15). This may be due to differential expression of $GABA_A$ receptor subunits (15).

www.manaraa.com

Together, morphological and electrophysiological characteristics suggest an anatomical and functional separation of intralaminar and intracolumnar inhibitory components (169).

These distinct firing patterns are not evident at birth. Studies in mice show that during the first two postnatal weeks, populations of layer IV regular-spiking and FS interneurons come from a single population of intermediate spiking cells (214). The early population of cells fires low-frequency action potential trains without accommodation or fast AHP. Characteristics of FS and RS cells begin to emerge during the first postnatal week, and these cells are encountered with increasing frequency until about P14 (214). Mature action potential firing patterns are dependent on a complement of specific ion channels in the neuronal membrane. In particular, the kinetics of the potassium-driven AHP may determine the distinctive rapid firing pattern of the FS cell. The Kv3 family of voltage-gated potassium channels appears to be necessary for this fast-spiking characteristic (212; 214). Comparatively, pyramidal cells lack Kv3 but do contain Kv4 (212). The presence of mRNA for Kv3.1 is correlated with the FS phenotype (214), and FS cells from Kv3.2 knockout mice were found to have broader action potentials and a smaller AHPs than controls (189). Voltage-gated potassium channels formed from these subunits are activated with depolarization, causing the action potential to be followed by a large hyperpolarization, quickly preparing the cell to fire another action potential. Blocking Kv3.1 and Kv3.2 with tetraethylammonium resulted in disappearance of the typical AHP and a decreased firing rate in FS cells (104).

www.manaraa.com

1.4.3 Molecular markers of interneuron subtypes and development of their expression

Interneurons selectively express certain proteins and peptides, making cellular content a useful characteristic for distinguishing subtypes. Three main calcium-binding proteins used for this purpose are parvalbumin (PV), calbindin (CB), and calretinin (CR). Peptides present in interneurons include somatostatin (SS), neuropeptide Y (NPY), vasoactive intestinal peptide (VIP) and cholecystokinin (CCK,172; 173). Some of the peptides also serve as co-transmitters and may be released concomitantly with GABA. Somatostatin, for example, has been shown to inhibit the presynaptic release of both GABA and glutamate from neurons in the rat basal forebrain (230).

Within different areas of cortex, expression of some markers can be used to define separate, non-overlapping populations of cells. In layers II/III, V and VI, the three major cellular markers expressed in separate interneuron populations are PV, SS and VIP (175). CB is also prevalent in these layers, overlapping with a small percentage of PV interneurons and a substantial portion of SS interneurons. Specifically in the deep cortical layers, nearly the entire CB cell population also expresses SS (184). VIP-containing interneurons may also express CCK and CR, but CR is not co-expressed with SS or PV (60; 175). For some peptides, stereotypical morphologies can be correlated. One group of SS interneurons has axons that ascend to layer I, giving off collateral branches in the intervening lamina (175). This morphology is indicative of Martinotti cells, which have been shown to express SS but never VIP or PV (209). VIP is characteristically expressed in bipolar cells (209). The molecular markers are associated with certain physiological cell types as well. PV expression is correlated with FS

www.manaraa.com

electrophysiology (60; 173; 175). Expression of CB (173; 175) and SS (131) are observed in cells with LTS firing characteristics. Further, analysis of mRNA in LTS interneurons indicates that SS is the most commonly expressed neuropeptide in those cells (60).

The development of the molecular marker phenotype may depend on cues in the cortical environment, as opposed to being genetically predetermined, since not all cells that derive from the same precursor contain the same calcium-binding protein (226). One example of this is NPY, the expression of which is a transient characteristic for some cells in cortex. NPY is a peptide that appears to act presynaptically, preventing the release of glutamate. It has also been shown to reduce excitation in the hippocampus (75). During development, a number of immature interneurons are immunopositive for NPY. Due in part to the influence of thalamocortical afferent input, the subset of these cells that also eventually express PV shows a decrease in NPY production (359). A change in the balance of inhibitory and excitatory input to a developing interneuron may also have an effect on its cellular contents. In hippocampal slice culture, application of the $GABA_A$ receptor blocker bicuculline produced a slight increase in the number of CR-expressing cells and a dramatic increase in the number of SS-producing cells (213). Application of the AMPA receptor blocker DNQX shifts the balance of inputs to favor inhibition, and while it did not appreciably alter the number of CR-expressing cells, it did cause a large drop in the number of cells containing SS (213). Assuming the same phenomenon occurs in neocortex, increased excitation during development, then, has the potential to lead to an increase in number of somatostatin-expressing cells.

www.manaraa.com

Furthermore, cluster analysis of gene expression has revealed a correlation between the mRNA for three main classes of ion channel expression and the three identified calcium-binding proteins (349). This indirectly strengthens the link between specific cellular contents and particular electrophysiological properties, as ion channels are responsible for the characteristics of action potential firing. For example, interneurons expressing mRNA for CR also contain a cluster of genes for ion channels that are associated with accommodation (349). The ion channels correlated with CB are associated with bursting behavior (349). PV is present in cells with ion channels that are appropriate for high frequency discharge (72; 349), and it also correlates with interneurons demonstrating FS firing patterns (60). Although it is not possible to unambiguously place each and every interneuron in a strictly defined group (209), the connections between morphology, electrophysiology and molecular markers make it possible to more clearly segregate the roles that may be shared by similar cells.

1.4.4 Interneuron connectivity and circuitry

The morphological and electrophysiological differences between interneuron subtypes can be translated into functional differences as well. Subtypes of interneurons may be able to perform particular roles by virtue of the fact that they target specific domains on an excitatory cell (175; 209; 324). Interneurons that send synapses to the soma affect the local generation of sodium dependent action potentials, while those that synapse on distal dendrites may modulate calcium-dependent action potentials (217; 225). Interneurons that synapse on dendrites are more suited to have a modulatory role in

www.manaraa.com

general, due to their distance from the soma, while cells synapsing on or near the cell body can effect stronger inhibition. A particularly good example is the chandelier cell; synapsing selectively on the axon initial segment of pyramidal cells, it provides the final inhibitory control before the action potential is allowed to propagate down the axon (323). Interneurons with different electrophysiological properties can also elicit postsynaptic responses that can be differentiated from each other. For example, IPSCs recorded in pyramidal cells are typically larger when produced by FS cells than when they are produced by LTS cells (369).

GABAergic neurons also create synapses with various classes of other inhibitory cells (141; 324) and, through autapses, themselves (324). This connectivity is determined by morphology and cell type; while some are highly connected, others are not. For example, there are no chandelier cell-chandelier cell connections (337). Basket cells can synaptically target double bouquet cells, but more frequently, they target other basket cells (337). Paired recordings have demonstrated that functional chemical synapses exist between FS and LTS cells, although of the various possible synaptic combinations, there is the least LTS to LTS cell inhibition (131). Electrical coupling through gap junctions occurs in neocortex as well, connecting one interneuron to others of the same electrophysiological type (125).

With regard to the excitation of interneurons, the GABAergic cells receive glutamatergic input for one of two purposes: (1) to produce feed-forward inhibition in response to direct excitation, or (2) to complete a feedback mechanism, usually initiated by axon collaterals from principal cells. The EPSCs recorded from interneurons are

www.manaraa.com

faster than the corresponding events in pyramidal cells (51; 128; 149). Interneurons with basket cell morphology and somatic targets tend to receive fewer synapses from a single pyramidal cell than dendrite-targeting or bipolar interneurons (51). However, thalamocortical input to GABAergic cells preferentially innervates FS over LTS interneurons in neocortex (131). Additionally, it has been shown that thalamocortical fibers produce EPSPs that have larger amplitudes and are more reliable in FS cells than in nearby spiny cells (330).

Target-cell-specific modification of excitatory input has also been shown to differ between interneuron subclasses. Generally, paired pulse depression occurs in interneurons that target perisomatic domains, but paired pulse facilitation is observed in dendrite-targeting interneurons (276). Confirming this, in bitufted cells that express somatostatin, facilitating eEPSCs are elicited. Multipolar cells with parvalbumin immunoreactivity demonstrate a depressive response (276). Also, when postsynaptic responses are recorded from different interneurons innervated by the same pyramidal cell, facilitation and depression are both observed, suggesting that the differential effect on eEPSPs is due to factors unique to each synapse, dependent on the postsynaptic interneuron subtype (276; 360). Furthermore, a single interneuron produces the same characteristic response (either facilitating or depressive) when stimulated by several different pyramidal cells, although each of them may have a different time course (210). The cellular location of excitatory afferents may play a role in this temporal disparity.

Chemical synapses between interneurons allow the formation of circuits, but more specialized networks are formed when certain interneuron subtypes are joined

www.manaraa.com

through electrical connections. Dye coupling has been observed between interneurons in hippocampus (224) and in neocortex (78), indicating that these cells are contiguous. Coupling occurs at a greater frequency and for a larger number of interconnected neurons in juvenile cortex (two weeks postnatal) than for adult cortex (78; 253). Specifically, gap junctions between PV immunopositive interneurons with FS characteristics have been described in neocortex (79; 122; 131), and electrical connections between SS-containing LTS cells have also been demonstrated (79; 87; 131). Synchronous responses in pairs of LTS cells following the application of a metabotropic glutamate receptor agonist have been shown to depend on electrical coupling (27). Molecular work and immunohistochemical studies have supported the presence of a gap junction protein nearly specific for neural tissue, Cx36 (76; 83; 272). Cx36 is sparsely expressed in adult rat cortex but has a fairly global presence in neurons of the early postnatal cortex, as measured by both immunohistochemistry and in situ hybridization (29; 30). Both PV and SS-expressing interneurons can be identified by a β-gal reporter activated by the Cx36 promoter, indicating that Cx36 is likely responsible for the electrical connections in both types of interneuron (87). Knock-out mice that lack Cx36 have shown a loss of electrical communication between inhibitory cells in cortex, as well as a severe impairment in LTS-driven oscillatory activity (87). While FS and LTS cells do inhibit each other through synaptic contacts they are virtually never electrically connected to each other (131).

www.manaraa.com

1.4.5 Modulation of activity

Neuromodulatory transmitters provoke a variety of responses in interneurons based on cell type. Acetylcholine, for example, hyperpolarizes FS cells but excites LTS cells in rat visual cortex (368), providing a mechanism for differential control of interneuron subpopulations. Dopamine differentially modulates inhibitory transmission from separate interneuron subtypes as well (126; 351). Norepinephrine and serotonin have heterogeneous effects on interneurons (14). There is also evidence that specific interneuron subpopulations are selectively targeted by serotonergic afferent inputs (106; 249).

Interneurons have the capability to modulate their own activity as well. Neocortical FS cells use GABAergic autaptic (self-synapsing) transmission, which is largely responsible for the precision of the action potential train they are able to fire in response to an injected depolarizing pulse (12). By virtue of the fact that FS cells synapse on themselves and other FS interneurons, simultaneous autaptic and synaptic inhibition could contribute to synchronous activity within a population of these cells. Experiments blocking autaptic transmission with gabazine increased the variability of spike firing in FS cells, while simulating autaptic transmission on pyramidal cells resulted in increased precision of action potential firing (12). Corroborating this with morphology, immunohistochemical data shows that both basket cells and dendrite-targeting cells form numerous autapses (336); however, double bouquet cells do not form as many (324). Bacci et al. demonstrated that LTS cells in neocortex generally do not provide self-inhibition via autaptic connections, but they can modulate their own activity

www.manaraa.com

by producing endocannabinoids that function in an autocrine manner (13). This has been referred to as a slow self-inhibition in which the experimental application of multiple trains of action potentials results in a prolonged hyperpolarization of the membrane potential. This long-lasting effect specific to LTS cells is similar to a subtype-specific long term depression (13).

1.5 Development of interneurons

In order for the cellular components of the neocortex to perform their correct functions, proper development must ensure the correct lamination and connections. Disruption of this process produces the malformations described earlier in this chapter. The following sections discuss our current understanding of interneuron development and migration in normal cortex, a process that has some differences compared to pyramidal cell migration. Cortical excitatory neurons are generated in the ventricular zone and form the preplate, the platform for the developing neocortex. When neurons divide and exit the cell cycle to differentiate, they split the preplate into two parts, the subplate (near the ventricle) and the marginal zone (close to the pial surface). A scaffolding of radial glia guides migrating pyramidal neurons to their proper layer, determined by neuronal birth date. Cortical GABAergic neurons, on the other hand, originate in one of several interneuron progenitor regions in the subpallial telencephalon and migrate tangentially to the cortex (112).

www.manaraa.com

1.5.1 Neurogenesis, migration, maturation

The medial, lateral, and caudal ganglionic eminences (MGE, LGE, CGE) of the developing basal ganglia are the source of cortical interneurons in rodents (6; 237; 363). The formation of different subtypes of interneurons from these sources may be due to separate pools of progenitors, factors present in the cortex during their time of migration, or a combination of both of these (54; 112). The MGE appears to be the source of cells expressing somatostatin and parvalbumin, but not calretinin (370). *In vivo* studies in mice that lacked the regionalization-regulating transcription factor Nkx2.1 revealed a very poorly developed MGE, and only fifty percent of expected GABAergic cell population was present by E18.5 (332). In this model, there was almost a complete lack of cells immunopositive for somatostatin (6). In conjunction with this, electrophysiological studies of MGE and CGE-derived interneurons also reveal two main cell types. Recordings from MGE-derived cells indicate that the predominant mature interneuron type formed is the FS cell (54). This parallels the finding that parvalbumin positive cells derive from the MGE precursor population (370). The second most populous type had firing characteristics similar to LTS cells, which is consistent with the firing patterns of cells described previously to contain somatostatin (54; 60). In the mouse, cells that originate in the MGE migrate through the neocortical SVZ in order to populate the neocortex with a large proportion of its inhibitory cells (363). Although cells from the LGE were originally thought to populate the cortex as well, they generally remain in the basal forebrain and migrate to the olfactory bulb (363). CGE-derived cells migrate to layer V of the neocortex but also to hippocampus and several basal ganglia

www.manaraa.com

structures (237; 363). While cells from the MGE appear to migrate laterally and spread widely, CGE-derived cells travel more specifically toward the caudal end of the telencephalon, and they do it more rapidly than cells from the MGE (223).

1.5.2 Cortical organization and lamination

Cortical organization is complex, including layer-specific targets and outputs as well as local circuitry, and it is important that inhibitory cells migrate to the appropriate position within the neocortex. Interneurons follow the same inside-out developmental pattern used by neocortical projection cells (7; 354). The reelin pathway is a crucial signaling pathway for the proper development of lamination by projection neurons, and it has recently been implicated in the laminar distribution of interneurons as well. Studies in Reelin and Dab-deficient mice demonstrate that early-born interneurons in animals lacking this signaling pathway (E12.5-13.5) have a pattern of layer inversion, but late-born cells (E15.5-16.5) are randomly dispersed throughout the entire cortex (143). To investigate whether this was actually due to a deficit in reelin signaling or if the cause was simply an insufficiency in local cues caused by the distorted arrangement of projection cells, a p35 mutant displaying aberrant cortical structure but intact Reelin was used. In this case, the late-born interneurons found their proper destination (143). It is possible, then, that the early-born cells may rely more on environmental cues from other cellular elements for their proper lamination, while late-born interneurons depend heavily on reelin signaling. Interestingly, late-born interneurons transplanted into younger tissue are able to adopt the fates expected for early-born interneurons, and the converse is also

www.manaraa.com

true (354). This suggests that while the birth date of interneurons is a key determinant for ultimate laminar identity, the migrating cells also rely on extracellular cues to find their place in the developing neocortex. In the freeze-lesion model, the combination of ischemia and cell death may affect these cues and, as a result, interneuron migration. In fact, Reelin deficiency has a demonstrated association with the development of microgyric lesions (277). Disrupted organization of Reelin-secreting Cajal-Retzius cells was also observed within this malformation. These observations were made in a transgenic mouse overexpressing brain-derived neurotrophic factor (BDNF), which appears to downregulate the expression of Reelin (277). This is interesting in light of the fact that the presence of Cajal-Retzius cells is actually prolonged in the freeze-lesion model (331). The presence of persistent reelin-positive cells resembling Cajal-Retzius cells has also been observed in a number of patients with polymicrogyria (103). If excess BDNF affects both Reelin and Cajal-Retzius cells, perhaps some abnormality in this neurotrophic factor contributes to their extended presence in PMG cortex.

Interneurons also exhibit a type of movement called 'ventricle-directed migration.' GABAergic cells generated in the ganglionic eminences migrate tangentially toward the ventricular zone, where excitatory cells are undergoing neurogenesis. At that point they stop, then continue in a radially directed manner toward their final destination in the neocortex (223; 235). BrdU labeling studies have shown that cells immunopositive for GABA are post-mitotic when they are present in the ventricular zone, indicating that they are not being generated in that location (243). Perhaps this migratory route through the ventricular zone provides the interneurons with signaling information to facilitate the

www.manaraa.com

integration of these cells into cortical layers in a manner that is coherent with their isochronic excitatory counterparts.

1.6 Summary and hypothesis

Hyperexcitability in malformed, epileptogenic cortex is a complicated phenomenon that likely requires the contribution of several cortical components. At this point, it is known that epileptiform activity can be evoked from the freeze-lesioned cortex beginning abruptly at P12 (157), but increased functional excitatory input to pyramidal cells develops gradually during the preceding week of postnatal development (375). The delay prior to the expression of hyperexcitability suggests that developmental processes may "mask" the effect of increased excitation until the end of the second postnatal week. Of the other cell types in neocortex that may play a role in this, interneurons are an attractive target for several reasons. During the first two postnatal weeks, these cells are in the process of maturing with regard to the action of GABA (278), expression of calcium binding proteins (4) and firing pattern (214). As persistent immature characteristics are observed in this model (290), one possibility is that the normal development of interneurons is delayed. By the second postnatal week, insufficient inhibitory control may simply permit excitation to dominate. However, inhibitory function appears to keep excitation in check until that time. Furthermore, there is indirect evidence of increased excitatory input to inhibitory cells in this model (160). A second possibility, and the one addressed by this study, is that the interneuron population is altered during development in a way that actively contributes to hyperexcitability.

www.manaraa.com

Evidence of interneuron alteration has been demonstrated in experimental paradigms of hyperexcitability and epilepsy, including the freeze-lesion model. In addition, immunohistochemical studies support the concept that this effect can be subtype-specific (49; 93). Rosen et al. have demonstrated a selective decrease in PV immunostained cells in PMG cortex (288). There is a corresponding decrease in the number of cells expressing PV in human tissue removed from patients with intractable temporal lobe epilepsy (91). However, contrasting evidence from a separate study shows no change in the number of PV cells in PMG cortex (308). One possible reason for this discrepancy is that while Schwarz et al. counted cells within columns spanning the entire distance from pia to white matter, Rosen et al. considered the superficial and deep layers as separate populations. By separating the populations, the authors revealed an infragranular -specific decrease in the PV-expressing interneuron population (288). Partially for this reason, layer V was chosen for the studies reported here. A transient decrease in PV expression was also observed in supragranular layers that resolved after P21 (288). Comparatively, at the time that epileptiform activity can first be evoked in the freeze lesion model (P12), there appears to be no change in the number or density of the subset of interneurons expressing SS in PMG cortex (250). The experiments described in the following chapters investigate whether this type of selective alteration is also observed with regard to the intrinsic properties and/or functional connectivity of interneurons.

The general hypothesis of this study is that interneuron populations in the freeze-lesion model are differentially affected in a pro-epileptogenic manner. More specifically,

www.manaraa.com

these experiments are based on the premise that increased vertical inhibition, due to alterations in the LTS population, could promote columnar synchrony; while decreased horizontal inhibition, due to alterations in the FS population, could lead to the spread of this synchronous activity to neighboring columns. Prior to making statements about the network activity of these interneuron populations, however, it is important to understand the properties of each subtype in order to determine what pertinent changes occur at the cellular level. Therefore, the three main questions addressed by the work presented in this dissertation are:

(1) Is interneuron subtype identity maintained in lesioned cortex, and are the intrinsic properties of these subtypes differentially affected by this developmental insult?

(2) Is the excitatory synaptic input to interneuron subtypes differentially altered in malformed, epileptogenic cortex?

(3) Is the inhibition mediated by vertically-oriented LTS cells increased in lesioned cortex?

www.manaraa.com

Chapter 2

Altered Intrinsic Properties of Neuronal Subtypes in Malformed, Epileptogenic Cortex

Introduction

Neuronal output is shaped by intrinsic properties that influence the reliability and pattern of action potential firing in response to synaptic input (25; 33; 180). These properties are secondary to the complement of ion channels located in the neuronal membrane, as well as the currents that pass through them (25; 164; 372). Increasingly, CNS disorders such as epilepsy are being linked to aberrant ion channel expression and the corresponding current alterations (35; 56; 165). In particular, this has been demonstrated in pediatric epilepsy related to cortical dysplasia (64; 215). Although the mechanisms that underlie epilepsy are not fully known, it is likely that changes to both neuronal intrinsic properties and synaptic connectivity play a role (53; 270). In fact, when modeling epilepsy in a paradigm that does not include disinhibition, alteration of intrinsic properties is necessary for the development of epileptiform activity (53). Specifically, the creation or enhancement of a neuron's capacity to generate bursts of action potentials promotes the development of hyperexcitability (65; 267; 296; 361).

Alterations to the intrinsic cellular properties that appear to play a role in the pathology of hyperexcitability have been demonstrated in various animal models. For

www.manaraa.com

example, in the TISH rat that mimics subcortical band heterotopia, pyramidal cells identified by morphology and firing pattern had resting potentials that were more depolarized than those in control cells (352). In a model of post-traumatic cortical hyperexcitability, pyramidal cells demonstrate higher input resistance, a longer time constant and a steeper f-I slope than control (270). Also, in the methylazoxymethanol (MAM) model of cortical dysplasia and heterotopia, some pyramidal cells exhibited smaller peak amplitudes, higher input resistance, longer action potential duration, less adaptation and higher firing frequency than control (56). Abnormal potassium channel expression in hippocampus (56) and excessive bursting behavior in neocortex (297) were also observed. In the freeze-lesion model used for the present study, pyramidal cells in layer II/III have altered intrinsic properties, such as decreased spike amplitude, maximum rate of spike rise, dV/dt ratio and primary F-I slope (201). These characteristics reflect delayed maturation, which has emerged as a theme in this model (142; 290; 331) and is also characteristic of human cortical dysplasia (62). For the purpose of comparison with the layer II/III results, but also because epileptiform activity likely originates in layer V (341), the focus of this work will be on layer V(342). In the freeze-lesioned cortex, excitatory synaptic input to layer V pyramidal cells gradually increases during the second postnatal week (375), but epileptiform activity cannot be evoked until postnatal day (P)12 (157). It is possible that until P12, concurrent developmental processes in the inhibitory cell population are sufficient to dampen the effect of increased excitation. Normally, by the end of the second postnatal week, a number of properties of both inhibitory and excitatory neurons approach mature values (4; 118; 214; 220; 278). If maturation of

www.manaraa.com

intrinsic properties is delayed or otherwise altered in either population, it may be sufficient to "unmask" the synaptic changes. Therefore, we have chosen to investigate the intrinsic properties not only of pyramidal cells, but also interneurons of layer V in lesioned cortex.

Interneurons exhibit a multiplicity of properties that have been used to categorize them into a number of distinct groups (60; 61; 170; 173). The morphological variety of inhibitory cell types suggests that there is normally an anatomical division of labor among the interneurons of the cortex (209). Previous epilepsy studies suggest that interneuron subtypes can be selectively affected in both animal model and human patient tissue (49; 91; 288). For this reason, it is necessary to compare not only excitatory and inhibitory cell types, but also interneuron subtypes individually. In particular, fast-spiking (FS) and low-threshold-spiking (LTS) interneurons have been well-described and differ significantly on a number of intrinsic characteristics (28; 131; 169; 173). FS interneurons are immunopositive for PV (60; 170), have basket cell or chandelier cell morphology (170; 172), receive powerful thalamocortical input and synaptically target cell bodies and thick dendrites (175). In FS cells, action potential half-width is typically less than 1 ms and there is little to no adaptation in the characteristically high action potential firing frequency (60; 173). In contrast, LTS interneurons have an action potential half-width slightly greater than 1 ms and an action potential firing pattern that shows clear adaptation (173). LTS interneurons are often immunopositive for SS (60; 170), have bipolar or bitufted morphology (170; 172), receive little input from thalamus, and synaptically target thin dendrites distant from the soma (175).

www.manaraa.com

Here we have examined the intrinsic properties of layer V pyramidal cells and two subtypes of interneurons to determine: (1) whether subtype identity is maintained in malformed cortex; (2) if the focal loss of deep layers during the last stages of neuroblast migration into the cortical plate can alter intrinsic properties; and (3) whether neuronal subtypes are differentially affected by this developmental insult.

Materials and Methods

Freeze lesion surgery

Freeze lesions were made as described previously (375). Rat pups aged postnatal day (P)1 were anesthetized with hypothermia by placing them in ice for 4-6 minutes, and an anterior-posterior incision was then made in the scalp. The freeze probe, consisting of a copper bar with a 2x5 mm rectangular tip cooled to -50°C, was applied to the exposed skull over the somatosensory cortex of the left hemisphere for 5 seconds. The skin was sutured, the pup warmed and returned to the dam.

In vitro slice preparation and electrophysiology

Lesioned animals and unoperated control rats aged P12-17 were anesthetized with isoflurane and decapitated. The brain was quickly removed and immediately placed into cold (4°C) sucrose slicing solution containing (in mM): 2.5 KCl, 1.25 NaH_2PO_4, 10 $MgCl_2$, 0.5 $CaCl_2$, 26 $NaHCO_3$, 11 glucose and 234 sucrose. For interneuron recordings, coronal sections 300 µm thick were made and transferred to a holding chamber filled

www.manaraa.com

with artificial cerebrospinal fluid (aCSF) containing (in mM): 126 NaCl, 3 KCl, 1.25 NaH_2PO_4, 2 $MgCl_2$, 2 $CaCl_2$, 26 $NaHCO_3$, and 10 glucose. In attempts to select and record from various interneuron subtypes, the inclusion of some pyramidal neurons in the group of recorded cells is inevitable. As an aid to determine which cells were pyramidal, we have included here, for comparison, the intrinsic properties of pyramidal neurons recorded in a separate study. The focus in that separate study was to isolate layer V pyramidal neurons from other laminar influences, and therefore, the slices were cut horizontally (300 µm) through layer V. Neurons in the control horizontal slices had intrinsic properties similar to those previously reported for layer V pyramidal neurons in coronal slices (201). After sectioning, slices were transferred to a holding chamber filled with artificial cerebrospinal fluid (aCSF) containing (in mM): 126 NaCl, 5 KCl, 1.25 NaH_2PO_4, 2 $MgCl_2$, 2 $CaCl_2$, 26 $NaHCO_3$, and 10 glucose. For these cells, recordings were made in normal aCSF containing dinitroquinoxaline [(6,7)],2,3(1H,4H)-dione (DNQX, 20 µM) and D,L-2-amino-5-phosphonopentanoic acid (APV, 100 µM) to block AMPA and NMDA receptors, respectively. Sections were maintained at 34°C for 45 minutes and at room temperature thereafter. All solutions were infused with 95%O_2/5%CO_2, maintaining pH at 7.4. Recordings were made in aCSF at 30-32°C, osmolarity was adjusted to ~290 mOsm.

The whole-cell patch clamp technique was used to record from layer V interneurons and pyramidal cells in somatosensory cortex from both control and malformed cortex. Prior to recording, access resistance (Ra) was measured, and only those cells with Ra less than 23MΩ were used for analysis. Recordings were terminated

www.manaraa.com

if access resistance increased more than 20% or if there was any evidence of declining cell health. The cortical area used for recording was 0.5-1.5 mm on either side of the lesion and from homotopic cortex in controls. Interneurons were selected based on morphological criteria identified under DIC optics: absence of the apical and basal dendrites and smaller soma than the typical layer V pyramidal cell. These recordings specifically targeted LTS and FS cells. LTS cells were identified by their spindle-shaped appearance and large processes extending towards both the pial surface and subcortical white matter. FS cells had smaller somata with thinner processes in a multipolar distribution. Pyramidal cells were identified by their relatively larger somata and prominent apical dendrites. The intracellular solution used for interneuron recordings contained (in mM): 130 K-gluconate, 10 Hepes, 11 EGTA, 2 $MgCl_2$, 2 $CaCl_2$, 4 Na-ATP, and 0.2 Na-GTP. Patch solution for pyramidal cell recordings in horizontal slices contained (in mM): 70 K-gluconate, 70 KCl, 10 Hepes, 4 EGTA, 2 NaCl, 4 Na-ATP, 0.3 Na-GTP. Osmolarity and pH of the intracellular solution were adjusted to 275-285 mOsm and pH 7.3. In some cases biocytin (0.05-0.2%) was included in the pipette in order to identify neuronal morphology with subsequent staining. Biocytin-filled cells were visualized using fluorescein-conjugated streptavidin (10 µg/mL, Molecular Probes).

Recordings in current clamp were made using a Multiclamp 700A (Axon Instruments) and digitized with a Digidata 1320A and pClamp software (Axon Instruments, at 20 kHz). The resulting files were analyzed using Clampfit (Axon Instruments) and Minianalysis (Synaptosoft) software.

www.manaraa.com

Intrinsic property measurements

Each cell was injected with a series of hyperpolarizing and depolarizing square pulse currents, 400 ms in duration. Current was delivered at an initial level of -40 nA, then increased by steps of 20, 30, or 40 nA to the point where the cell fired at a maximal rate. From these recordings, a number of intrinsic properties were calculated for both pyramidal cells and interneurons. Adaptation was calculated three ways. Total adaptation was calculated by dividing the frequency of the last two action potentials by the frequency of the first two. Early adaptation was calculated as the ratio of the frequency of action potential firing at 200 msec to the frequency of the first pair of action potentials. Late adaptation was calculated as the ratio of the frequency of the last pair of action potentials and the fourth pair. A ratio of one represents no adaptation, while increased adaptation is reflected by an increasingly smaller number. Other measures included action potential half-width, percent increase in half-width from the first to second action potential, peak of first and second afterhyperpolarizations (amplitude measured relative to the threshold for action potential firing), time to peak for the first AHP (relative to the first action potential peak), accommodative hump (the difference between the peak of the smallest action potential and the peak of the subsequent largest action potential), minimal discharge frequency and time of minimal discharge. Action potential amplitude, maximum rates of rise and decay, dV/dt ratio and primary F/I slope were also calculated as described previously (201). Briefly, the amplitude and the max rise and decay rates were determined for the initial action potential in the first sweep with a suprathreshold current. Primary F/I slope was determined from a plot of the frequency

www.manaraa.com

of the first two action potentials (Hz) versus the magnitude of injected current (nA). *t*-tests were used to compare control vs. PMG for each group, $p < 0.05$ was considered to be significant.

Immunohistochemistry

Rats aged P13-14 were anesthetized with isoflurane and transcardially perfused with 4% paraformaldehyde. The rats were decapitated, each brain removed and stored in paraformaldehyde at 4°C overnight. Parasagittal sections 80 µm thick were made from the left hemisphere of both lesioned animals and un-operated controls. Simultaneous triple immunohistochemical staining was performed for SS (rabbit anti-SS, 1:1000, Peninsula Labs; AlexaFluor 568 goat anti-rabbit, 1:100), PV (mouse anti-PV, 1:5000, Sigma; AlexaFluor 405 goat anti-mouse, 1:100) and vasoactive intestinal peptide (VIP, guinea pig anti-VIP, 1:1000, Peninsula Labs; Fluorescein goat anti-guinea pig, 1:200). Sections were incubated in primary antibody solution for SS, PV and VIP on the shaker overnight at room temperature (10%NGS, 2%BSA, 0.5%TritonX-100/TBS). Sections were washed in TBS, incubated in secondary antibody solution for three hours on the shaker at room temperature (10%NGS, 2%BSA, 0.5%TritonX-100). Sections were mounted on unsubbed slides and coverslipped with Prolong Anti-fade mounting medium. Images were obtained using a Leica TCS-SP2 AOBS confocal laser scanning microscope at the Virginia Commonwealth University Department of Anatomy and Neurobiology Microscopy Facility.

www.manaraa.com

Results

Classification of cortical neuronal subtypes

Whole cell recordings were made in current clamp from neurons in layer V of control and PMG cortex. Cells were depolarized with a series of currents (400 ms duration step pulse), eliciting low and high frequency trains of action potentials (Fig. 2.1). Within PMG cortex, we observed a range of neuronal action potential firing patterns that was similar to what was seen in control cortex. A number of previously published studies have used these characteristic patterns to identify interneuron subtypes (13; 15; 27; 28; 131; 169; 170; 367). Based on firing patterns, the recorded cells were placed into one of three groups; pyramidal neurons (Fig. 2.1A,B), FS interneurons (Fig. 2.1C), or LTS interneurons (Fig. 2.1D). Some neurons that were initially selected as potential interneurons based on the DIC image prior to recording showed firing patterns similar to pyramidal cells, so we have called these "suspected pyramidal cells" (Fig. 2.1B). To help classify these cells, the firing patterns from pyramidal cells identified in a separate study were used here for comparison (Fig. 2.1A).

A quantitative confirmation of this pattern-based group assignment is shown in figure 2, where total adaptation is plotted against the amplitude of the first AHP minus the amplitude of the last AHP for individual cells (AHP difference). Adaptation of action potential firing frequency is commonly used to distinguish LTS from FS interneurons (28; 169). AHP difference has also been shown to reliably distinguish pyramidal cells from LTS interneurons (28). In order to confirm that this measure could be used in our

www.manaraa.com

data to separate LTS cells from the pyramidal cells mistakenly recorded while looking for interneurons, we included the previously identified pyramidal cells in this plot as well. This graph shows a clear demarcation between three neuronal cell types (pyramidal, FS, LTS) for both control and PMG populations (Fig. 2.2). Using this methodology, several cells were not classified as FS, LTS, or pyramidal cells. The AHP difference indicated that these cells were unlikely to be pyramidal, but their adaptation ratio did not clearly align them with one of the two interneuron subpopulations. It is likely that these cells represent one or more additional subtypes of interneurons that are beyond the scope of this study. Additionally, the "suspected pyramidal cells" clearly segregated with the group of known pyramidal cells (Fig. 2.2).

Intrinsic properties of cortical neuronal subtypes

A number of intrinsic properties have been useful in differentiating interneuron subtypes (60; 61; 169; 172). Here we have made the same measurements as Cauli et al (60; 61), as they had the most extensive list of properties that clearly separated cell types. This analysis allows us to determine if the intrinsic properties that differentiate interneuron subtypes are altered in PMG cortex. It also confirms whether each action potential firing pattern correlates with a specific array of intrinsic properties in PMG cortex as it does in control. For control cells, our values were very similar to those reported by Cauli et al in most cases, including first and second action potential duration, percent increase in action potential duration, first and second afterhyperpolarization amplitudes, and relative values for early adaptation ratio (Table 2.1). Our LTS cells were

www.manaraa.com

similar to their RSNP-SS interneurons. There were some dissimilarities between our values and Cauli's for accommodative hump, minimal firing frequency and time of minimal firing frequency. All of these discrepancies are likely due to the difference in the length of our depolarizing step (400 msec) compared to theirs (800 msec). In addition, we did not restrict our calculation of minimal frequency to sweeps that began with frequencies of 100 Hz or more. However, even with these differences, minimal firing frequency showed the same relative differences between FS and LTS cell populations in our data (LTS significantly lower than FS, Table 2.1) as FS and RSNP-SS did in Cauli's. The other measures that distinguished FS and LTS interneurons within the control group were the first and second action potential duration, percent increase in action potential duration, AHP peak, early and late adaptation ratios, and accommodative hump (Table 2.1, Fig. 2.3).

Pyramidal cell intrinsic properties

A previous study of layer II/III pyramidal neurons in freeze-lesioned microgyral cortex found that cells in lesioned cortex exhibited slower action potentials compared to control, suggesting delayed maturation of this intrinsic property (201). Similarly, we found that in a train of action potentials, the half-width of the second action potential was wider for layer V pyramidal neurons in PMG cortex compared to control (Fig.2.3). For other measures, including maximum rate of rise or decay, or primary F/I slope, we found no differences between control and PMG layer V pyramidal neurons (Table 2.2), in contrast to previous findings in layer II/III.

www.manaraa.com

Interneuron subtype identity is maintained in malformed cortex

For a number of intrinsic properties, there was no difference between control and PMG interneurons, including the first and second action potential duration, percent increase in this duration, first and second AHP duration, early and late adaptation ratios, accommodative hump, minimal frequency and time for minimal frequency (Table 2.1, Fig. 2.3). The measures that distinguished FS and LTS interneuron subtypes in control cortex also distinguished these subtypes in PMG cortex (Table 2.1). Some of these parameters, including action potential half width and AHP amplitude have repeatedly been used to distinguish these two subtypes in normal neocortex (60; 61; 169; 265).

The intracellular content of interneurons provides an additional basis for subtype identification. Molecular markers PV, SS, calbindin (CB), calretinin (CR) and VIP are each found within selective subpopulations of interneurons (173; 174; 184). These identifiers are often correlated with particular morphologies and electrophysiological characteristics (61; 173). One helpful feature of these markers for distinguishing interneuron subtypes is that some of them are present in non-overlapping populations of interneurons (PV, SS, VIP, 175). These markers are present early in development (152) and therefore may be a useful tool to assess whether the path of neuronal differentiation is altered during the formation of microgyria. Therefore, we addressed the specific question of whether these markers were also found in non-overlapping populations in PMG cortex. The quantitative assessment of the numbers of neurons has previously been done for both PV (288) and SS (250) and is beyond the scope of this analysis, since we

www.manaraa.com

are concerned here with interneuron identity rather than number. High power z-stack images show that no cells contained more than one of the immunohistochemical labels in either control or PMG cortex (Fig. 2.4H,L,P,T). This finding was confirmed by examining twelve separate fields in each of two control and two freeze-lesioned brains. In no case was an overlap of any of the three markers present within a single cell. High power images in control cortex show that PV-stained cells had a rounded somata and multipolar morphology typical of basket cells (Fig. 2.4E,I). In PMG cortex, the morphology of PV cells is similar, although individual neurons are less heavily stained, with less clear dendritic arbors. In both control and PMG cortex, SS-stained neurons had ovoid somata typical of bipolar neurons (Fig. 2.4F,J,N,R). VIP neurons were less prevalent, but no differences in morphology were evident between control and PMG cortex.

Dendritic and axonal morphology can also be used to distinguish interneuron subtypes. While not all cells recorded and filled with biocytin can be recovered in subsequent processing, in this study dendritic and/or axonal morphology was clear in 40 control and 43 PMG neurons from coronal slices. Quantitative examination of this morphology will be performed in a separate study. Here we have made the following qualitative classification of cell morphologies: (1) pyramidal neurons having a clear apical dendrite (large, single dendrite directed toward the pia); (2) bipolar neurons having multiple dendrites and/or axons that project vertically, typically both towards the pia and towards the white matter, and typically crossing into other laminae; and (3) basket neurons that have a round field of dendritic projection (approximately equal vertical and

www.manaraa.com

horizontal distance of dendritic projection) within layer V. Clear examples of all of these cell types were found in PMG cortex (Fig. 2.5). After classification of the morphological type, this was compared to the electrophysiological type. In the majority of cases for both control and PMG cortex, there was a match. In control cortex, 77% of electrophysiologically-identified pyramidal neurons had a clear apical dendrite. The same was true for 89% of PMG pyramidal neurons. In control cortex, 92% of LTS neurons had a clear bipolar morphology, while this was true for 69% of PMG neurons. In control cortex, 60% of FS cells had clear basket cell morphology, and this was true for 64% of PMG FS neurons. There were 2 cells in each of control and PMG cortex whose morphology could not be clearly characterized.

Interneuron firing rate is altered in PMG cortex

Although many intrinsic properties are unchanged in PMG interneurons compared to control, several characteristics were altered that may affect inhibitory tone in malformed cortex. Interestingly, these characteristics were differentially altered for LTS and FS interneurons. In PMG cortex, the maximum firing frequency is decreased for FS interneurons compared to control FS cells (Fig. 2.6A,C). In contrast, PMG LTS interneurons have an increased maximum frequency compared to control LTS cells (Fig. 2.6B,C). These respective changes result in maximum firing frequencies for LTS and FS interneurons that are not different from each other in PMG cortex, while this measure is significantly different for the two interneurons subtypes in control cortex. The increase in firing frequency for LTS interneurons may be due, in part, to the decreased duration of

www.manaraa.com

the first AHP (Fig. 2.6D,F). In particular, the early action potentials fire at a faster rate in PMG LTS cells than in control. Despite the faster initial firing, adaptation still occurs in PMG LTS cells. The shorter AHP and higher frequency at the beginning of the train contribute to the increase in total adaptation observed in PMG compared to control LTS interneurons (Fig. 2.6E,G). LTS interneurons also had a slightly less negative resting potential in PMG compared to control (Table 2.2). FS interneurons in PMG cortex fired action potentials with slightly larger amplitudes than FS cells in control cortex (Table 2.2).

Discussion

Based on intrinsic properties, pyramidal, FS and LTS neuronal subtypes can clearly be distinguished in control cortex (15; 61; 131). Here we have found that this still holds true for malformed, epileptogenic cortex (Fig. 2.2B). Thus the identity of these neuronal subtypes is not altered by a developmental insult in the late stages of cortical migration. While unique cell types can still be distinguished, some intrinsic properties are altered in the PMG. This includes a slowing of the second action potential in a train for pyramidal cells, suggesting that this property is at an immature state. The changes also included a decrease in the maximum firing frequency for FS, but an increase in this rate for LTS interneurons. Both of these changes are unlikely to be explained by the same alteration in, for instance, potassium channels. These results demonstrate that neuronal subtypes are in fact differentially altered during the formation of a microgyrus and the adjacent hyperexcitable region of neocortex. In addition, the changes in

www.manaraa.com

maximum firing rate suggest that the ratio of synaptic input from FS versus LTS interneurons could be altered, with that from LTS increasing while that from FS decreases. Whether this occurs in individual neurons and how it might contribute to epileptiform activity requires further exploration.

Maintenance of interneuron subtypes in PMG suggests that differentiation proceeds normally after the lesion is made, or that most mechanisms defining cell type are complete in layer V prior to the lesion and are unaffected by it. This is consistent with our current understanding of interneuron subtype determination. First, the cells that will eventually populate the PMG cortex are already born when the lesion is induced (291). Secondly, interneurons likely receive their subtype-instructive information at the place of origin, rather than from signals during migration (364). The source of cortical interneurons in rodents includes the medial (MGE), lateral and caudal ganglionic eminences (6; 237; 363), with the MGE serving as the major point of origin for cells expressing somatostatin and parvalbumin (370). Parallel electrophysiological findings indicate that the two predominant mature interneuron types formed from the MGE exhibit firing characteristics of FS and LTS cells (54). In the MGE, prenatally active transcription factors are important for determining the eventual interneuron fate, identified by the expression of PV and SS (6; 97; 332).

It is clear from our data that selective intrinsic properties may be altered, leaving others intact. Previously, an altered number of PV neurons in deep layers has been demonstrated in PMG cortex (288), while the number of SS interneurons appears unchanged (250). A selective change in particular interneuron subpopulations has been

www.manaraa.com

observed in other epilepsy models as well. Typically, it is the PV neurons that are selectively decreased in neocortical models (266; 352), while SS-labeled neurons are selectively reduced in some hippocampal temporal lobe models (47; 119; 328), as well as in human temporal lobe epilepsy (239). The expression of PV in the rodent is not observed with immunohistochemistry until the second postnatal week (4; 322), and may be influenced by factors such as early activity (251), dopamine (264) and estrogen (292). If the observed decrease in PV-stained neurons in the PMG (288) represents a developmental alteration in protein expression, rather than simply the loss of some GABAergic-PV cells, it is possible that incorrect protein expression or aberrant overlap of several proteins within the same cell could occur. This would result in an altered identity based on intracellular contents. Typically in epilepsy studies, changes in single intracellular markers for interneurons have been studied without determining whether there is any change in the co-localization of these markers. Here we have specifically shown that the lack of co-localization of PV, SS and VIP in control tissue is maintained in the PMG (Fig. 2.4), further suggesting that this aspect of interneuron subtype identity is preserved.

In addition to the expression of calcium-binding proteins (152), dendritic outgrowth (353) and some complex firing properties of interneurons (197) have reached near-adult levels by the end of the second postnatal week. Firing properties and action potential characteristics of pyramidal cells also approach mature values by the second and third postnatal weeks (118; 220). Alterations in one or more of these properties during development may contribute to the abnormal activity seen in epileptogenic cortex (25).

www.manaraa.com

This appears to be true in human dysplastic cortex, where the presence of dysmorphic, immature cells indicate disruption of maturational processes (62; 64). For example, cytomegalic neurons demonstrate abnormal membrane properties (64) and the ability to generate calcium spikes with little provocation, possibly suggesting a role in epileptiform activity (63). It is often difficult to discern whether intrinsic property alterations cause the observed pathologies or occur in response to it, but neuronal alterations in disease states tend to resemble non-homeostatic changes, rather than compensatory mechanisms (25). Often these changes include mis-expression of channels or subunits that are important for excitability or repolarization. For example, increased neuronal activity (modeled with short term LTP induction or glutamate application) can cause altered expression of voltage-gated potassium channels (179; 228), directly affecting cellular excitability (228). A lack of functional Kv2.4 channels in heterotopic neurons of the MAM model (56), as well as an upregulation of intrinsic bursting behavior following pilocarpine-induction of status epilepticus (361) both create a tendency for hyperexcitability. Interestingly, the type of alteration that occurs for a given channel or type of current appears to depend both on the experimental model and the developmental state of the animal. In immature rats (P10-11), hyperthermia-induced seizures resulted in an enhanced I_h (71) that contributed to hyperexcitability, while kainate seizure induction in more mature animals (five to six weeks) caused a decrease in I_h and the responsible HCN channel subunits (312). Channel alterations likely underlie changes in firing mode that have also been shown to promote epileptiform activity, including the development of intrinsic bursting in layer V (296), increased bursting in CA1 following *in utero* treatment

www.manaraa.com

with MAM (17), and a transient suppression of AHP and increased firing frequency in the kindling model (26). Selke et al. (311) have also demonstrated the dual loss of one AHP component and adaptive firing behavior in hippocampal granule cells, causing transient hyperexcitability in this population.

Pyramidal cell intrinsic property delayed maturation

A number of findings have contributed to the theme of delayed maturation associated with malformation models (158). In the freeze lesion/PMG model, this includes delayed expression of mature GABA subunits (89; 142) and chloride transporters (316), as well as persistent radial glia (290) and Cajal-Retzius cells (331). There is previous evidence of an immature state in pyramidal cell intrinsic properties within layer II/III (201), and we find at least some similarities with an increased duration of the action potential in the layer V pyramidal neurons recorded here (Fig. 2.3). Typically, action potentials become shorter in duration and larger in amplitude by the end of the second postnatal week (118; 220). Accompanying this change is a larger action potential peak and a faster rate of rise and fall (220). Although we did not observe as many changes in the pyramidal cell intrinsic properties, this may reflect the older age of the animals at the time of recording in the previous study or a true difference between laminae. In any case, both layers show an increased duration of the action potential under some conditions. Prolonging the action potential could limit high frequency firing or bursting, however, and may actually have an anti-epileptogenic effect in PMG (38).

www.manaraa.com

Differential alterations in interneuron subtypes

While the FS and LTS subtypes have maintained their identity in PMG cortex, specific changes in their firing frequencies may represent altered efficacy for each cell type, with interesting implications for interneuron function, as well as potential underlying subcellular mechanisms. In particular, PMG LTS interneurons have an increased maximum firing frequency (Fig. 2.6). One possible mechanism for increased frequency is the elevated expression of voltage-gated potassium channels that permit rapid re-polarization responsible for high-frequency firing. These channels normally have a differential expression pattern in neuron subpopulations for both neocortex (68; 349) and hippocampus (46). The rapid action potential firing capabilities of FS cells may rely, at least in part, on the expression of a specific potassium channel, Kv3.1 (72; 349). Aberrant expression of channels like this could endow LTS cells with increased firing capability. A decreased expression of this channel could contribute to retarding the speed with which FS interneurons fire in the PMG. However, adaptive behavior typical of LTS cells in normal cortex still occurs in PMG, and is actually increased due to a higher initial firing frequency (Fig. 2.6).

Morphological properties associated with specific interneuron populations indicate that tasks performed by each inhibitory population are likely assigned to a specific subtype. LTS interneurons that are capable of firing at an increased rate could create a more powerful inhibitory effect, perhaps augmenting their ability to synchronize surrounding neurons. Even in the absence of excitatory synaptic input, networks of LTS cells can exhibit synchronous, oscillatory behavior, resulting in synchronous IPSPs in

www.manaraa.com

neighboring regular-spiking cells (27). Furthermore, inhibitory input to dendrites can alter the phase of dendritic spiking (178), potentially synchronizing the probability and timing of excitatory events in the dendrites that will ultimately influence cellular output. Based on the vertical orientation and dendrite-targeting of the LTS cells (170; 172; 175), this means that these cells may produced interlaminar, intracolumnar synchrony. At the same time, the lower maximum firing frequency observed in FS interneurons could result in a less powerful horizontal or intercolumnar inhibition. Both of these changes could sway the balance of inhibition to allow the increased excitatory input (160) to contribute to unregulated synchronous firing. It is yet to be determined whether or not increased LTS firing is sufficient to synchronize cortical activity to the extent necessary to promote epileptiform activity. This is currently being investigated through selective activation of LTS interneurons.

Taken together, these data suggest that the differentiation of neuronal subtypes proceeds relatively normally during reorganization of the cortex induced by focal loss of deep layer neurons during the time of cortical migration. However, subtle changes in the firing behavior of LTS and FS interneurons may supply enhanced interlaminar synchrony and suppressed intercolumnar inhibition, ultimately contributing to hyperexcitability in malformed cortex.

www.manaraa.com

Table 2.1 Intrinsic properties of layer V interneurons and pyramidal cells.

Electrophysiological Parameter	FS Control (n=34) PMG (n=30)		LTS Control (n=33) PMG (n=23)	Pyr Control (n=29) PMG (n=22
1st spike duration, ms	0.77 ±0.04 0.81 ±0.06	§ §	1.08 ±0.05 1.03 ±0.05	1.86 ±0.08 2.03 ±0.12
2nd spike duration, ms	0.79 ±0.04 0.84 ±0.07	§ §	1.23 ±0.06 1.17 ±0.06	2.35 ±0.13 2.84 ±0.22**
Duration increase, %	2.8 ±0.6 2.7 ±1.0	§ §	13.4 ±1.4 12.6 ±1.7	25.8 ±4.4 39.6 ±6.9
1st spike AHP, mV	-11.8 ±0.6 -11.5 ±0.6	§ §	-8.6 ±0.6 -7.2 ±0.9	-3.9 ±0.7 -3.3 ±0.6
2nd spike AHP, mV	-14.9 ±0.6 -14.6 ±0.6	§ §	-11.2 ±0.6 -10.0 ±0.9	-14.0 ±0.8 -14.8 ±0.8
Early adaptation ratio	0.08 ±0.02 0.09 ±0.02		0.11 ±0.02 0.07 ±0.01	0.22 ±0.02 0.16 ±0.03
Late adaptation ratio	0.86 ±0.02 0.83 ±0.01	§ §	0.55 ±0.03 0.55 ±0.04	0.77 ±0.02 0.76 ±0.01
Accommodative hump, mV	4.8 ±0.6 4.3 ±0.6	§ §	1.5 ±0.2 2.2 ±0.6	3.4 ±1.1 3.1 ±1.3
Minimal frequency, Hz	32.4 ±3.6 25.5 ±3.3	§ §	9.2 ±0.6 11.6 ±2.3	6.3 ±0.3 6.7 ±0.5
Time for min. freq., ms	188 ±21 171 ±17		201 ±14 170 ±16	175 ±9 176 ±12

Values are means ±SEM. n, number of cells; FS, fast-spiking cells; LTS, low-threshold spiking cells; Pyr, pyramidal cells; Student's *t*-test between control and PMG for each group, ** indicates $p < 0.05$., Student's *t*-test between FS and LTS in control and PMG populations, § indicates $p < 0.05$.

www.manaraa.com

Table 2.2 Intrinsic properties of layer V interneurons and pyramidal cells.

Electrophysiological Parameter	FS Control PMG	LTS Control PMG	Pyr Control PMG
Resting membrane potential, mV	-62.7 ±6.3 (31) -63.0±7.3 (24)	-55.4 ±4.2 (31) -58.7±5.2 (19)**	-56.2 ±5.3 (28) -57.3±8.2 (22)
Input resistance, MΩ	120 ±7 (32) 123 ±7 (25)	191 ±16 (32) 173 ±22 (21)	121 ±16 (29) 140 ±18 (21)
Spike amplitude, mV	81.8 ±1.1 (34) 85.3±1.3 (30)**	99.2 ±1.4 (33) 96.3 ±1.7 (23)	103.6 ±0.8 (28) 102.4 ±1.0 (16)
Max rate of rise, V/s	256 ±12 (34) 253 ±13 (30)	244 ±13 (33) 239 ±11 (23)	287 ±11 (28) 272 ±13 (16)
Max rate of decay, V/s	117 ±7 (34) 115 ±9 (30)	85 ±4 (33) 84 ±5 (23)	42 ±2 (28) 39 ±2 (16)
dV/dt ratio	2.3 ±0.1 (34) 2.4 ±0.1 (30)	2.9 ±0.1 (33) 2.9 ±0.1 (23)	6.9 ±0.2 (28) 7.1 ±0.3 (16)
Primary F/I slope (Hz/nA)	407 ±25 (34) 400 ±23 (30)	471 ±33 (33) 481 ±41 (23)	87 ±18 (28) 97 ±20 (16)

All data are expressed as means ±SE (n cells). Student's *t*-test was used to compare control and PMG values within each group, ** indicates $p < 0.05$.

www.manaraa.com

Figure 2.1 Example traces of neuronal responses to a series of current steps. Firing patterns recorded in control (1,3) and PMG (2,4) cortex in response to depolarizing current. Traces are shown for low frequency responses to small current steps (3,4) and high frequency responses to larger steps in the same cells (1,2). These traces demonstrate patterns typical for: **A.** Pyramidal cells identified in horizontal slices; **B.** Suspected pyramidal cells recorded in coronal slices; **C.** FS; and **D.** LTS interneurons recorded in coronal slices.

www.manaraa.com

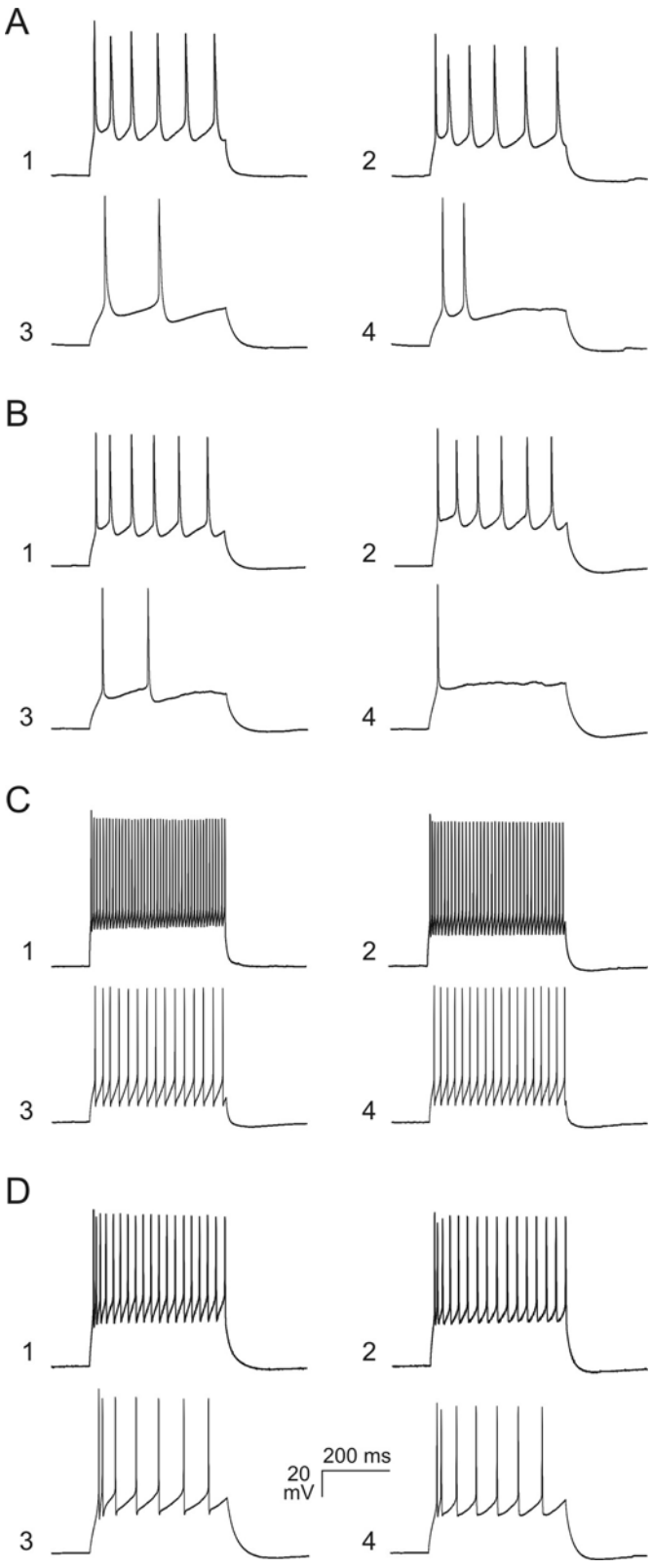

www.manaraa.com

Figure 2.2 Identification of neuronal subpopulations based on action potential firing properties. The difference between first and last AHP amplitudes is plotted against total adaptation ratio, which is the frequency of the first two action potentials divided by the frequency of the last two action potentials. Each symbol shows the result for a single cell. **A.** Control cells. **B.** PMG cells. Five cell types are represented: 1) FS = fast-spiking; 2) LTS = low threshold-spiking; 3) pyramidal; 4) Suspected pyramidal (initially expected to be interneurons but characterized as pyramidal cells based on action potential characteristics); 5) unknown cell type (non-pyramidal, unclassified interneurons).

www.manaraa.com

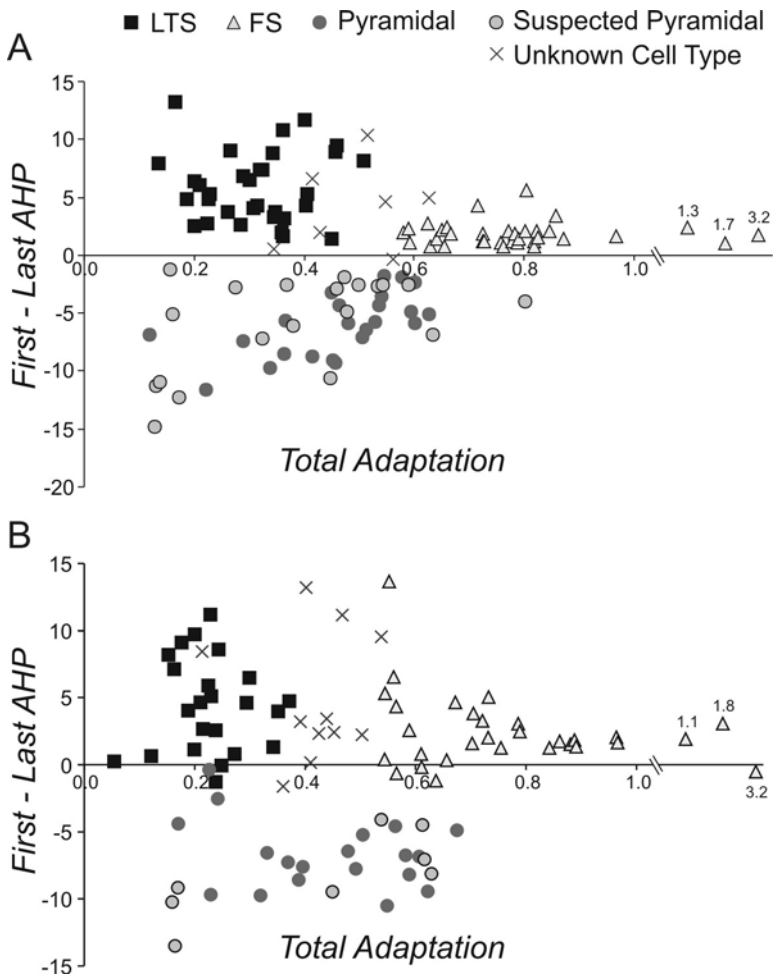

www.manaraa.com

Figure 2.3 Comparison of action potential half-width in pyramidal, FS and LTS cells. **A.** Example traces from pyramidal cells in control (1) and PMG (2). **B.** Enlarged versions of the first (1) and second (2) action potentials from the traces shown above in A, for control (gray, thicker line) and PMG (black, thinner line). **C.** Mean second action potential half-width in control (gray) and PMG (black) for 29 and 22 pyramidal cells, 34 and 30 FS cells, and 33 and 23 LTS cells, respectively. * = *t*-test, $p < 0.05$.

www.manaraa.com

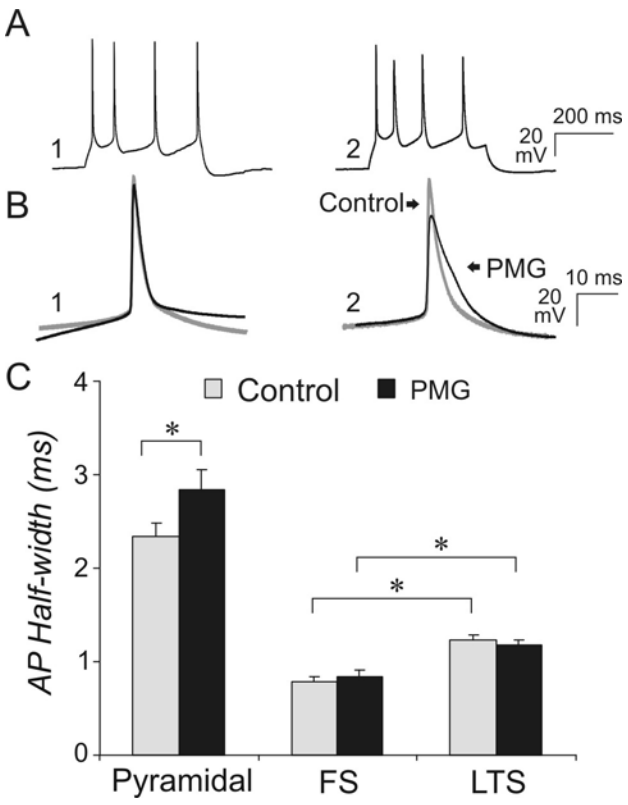

www.manaraa.com

Figure 2.4 Confocal images of parasagittal sections at low power **(A-D)** and high power **(E-T)** showing immunohistochemistry to visualize parvalbumin (blue), somatostatin (red), and vasoactive intestinal peptide (green). To prevent cross-talk between channels, a sequential scanning procedure was used. Panel **A**, overlay of all three fluorophores in control cortex. Panels **B-D**, overlay of all three fluorophores in PMG cortex at locations within, near, and distant from the microgyrus, respectively. Panels **E-H**, images of each fluorophore separately followed by overlay of the three (same visual field) taken from layers II/III in control cortex. Panels **I-L**, images taken from layer V in control cortex. Panels **M-P**, images taken from layer II/III in PMG cortex. Panels **Q-T**, images taken from layer V in PMG cortex. For **E-T**, images are z-stacks with a 1.5 μm slice. Scale bar in **D** for **A-D** = 200 μm, scale bar in **T** for **E-T** = 20 μm.

www.manaraa.com

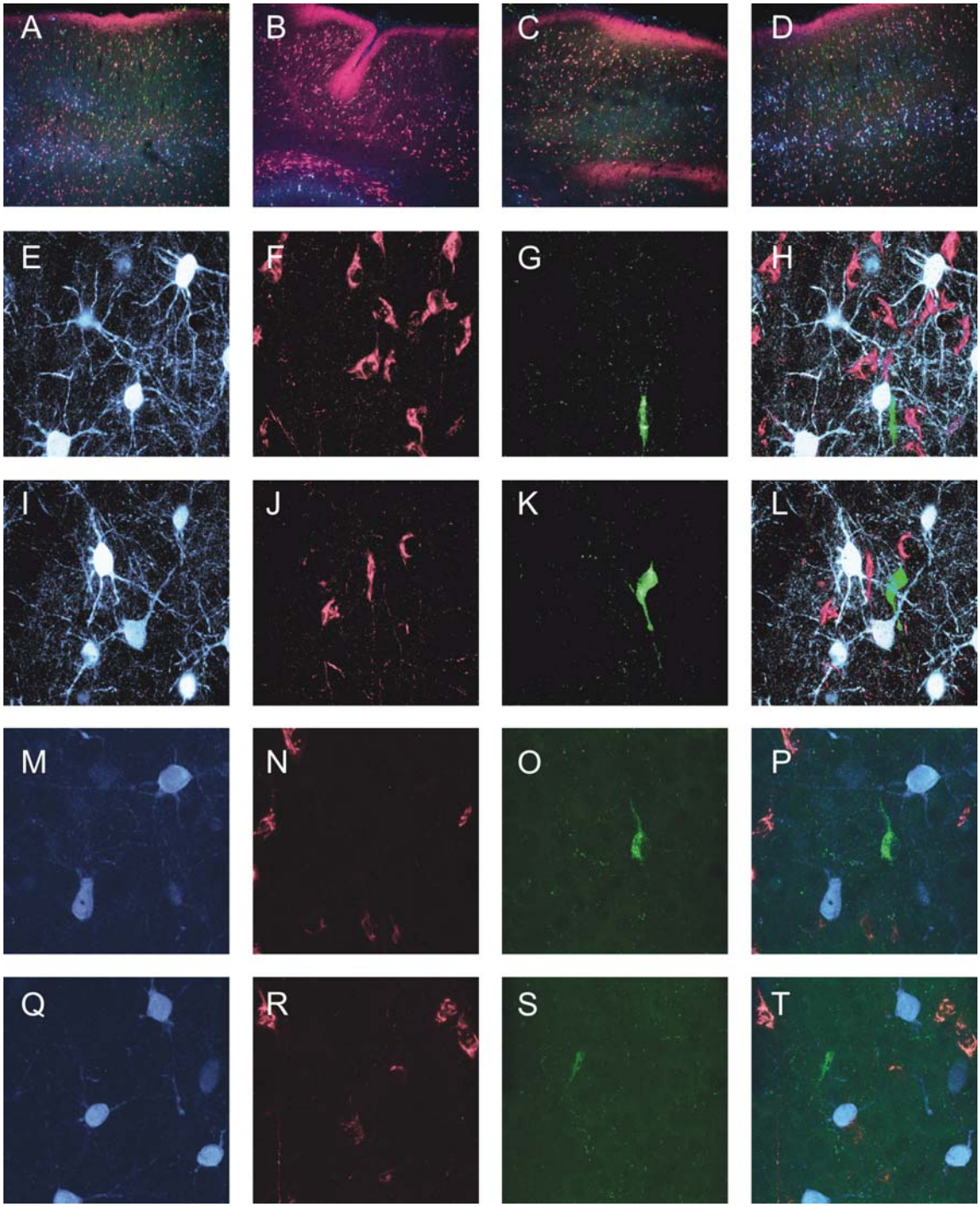

www.manaraa.com

Figure 2.5 Confocal images of individual cells that were recorded and later visualized with fluorescein-conjugated biocytin. All cells are from PMG cortex and are examples of **A.** bipolar, **B.** basket and **C.** pyramidal cell morphology. Scale bar = 10 μm.

www.manaraa.com

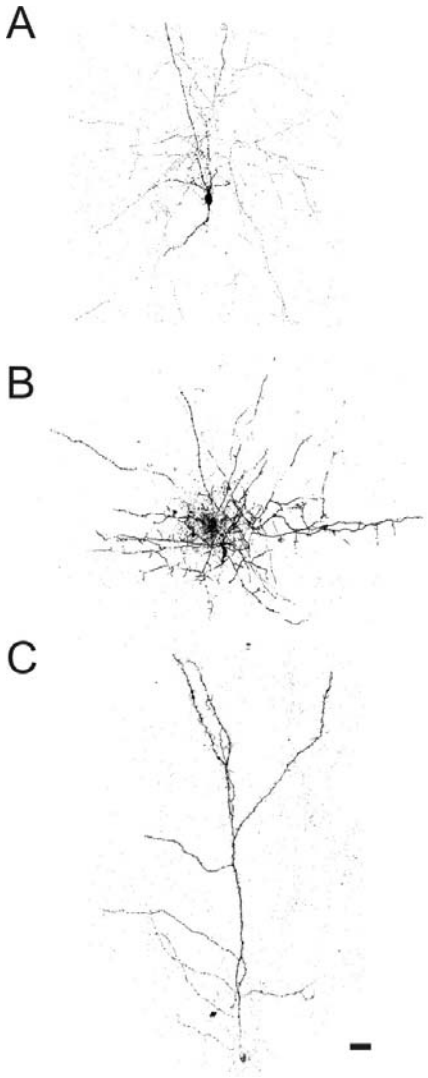

www.manaraa.com

Figure 2.6 Altered action potential firing properties in neuronal subpopulations. A. Example traces from FS cells in control (1) and PMG (2) demonstrating decreased maximum firing frequency in PMG. **B.** Example traces from LTS cells in control (1) and PMG (2) demonstrating increased maximum firing frequency in PMG. **C.** Maximum firing frequency in pyramidal, FS and LTS cells. **D.** Example traces of initial action potential firing from typical control (1) and PMG (2) LTS cells, showing decreased AHP duration in PMG. **E.** Full trains of action potentials showing adaptation in control (1) and PMG (2) LTS cells, increased in PMG. **F.** Duration of AHP. **G.** Average total adaptation. Control (gray) and PMG (black) for 29 and 22 pyramidal cells, 34 and 30 FS cells and 33 and 23 LTS cells, respectively. * = *t*-test, $p < 0.05$.

www.manaraa.com

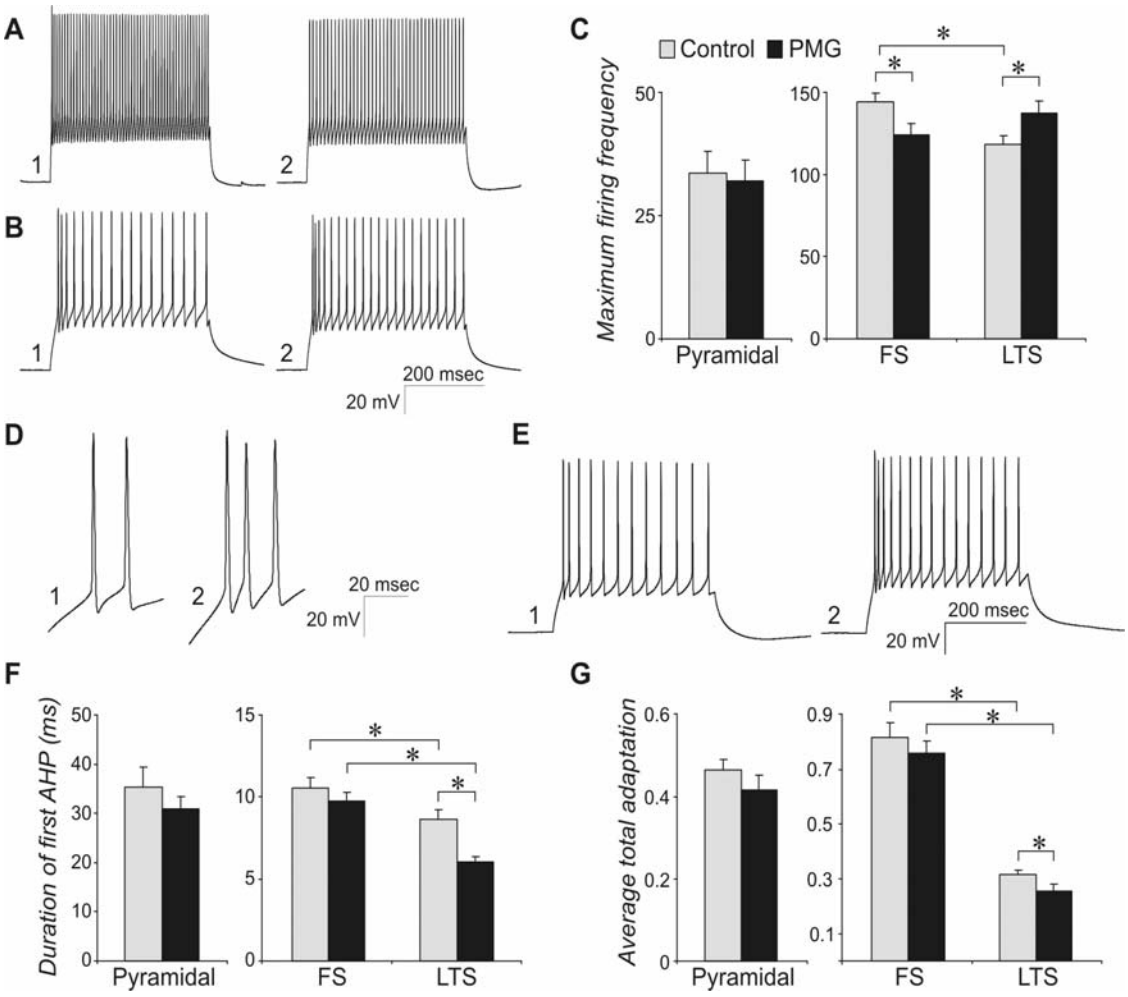

www.manaraa.com

Chapter 3

Excitatory Synaptic Input to Interneurons is Differentially Affected in Malformed Epileptogenic Cortex, Based on Subtype

Introduction

Many of the existing anti-epileptic drugs (AEDs) are ineffective when used alone to treat seizures (187), especially for children who can attribute their seizures to cortical malformations (263). Polymicrogyria, a developmental malformation involving the focal loss of cortical deep layers, is associated with epilepsy and often causes intractable seizures that require surgical intervention (186; 246; 318). Selecting a surgical site is difficult; however, as the epileptogenic region of cortex extends beyond the anatomical malformation in many of these patients (70; 137; 139). In addition, the underlying mechanism responsible for hyperexcitability in polymicrogyria is not fully known.

In the freeze-lesion model of polymicrogyria, not only do the histological changes in the rat mirror those of the human (99; 100) but an analogous electrophysiological abnormality is also reliably demonstrated (156; 157; 202). About two weeks after the lesion is made, epileptiform activity can be evoked consistently from the cortex surrounding the lesion (156). Abnormal connectivity has been demonstrated, suggesting that fibers that originally targeted the lesioned cortex have been redirected to the surrounding paramicrogyral area, producing hyperinnervation with glutamatergic

www.manaraa.com

afferents (159; 160; 286) . We have previously demonstrated a functional increase in excitatory input to cortical PMG pyramidal cells prior to the onset of epileptiform activity (375). The timing of this indicates that increased excitation alone does not account for the abnormal activity, and a concomitant alteration of inhibitory cells may be necessary to "unmask" the network hyperexcitability that is observed at P12. There is increased excitatory input to at least some inhibitory postsynaptic targets as well (160), but measures of overall inhibition do not demonstrate a clear change in this model (268; 269). Individual interneuron subtypes may be differentially affected by the aberrant innervation in a way that is not obvious when inhibitory activity is examined as a whole. This would mean that selective and specific connectivity, not random hyperinnervation, is responsible for the generation of epileptiform activity.

Previous work has provided evidence of selective alterations that occur in both the human condition and in epilepsy models. Evaluation of hippocampal tissue from patients with temporal lobe epilepsy (279) and both the kainic acid (49) and kindling models (321) revealed the presence of fewer somatostatin (SS)-immunopositive cells than control. Also in the kainic acid model, a subset of parvalbumin (PV)-immunopositive cells was selectively spared from injury (37). With regard to neocortex, a decrease in the number of PV-immunopositive cells has been demonstrated in the TISH model, accompanied by a lower frequency of sIPSCs (352). In the freeze-lesion model, Rosen et al. have shown a selective decrease in the number of PV-immunopositive neurons in this model (288; but see 308), while Schwarz et al. have demonstrated an increase in the number of calbindin (CB)-stained cells (308). In contrast to the hippocampal studies, the

www.manaraa.com

number of interneurons containing SS appears to remain unchanged at the onset of hyperexcitability (250). Some intrinsic properties of LTS and FS interneurons also appear to be differentially altered in lesioned cortex (Chapter 2). In conjunction with these results, is important to determine whether there are corresponding functional alterations that occur in specific inhibitory cell populations.

The network of interneurons does not create a straightforward "off" switch, and different interneuron subtypes have unique roles in neocortex (36; 209). For example, FS interneurons that express PV have basket cell or chandelier cell morphology (170; 172). Their axonal arbors have an intralaminar distribution that targets adjacent somata (175), making them well-suited to deliver powerful inhibition and prevent the spread of excitation to neighboring cortical columns. LTS interneurons that express SS have bipolar morphology and a vertical bias (170; 172). These cells target distal dendrites for synapse formation (175), and their distance from the site of action potential initiation allows them to function in a modulatory capacity. Interestingly, there are situations in which dendritic and somatic inhibition may be differentially altered. In the pilocarpine model of temporal lobe epilepsy, for instance, a specific decrease in SS-immunopositive, dendrite-targeting interneurons was observed in the hippocampus, paralleled by a selective decrease in functional dendritic, but not somatic, inhibition of pyramidal cells (80). The hypothesis addressed with the present study is that a similar phenomenon occurs in PMG cortex, namely that dendrite-targeting LTS cells demonstrate increased efficacy, while soma-targeting FS cells have less. These alterations would theoretically leave overall inhibition intact while producing functional, pro-epileptogenic

www.manaraa.com

consequences specific to each cell type. For example, an increase in LTS/SS cell function might increase columnar synchrony. An augmentation of this nature could be achieved by increasing the excitatory input to LTS cells. In fact, this type of change was noted in the pilocarpine model, where a greater number of action potential-driven events was observed in the cells that provide somatic inhibition (80). In order to determine if such a change occurs in PMG neocortex, excitatory postsynaptic potentials were recorded from both FS and LTS interneurons.

Materials and Methods

Freeze lesion surgery

Freeze lesions were made as described previously (375). Rat pups aged P1 were anesthetized by placing them in ice for 4-6 minutes. An incision was made to expose the skull overlying somatosensory cortex of the left hemisphere. The freeze probe, consisting of a copper bar with a 2x5 mm rectangular tip cooled to -50 $^{\circ}$C, was applied to the exposed skull for 5 seconds. The skin was sutured, the pup warmed and returned to the dam.

In vitro slice preparation

Lesioned animals and unoperated control rats aged P12-17 were anesthetized with isoflurane and decapitated. The brain was quickly removed and placed into cold (4°C) sucrose slicing solution containing (in mM): 2.5 KCl, 1.25 NaH_2PO_4, 10 $MgCl_2$, 0.5

www.manaraa.com

$CaCl_2$, 26$NaHCO_3$, 11 glucose, and 234 sucrose. Coronal sections were cut at a thickness of 300μm and transferred to a holding chamber filled with artificial cerebrospinal fluid (aCSF) containing (in mM): 126 NaCl, 3 KCl, 1.25 NaH_2PO_4, 2 $MgCl_2$, 2 $CaCl_2$, 26 $NaHCO_3$, and 10 glucose. Sections were maintained at 34°C for 45 minutes and at room temperature thereafter. All solutions were perfused with 95%O_2/5%CO_2, maintaining pH at 7.4.

Electrophysiology

The whole-cell patch clamp technique was used to record spontaneous (s), miniature (m) and evoked (e) excitatory postsynaptic currents (EPSCs) from layer V interneurons in somatosensory cortex. Interneurons were differentiated from pyramidal cells under DIC by their small, rounded or oblong somata and lack of clear apical or basal dendrites. Recordings were made from an area of cortex 0.5-1.5 mm from the sulcus and from homotopic cortex in controls. The intracellular solution used for recordings contained (in mM): 130 K-gluconate, 10 Hepes, 11 EGTA, 2.0 $MgCl_2$, 2.0 $CaCl_2$, 4 Na-ATP, and 0.2 Na-GTP. With this solution E_{Cl^-} = -71.5 mV. All voltage clamp recordings were made at a holding potential of -70 mV, allowing excitatory events to be recorded in isolation. The osmolarity and pH of the intracellular solution were adjusted to 275-285 mOsm and pH 7.3, respectively. Recordings were made in aCSF at 30-32°C. For some recordings, modified aCSF solution was used to increase the probability of neurotransmitter release. This solution contained, (in mM): 126 NaCl, 3 KCl, 1.25 NaH_2PO_4, 0.5 $MgCl_2$, 3.5 $CaCl_2$, 26 $NaHCO_3$, and 10 glucose. For miniature events,

www.manaraa.com

tetrodotoxin (TTX, 1 μM) was added to the bathing solution. Recordings where made after nearby extracellular stimulation could no longer evoke a postsynaptic current (~5 min). For evoked EPSCs, a glass electrode filled with 1M NaCl was placed in the slice at a 250 μm horizontal distance from the recorded cell and used to apply a series of currents. Threshold was determined as the smallest amount of current able to elicit a fifty percent response rate at a pulse width of 20 μsec. Stimulus intensity was changed by increasing pulse duration while maintaining the threshold level of current. A series of five intensities was applied (1x, 2x, 4x, 8x and 16x threshold). For each intensity level, the responses to three stimulus presentations were averaged. A 50 Hz train of four stimuli was applied to the slice using the maximum stimulus intensity (16x threshold). The responses to five stimulus train presentations were averaged for individual cells.

Data analysis

Recordings were made with a Multiclamp-700A amplifier (Axon Instruments), and only those with an access resistance less than 23 MΩ were accepted for analysis. Recordings were terminated if the resistance increased more than 20% or if there was other evidence of declining cell health. Data was digitized online (20 kHz) using software from Axon Instruments. Data analysis for voltage clamp experiments was performed using MiniAnalysis (Synaptosoft). Some intrinsic parameters were measured using Clampfit (Axon Instruments). Evoked data was analyzed using Igor software (Wavemetrics). Measurements are reported as means ±SEM. Student's *t*-test (Excel), z-test (SigmaStat), one way ANOVA and repeated measures ANOVA (SPSS) were used to

www.manaraa.com

test for significance where appropriate, and $p < 0.05$ was considered to be significant. Cumulative probability plots were generated to compare control and PMG mEPSC interevent interval (IEI) durations for LTS, FS and overall interneuron populations. For LTS, 200 events from each of nine cells with mEPSC frequencies closest to the median value were combined for a total of 1800 events per group. For FS, the first 300 events from each of six cells were used per group. For overall interneuron populations, 300 events from each of 23 cells per group were used to ensure that all cell types were represented. The data were fit with the exponential decay function: $y = A1 \exp(-x/t1) + y0$ and the percentage of IEI values that fell below a set duration threshold was determined. The Kolmogorov-Smirnov test was used to test for significance, $p < 0.05$ was considered to be significant.

Results

Excitatory input to the overall interneuron population is unchanged in PMG cortex

Recordings were made from a total of 73 control and 59 PMG interneurons using the whole cell patch clamp technique. To determine whether excitatory synaptic input is altered for interneurons in the freeze-lesion model, s- and mEPSCs were analyzed. The sEPSC frequency ranged from 0.5- 22.3 Hz in both control and PMG populations. This is similar to previously reported values for excitatory input to layer V pyramidal neurons (160). Comparable ranges for sEPSC amplitude were also observed for control (11.5-45.4 mV) and PMG (13.9- 48.8 mV). Mean sEPSC frequency and mean amplitude were

www.manaraa.com

the same for events recorded from interneurons in PMG cortex compared to those in control (Fig. 3.1). For mEPSCs, neither the frequency nor the amplitude of these events was different in PMG cortex compared to control (Fig. 3.1). Furthermore, the frequency of miniature events was not significantly different from that of the spontaneous events. Calculated for individual cells, mEPSC frequency was 93 ±9% of sEPSC frequency in control and 91 ±8% in PMG. In order to determine whether alterations occur that cannot be detected when all interneurons are considered together, subpopulations were examined separately.

FS and LTS interneurons receive different amounts of excitatory input in control cortex

To compare populations of interneurons, two groups were separated from each other based on firing patterns and intrinsic properties. In a separate study of intrinsic properties, we have found that interneuron subtypes exist in essentially the same spectrum in PMG as they do in control. We can readily separate different subtypes, as well as distinguish regular spiking neurons from interneurons (Chapter 2). This was accomplished using two measures, (1) the difference between the peaks of the first and final AHPs and (2) the total adaptation ratio. Once these groups were established, a number of other intrinsic properties were evaluated and found to be consistent for each cell type between control and PMG cortex. Several of those measures were used here to confirm the classification of FS and LTS interneurons.

Interneurons were visually identified under DIC and then assigned to a subtype category based on their responses to a series of depolarizing current steps producing both

www.manaraa.com

low and high frequency firing patterns (Fig. 3.2). LTS interneurons fired two or three temporally close action potentials in response to small current steps, followed by adapting trains of action potentials in response to increased current (Fig. 3.2A,B). FS interneurons fired high frequency action potential trains with little adaptation (Fig. 3.2C,D). Adaptation for individual cells was plotted against action potential halfwidth, separating the two populations of interneurons (Fig. 3.2E,F). Input resistance, action potential half width and AHP peak amplitude were also used to distinguish interneurons here (Fig. 3.3). For both interneuron populations, these control measures were consistent with previously reported values (60; 169).

For each interneuron subtype, levels of excitatory input were determined in control. FS interneurons had a higher frequency of sEPSCs than LTS interneurons, and mEPSC frequency was also greater in FS cells compared to LTS (Fig. 3.4). The amplitude of spontaneous and miniature events was larger in FS compared to LTS interneurons (Fig. 3.4), and rise time and decay for both sEPSCs and mEPSCs were faster in FS cells than LTS cells (Table 3.1). These differences were maintained in PMG cortex (Fig. 3.4, Table 3.1).

Excitatory input to interneurons is differentially altered in PMG cortex

For LTS interneurons, the mean frequency of spontaneous events was doubled in PMG compared to control cortex (Fig. 3.4). This occurred without alteration of the mean amplitude (Fig. 3.4F), rise time, or decay for these events (Table 3.1). There was also a higher mean frequency of miniature events in PMG LTS interneurons compared to

www.manaraa.com

control, but no difference in amplitude (Fig. 3.4G,H). Interestingly, neither the spontaneous nor the miniature event mean frequency was different in the PMG FS cell population compared to control (Fig. 3.4). To take into account the variation within each cell type, the range of frequencies was plotted with both the mean and median values for that group (Fig. 3.5A-B). As expected for the PMG LTS population, the upper limit of the range was increased, although the minimum value was the same (Fig. 3.5A). Not all of the cells had a higher frequency in the LTS population, but both the mean and median values were increased. In contrast, the action potential half-width, an intrinsic property and defining quality of interneuron subtype, were unaffected (Fig. 3.5A). Interestingly, neither the range of frequencies nor the mean frequency was different for PMG FS cells compared to control; however, the median value for mEPSC frequency was lower in the PMG FS population. As with the LTS interneurons, the action potential half-width measurement remained unchanged (Fig. 3.5B).

Cumulative probability plots were generated (See Materials and Methods) to compare the IEI distribution for the cells with mEPSC frequencies closest to the median value in each group (Fig. 3.5C-E). Not surprisingly, there was a significant separation between the distribution of the IEIs for control and PMG LTS cells (Fig. 3.5C). To investigate this difference further, the percentage of IEIs that were shorter than the set threshold of two seconds was compared between control and PMG. While 47% of the IEIs in control LTS cells were shorter than two seconds, 85% of IEIs in PMG LTS cells fell below this threshold. Unexpectedly, there was also a significant separation between the control and PMG populations of FS cells (Fig. 3.5D). Due to the higher mEPSC

www.manaraa.com

frequency observed in FS cells, a 400 msec threshold was used. For control cells, 75% of the IEIs were shorter in duration than the threshold, while for PMG FS cells, the IEIs were typically longer, with only 42% of the IEIs falling below the threshold level. A cumulative probability plot was also generated for interneurons without separating them by subtype, and the distribution was similar for both control and PMG populations (Fig. 3.5E). A 900 msec threshold was set for these IEIs, with 66% and 46% falling below this level for control and PMG, respectively.

Evoked responses

In response to a series of five stimuli with varied intensities, eEPSCs in both FS and LTS interneurons were graded in size relative to the increase in stimulus intensity (Fig. 3.6A,B). Some cells occasionally fired action potentials at the highest stimulus intensities. The mean area of the eEPSC was larger for FS interneurons than LTS interneurons (Fig. 3.6C). There was no significant difference in the threshold current used to evoke these responses for any of the groups (Control LTS = 73 ±15 µA, Control FS = 65 ±15 µA, PMG LTS = 65 ±10 µA, PMG FS = 31 ±4 µA, one-way ANOVA, N.S.). Time-to-peak of the eEPSC was shorter for control FS interneurons than both control and PMG LTS interneurons. There was, however, no difference in the time to peak for PMG FS interneurons in comparison to any of the other cell groups (Fig. 3.6D). The presence of all-or-none variable-latency evoked activity was also evaluated for each cell in response to this series of stimuli. In control, 6/22 FS cells (27%) and 5/22 LTS cells (23%) demonstrated this type of late activity on one or more sweeps. In PMG, it

www.manaraa.com

was present in 12/22 FS cells (55%) and 7/15 LTS cells (47%). Typically, late activity was observed following application of the lower intensity stimuli (Fig. 3.6E,F). The mean area of this activity was not different for control FS cells compared to either population of LTS cells, but late activity in PMG FS interneurons had a larger area than either control or PMG LTS interneurons (Fig. 3.6G).

Trains of four stimuli at a frequency of 50 Hz were also applied to the slice using the maximum stimulus intensity established for the preceding series. As has been previously reported, LTS cells demonstrated facilitating patterns, while FS cells had a depressive pattern (276) in response to repetitive stimulation (Fig. 3.7). Cells were identified as facilitating or depressive based on the percent change in eEPSC amplitude between the first and fourth responses to the stimulus train. In control, all FS cells showed depression, as expected (Fig. 3.7F). However, there were four control LTS cells that did not show clear facilitation (19%). In PMG, four FS cells showed a slightly facilitating response (18%). Only one PMG LTS cell was not facilitating (7%). There were no differences between control and PMG populations regarding the proportion of cells that demonstrated the expected, stereotypical response to repetitive stimuli (z-test, N.S.). It is interesting to note that of the facilitating PMG FS cells, the amount of facilitation between the first and fourth eEPSCs (159 ±27%) was not as extensive as is typically seen in LTS interneurons (322 ±34% in control, 338 ±60% in PMG). Also, while there was no significant difference in the characteristic response (facilitating vs. depressive) for either interneuron subtype, the extent of the response was altered in PMG cortex. In other words, the amount of depression in PMG FS cells was slightly increased

www.manaraa.com

compared to than that of control FS cells, as measured by the percent decrease in peak (*t*-test, $p < 0.05$, Fig. 3.7C). For the LTS population, the percent increase in peak amplitude for the final response was slightly larger in PMG LTS cells (*t*-test, $p < 0.05$, Fig. 3.7D).

Increased probability of release causes increased sEPSC frequency in both PMG and control

The increased s- and mEPSC frequencies observed in LTS interneurons could be due to the presence of more glutamatergic terminals or an increased probability of release from existing terminals. For this reason, sEPSCs were also recorded in modified aCSF containing low Mg^{2+} and high $Ca^{2+}$to increase the probability of presynaptic glutamate release (see Materials and Methods). A percent increase in sEPSC frequency of roughly equal magnitude was seen in the LTS cells from PMG (677 ±278 %) and control cortices (470 ±190 %, Fig. 3.8). This increase included a wide range of values for individual cells in both control and PMG cortex. In control LTS cells, this also reflected an increase in mean frequency from 1.2 ± 0.2 Hz in normal aCSF to 6.4 ± 2.5 Hz in modified aCSF (*t*-test, $p < 0.05$). In PMG, the corresponding values increased from 1.5 ±0.2 Hz to 9.9 ± 2.5 Hz (*t*-test, $p < 0.05$). FS interneurons also demonstrated a similar level of increase between control (100 ±61 %) and PMG (122 ±38 %) populations, as expected, although their increase was much smaller than that of the LTS interneurons (Fig. 3.8). For neither control nor PMG cortex was there an accompanying change in the amplitude of the spontaneous events.

www.manaraa.com

Discussion

The main finding of this study is that there is a selective increase in excitatory input to LTS interneurons in malformed, epileptogenic cortex. Additionally, there appears to be a subtle decrease in excitatory input to FS cells in PMG cortex. This is not reflected in the interneuron population as a whole; however, as sEPSC frequencies are not different when comparisons between control and PMG cortex include all interneurons.

After separating FS and LTS interneurons based on their intrinsic properties (13; 15; 28; 60; 61), we were able to note characteristic differences in physiological properties for these two groups in control. The sEPSCs recorded from FS interneurons typically have a higher frequency, larger amplitude and faster rise and decay times compared to LTS cells (see Results). This is not surprising, as both thalamocortical and local pyramidal cell inputs to FS cells tend to be reliable and precise (28; 330), while LTS cells have more failures in response to pyramidal cell synaptic stimulation and receive weak input from the thalamus (28). The characteristics that distinguish these two types of interneurons are also related to the observation that the cells normally function within separate networks. Electrically connected FS cells (28; 124; 131), for example, provide powerful inhibition (330) and elicit fast IPSCs in pyramidal cells (369). This allows the horizontally oriented FS cells that synapse on cell bodies (185) to powerfully and rapidly effect feed-forward inhibition, while vertically oriented LTS cells (173) modulate activity via dendritic synapses. Networks of LTS cells have a role in cortical synchrony (197) and elicit slower IPSCs than FS cells, likely due to their distal synapse location (369).

www.manaraa.com

These two types of interneurons also have a differential response to acetylcholine (171; 368), further suggesting that they subserve different functions. Interestingly, under control conditions in hippocampus, differences have also been demonstrated between the excitatory input to dendrite-targeting and soma-targeting interneurons (81). In hippocampus, for dendrite targeting interneurons, sEPSCs have been shown to be dependent on action potential firing, but sEPSCs in soma-targeting interneurons were largely independent of action potential firing (81).

Just as the balance of excitation and inhibition is important for normal cortical function, we propose that an imbalance between the function of distinct inhibitory networks may contribute to the observed electrophysiological abnormality in this model. Inhibition itself was not measured directly for this study, but the EPSC frequency measured in inhibitory cells demonstrates a selective increase in the PMG LTS population, suggesting that LTS cells may more frequently be depolarized to threshold potential in PMG cortex (Fig. 3.4). This in turn could create an increase in the inhibitory influence provided by the LTS population, enhancing vertically-oriented inhibition (173; 174). Due to connectivity provided by gap junctions and the subsequent coordinated activity of a number of LTS cells (197), this increase could result in columnar synchrony. In contrast, other studies have demonstrated decreased excitatory input to interneurons (367). While this may intuitively make more sense with regard to hyperexcitability, not all models of hyperexcitability show decreased inhibition (50; 269). Although the mean values for EPSC frequency were not different for FS cells, the separation between mEPSC IEI distributions for control and PMG also suggests that there is at least a

www.manaraa.com

subpopulation of PMG FS cells receiving less excitatory input. The range of mEPSC frequency is not different for PMG, and there is enough variation to produce similar means for each group, however, the lower median value indicates a shift toward lower mEPSC frequencies. The idea of decreased input to FS cells is also consistent with a study that showed a selective decrease in the strength of inhibition from FS cells in layer IV of somatosensory cortex (329). A loss of powerful feed-forward inhibition normally mediated by these cells could result in the absence of regulation needed to prevent uncontrolled spread of excitation.

Amplitude, rise time and decay were not altered in PMG for either LTS or FS interneurons, suggesting that the observed alterations in frequency comprise a pre-synaptic phenomenon. In addition, the observed sEPSC frequencies were very close to the mEPSC frequencies, indicating that under these conditions, there is a limited amount of spontaneous activity (Fig. 3.4). This suggests that the increased sEPSC frequency in PMG LTS cells is not action potential-dependent. Rather, the increased mEPSC frequency supports the idea that increased afferent contacts selective to the LTS cell population underlie increased excitation. In fact, previous work has suggested the possibility of increased excitatory drive on interneurons that occurs in a specific, non-random fashion (160). However, altered probability of release at the excitatory synapses could also have a role in the observed changes. To evaluate this, modified aCSF (containing high Ca^{2+}/low Mg^{2+}), was applied to enhance neurotransmitter release probability (352). We expected that if LTS cells in PMG cortex receive increased input due to a greater number of afferent fibers, the percent increase in frequency should mirror

www.manaraa.com

that of the control population, which it did (Fig. 3.8). A lesion-induced increase in presynaptic release probability for excitatory synapses on LTS cells would likely render their response to the modified aCSF similar to the smaller response seen in FS cells. The FS cells were expected to respond less robustly, as they are more reliably excited by presynaptic excitation (330) and have higher sEPSC frequency under normal conditions (Fig. 3.4). Conversely, if the probability of release was decreased in PMG FS cells, we would have expected to see a "rescue" effect following application of modified aCSF. While these data do not definitively prove that probability of release from excitatory synapses on interneurons is unaltered in this model, the idea of an altered number of afferent fibers and synapses is supported by other data that suggest an anatomical reorganization of afferent inputs (286). Ultrastructural studies to determine the number of excitatory synapses on interneuron subtypes would help clarify this issue. Ultimately, complex alterations to a number of characteristics may contribute to the observed changes, and our methods may be unable to distinguish each component.

It has been previously reported that FS cells exhibit a depressive response to repeated stimuli, while LTS cells show facilitation (276). Here, a 50 Hz stimulus train evoked depressive responses from FS cells and facilitating responses from LTS cells, with few exceptions. FS cells typically receive strong glutamatergic input from terminals that release enough neurotransmitter to produce a reliable postsynaptic response, resulting in depleted glutamate stores and their depressive response after repeated stimulation. Perhaps suggestive of a slight increase in release probability for the PMG FS neurons, "greater depression" was observed in these cells (Fig. 3.7). A subtle increase

www.manaraa.com

in the probability of release would make more glutamate available to be used in response to the later stimulations. For the LTS cells, facilitation is explained by the presence of glutamate in the presynaptic terminal that is only released subsequent to repetitive stimulation and increased calcium influx. Had release probability in PMG LTS cells already been increased, their response to repetitive stimulation would be expected to lose at least some facilitation, as the glutamate would be released at lower stimulus intensities under those conditions. The majority of LTS cells still responded to the stimulus train with a facilitating response, demonstrating that they did not exhaust glutamate stores and could still produce facilitating responses in PMG cortex (Fig. 3.7). However, if PMG LTS interneurons have a larger number of afferents, they should then have larger responses to threshold stimuli. Surprisingly, the area of the evoked response was not different in PMG cortex when compared to control. It is possible that the number of additional afferents required to double the initially low frequency of LTS interneurons might not be sufficient to cause a significantly increased evoked response, especially if there is a concomitant alteration in release probability. Interestingly, another indirect measurement of aberrant excitatory input, late evoked activity, was observed in twice as many PMG interneurons as in control (see Results and Fig. 3.6). This type of activity reflects excitation that resonates in the cortex prior to eliciting a postsynaptic response in the recorded cell. The increased FS activity is a good indicator of increased excitation in the cortex, due to the reliable response to synaptic input seen in this cell type (28; 330).

An intricate connectivity between excitatory and inhibitory cells that is only partially understood defines cortical organization and can be disrupted during

www.manaraa.com

development. For example, as the cortex matures, FS and LTS cells develop distinct relationships with neighboring pyramidal cells. FS cells form reciprocal connections that are stronger than one-way connections, while LTS cells do not have this same propensity (371). In addition, whether or not spatially related FS and pyramidal cells will receive excitatory input from the same afferents is dependent on these reciprocal partnerships, while for LTS cells, it is not (371). When the freeze-lesion is made, neuronal death causes some incoming glutamatergic afferents to be deprived of their targets. In particular, it appears that a number of FS cells are lost, evidenced by the decrease in PV-immunopositive cells (288). Even though thalamic and callosal afferents originally destined for the gyrus appear to hyperinnervate the paramicrogyral area (155; 286), there may be fewer pyramidal- FS pairs to receive these inputs. One potential consequence of this could be a decrease in the FS cell efficacy. If these interneurons are not stimulated at the same time as neighboring pyramidal cells, their role in feed-forward inhibition and control of horizontally spreading excitation could be hindered. Also relevant to this study is the potential availability of more glutamatergic afferents for the surviving pyramidal and LTS cells. The vertical orientation of LTS cells means that dendrites connected to layer V cell bodies may be located in layer IV, the main target of thalamic afferent fibers. Increased thalamic afferents could contribute to the increased EPSC frequency seen in these cells. Additionally, while a large number of afferents may come from projecting sources, it is also possible that local pyramidal cells will show sprouting and increased axonal development, as is seen in the undercut model of post-traumatic epilepsy (294). In fact, recordings of *in vitro* epileptiform activity evoked by thalamic stimulation

www.manaraa.com

suggest that the hyperexcitability relies on intracortical circuits more than thalamic input (329).

Although it was not addressed in this study, synaptic inhibition between interneuron subtypes may be affected as well. In normal cortex, FS cells synaptically inhibit LTS cells, but LTS cells tend not to inhibit each other (131). The presence of fewer or "less active" FS cells might result in decreased IPSC frequency for both interneuron populations. However, if other alterations occur, such as aberrant increased LTS-LTS synaptic inhibition, the extra excitatory input observed in this cell type may be "canceled out" and not cause the expected post-synaptic depolarization. It would be interesting to study the inhibitory input to these interneuron subtypes as well for this reason. It is known that FS cell IPSCs tend to be faster and larger than those in LTS cells, and eIPSCs often require higher stimulus intensities in LTS cells (15). Furthermore, the overall frequency of mIPSCs is unchanged in this model, indicating that if probability of release is not altered, the total number of inhibitory synapses is unchanged (160). It may be difficult to accurately assess inhibitory function in the slice preparation (269), but a general comparison between inhibition and excitation within a given subtype should help address this question.

The contribution of interneurons to the development of epileptogenesis occurs in the context of increased excitation and will take a significant amount of investigation to satisfactorily resolve. At this point we suggest that as extra afferent fibers infiltrate the area adjacent to the lesion during the first week or two of development, they have fewer potential targets. To make up for this, hyperinnervation of certain cells occurs, producing

www.manaraa.com

increased excitation of pyramidal cells (375) and selectively increasing excitatory events in LTS cells (Fig. 3.4). Although current seizure treatment strategies may contradict the idea of increased inhibition as a causative epileptogenic factor, a number of studies point to the maintenance or even enhancement of inhibition in epileptogenic cortex (50; 55; 269; 293). Focusing on one specific interneuron subtype helps to address some confusion regarding how this paradox exists. In the model used for this study, overall inhibition does not show an obvious change, but selective alterations of inhibitory subtypes may permit functional consequences while still allowing for maintenance of global inhibition. Even a subtle increase in the activation of LTS interneurons could cause asymmetry in the inhibitory population in the form of increased output of vertically-oriented interneurons, which may be a contributing factor to epileptogenesis in this model.

www.manaraa.com

Table 3.1 Properties of spontaneous and miniature postsynaptic currents.

	10-90 Rise (msec)*	Decay (msec)*	Area (pA*sec)#
sEPSCs			
Control LTS	1.1 ±0.05	6.0 ±0.2	70.2 ±3.3
PMG LTS	1.0 ±0.04	5.4 ±0.2	67.2 ±4.1
Control FS	0.65 ±0.02	4.3 ±0.1	66.2 ±2.1
PMG FS	0.71 ±0.04	4.3 ±0.2	64.7 ±3.5
mEPSCs			
Control LTS	1.1 ±0.05	5.9 ±0.3	69.0 ±4.7
PMG LTS	1.1 ±0.08	5.7 ±0.4	64.0 ±5.5
Control FS	0.64 ±0.04	4.1 ±0.1	58.1 ±2.2
PMG FS	0.68 ±0.05	4.1 ±0.1	56.1 ±3.0

* Significant difference between FS and LTS populations, t-test, $p < 0.05$

Significant difference between FS and LTS for control mEPSC only, t-test, $p < 0.05$

www.manaraa.com

Figure 3.1 Excitatory post-synaptic currents in inhibitory cells. Isolated outward excitatory currents recorded in normal aCSF (sEPSCs, **A**), and in the presence of TTX (mEPSCs, **B**). Mean sEPSC frequency **(C)** and amplitude **(D)** for all interneurons in control (gray, n = 73) and PMG (black, n =59) populations. Mean mEPSC frequency **(E)** and amplitude **(F)** for all interneurons in control (gray, n = 32) and PMG (black, n = 25) populations. There were no significant differences between control and PMG populations on any measure, *t*-tests.

www.manaraa.com

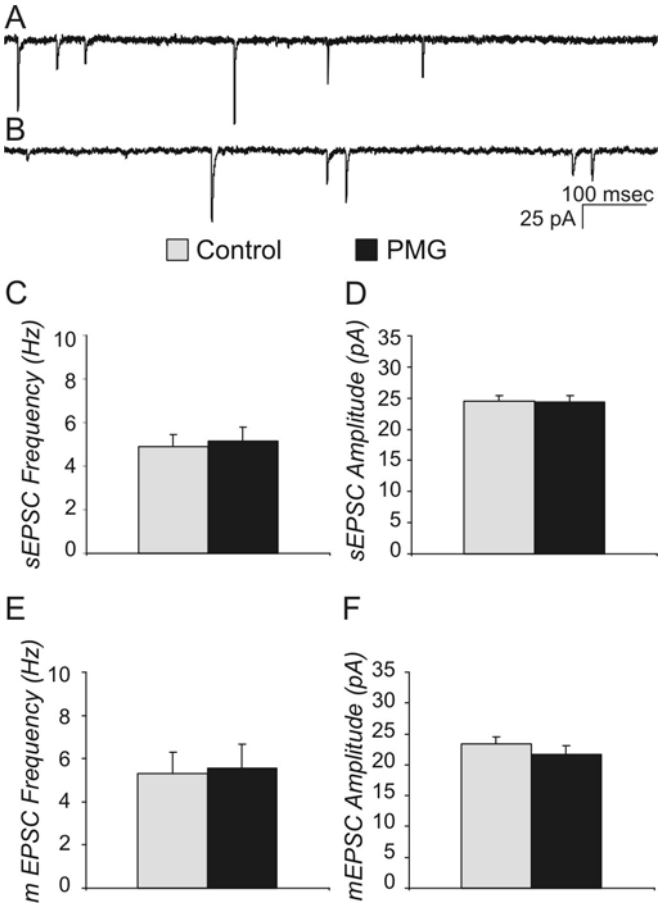

www.manaraa.com

Figure 3.2 Sample traces demonstrating typical firing patterns for LTS and FS interneurons. Responses to high (1) and low (2) current steps are shown for **(A)** control LTS, **(B)** PMG LTS, **(C)** control FS, and **(D)** PMG FS interneurons. Average action potential half-width plotted against total adaptation ratio for individual LTS (open square) and FS (filled triangle) interneurons from **(E)** control and **(F)** PMG cortex.

www.manaraa.com

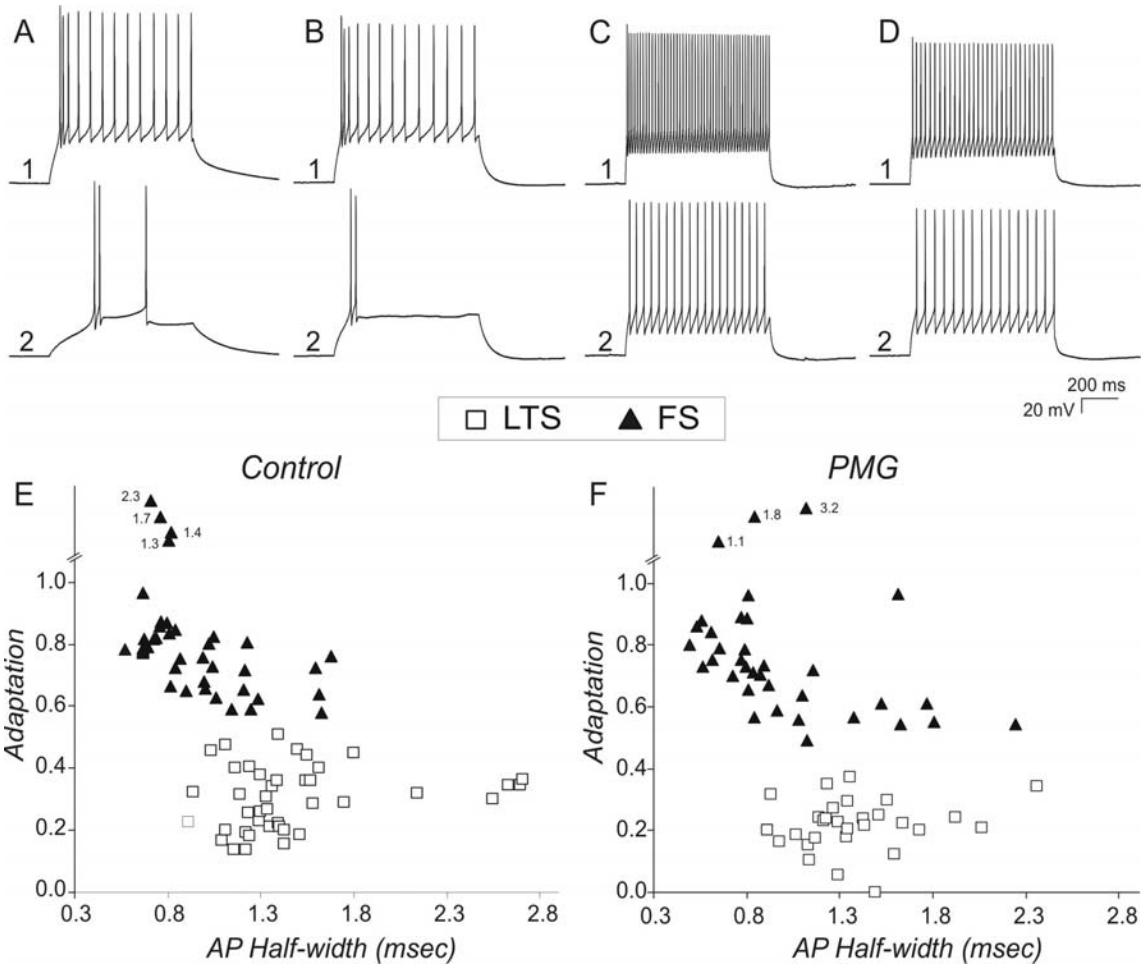

www.manaraa.com

Figure 3.3 Classification of interneuron subtypes based on intrinsic properties. FS and LTS interneurons could be differentiated from each other in control (gray, n = 39 for FS, n = 35 for LTS) and PMG (black, n = 29 for FS, n = 41 for LTS) populations based on **(A)** input resistance, **(B)** mean action potential half-width and **(C)** total adaptation. Total adaptation is the ratio of the frequency of the last two action potentials and the frequency of the first two action potentials fired in response to a 400 ms square current pulse. * = *t*-test, $p < 0.05$.

www.manaraa.com

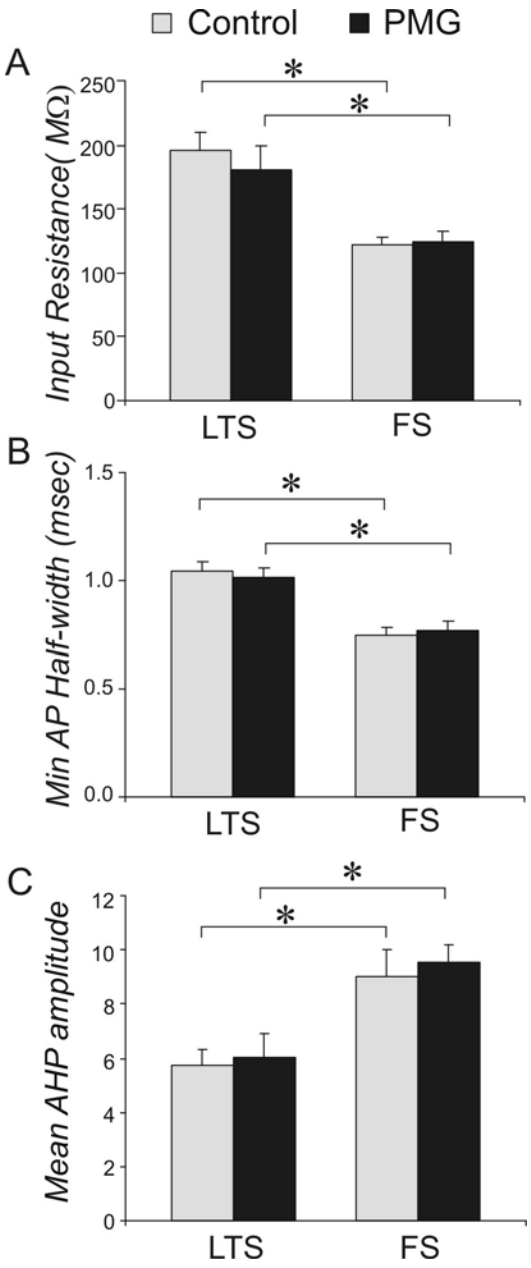

www.manaraa.com

Figure 3.4 Excitatory post-synaptic currents in FS and LTS interneurons. Sample traces showing typical mEPSCs recorded from FS interneurons in **(A)** control and **(B)** PMG, and typical mEPSCs recorded from LTS interneurons in **(C)** control and **(D)** PMG. Mean sEPSC frequency **(E)** and amplitude **(F)** measured in control (gray, n = 31 for LTS, n = 33 for FS) and PMG (black, n = 23 for LTS, n = 28 for FS) populations. Mean mEPSC frequency **(G)** and amplitude **(H)** measured in control (gray, n = 14 for LTS, n = 17 for FS) and PMG (black, n = 9 for LTS, n = 12 for FS) populations. * = *t*-test, $p < 0.05$.

www.manaraa.com

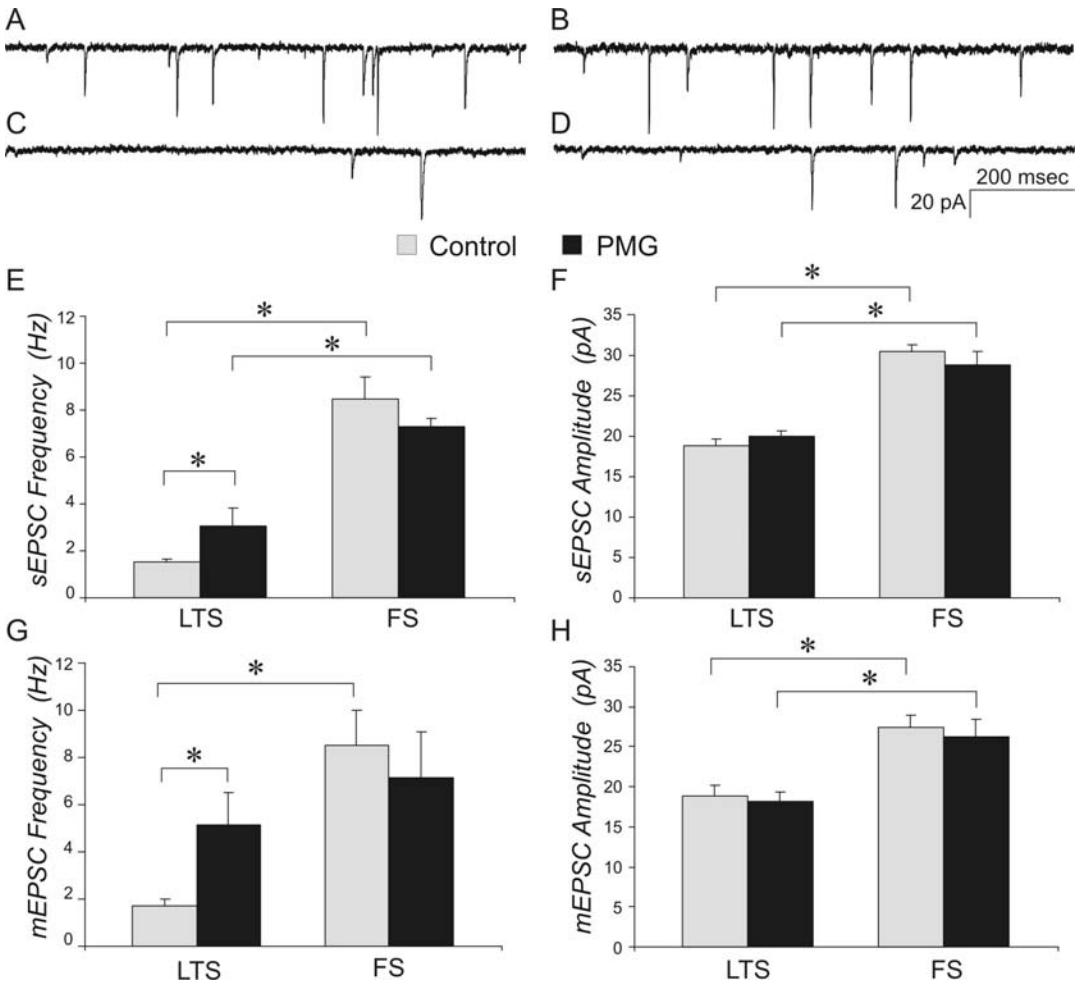

www.manaraa.com

Figure 3.5 Population distribution and IEI cumulative probability for mEPSCs. Population distribution is altered for synaptic but not intrinsic measures in LTS cells only. Shown are the distribution limits (maximum and minimum) as well as mean (x) and median (-) for each population, with AP halfwidth plotted on the left axis and mEPSC frequency plotted on the right axis. Control is shown with gray-filled symbols, PMG with black-filled symbols for **(A)** LTS interneurons and **(B)** FS interneurons. Cumulative probability of mEPSC IEI duration is altered for LTS and FS interneurons, but not for the overall interneuron population. Control is shown with gray line, PMG with black line. **(C)** Cumulative probability of IEI duration for LTS cells. For control and PMG, nine representative LTS cells were chosen from each group that had mEPSC frequencies closest to the median, and 200 events per cell were used for a total of 1800 events. Significant separation between control and PMG distributions, Kolmogorov-Smirnov test, $p < 0.05$. **(D)** Cumulative probability of IEI duration for FS cells. For control and PMG, 300 events were used from each of six representative cells, for a total of 1800 events per group. Significant separation between control and PMG distributions, Kolmogorov-Smirnov test, $p < 0.05$. **(E)** Cumulative probability of IEI duration for overall interneuron population. For control and PMG, 300 events from each of twenty three representative cells were included, for a total of 6900 events.

www.manaraa.com

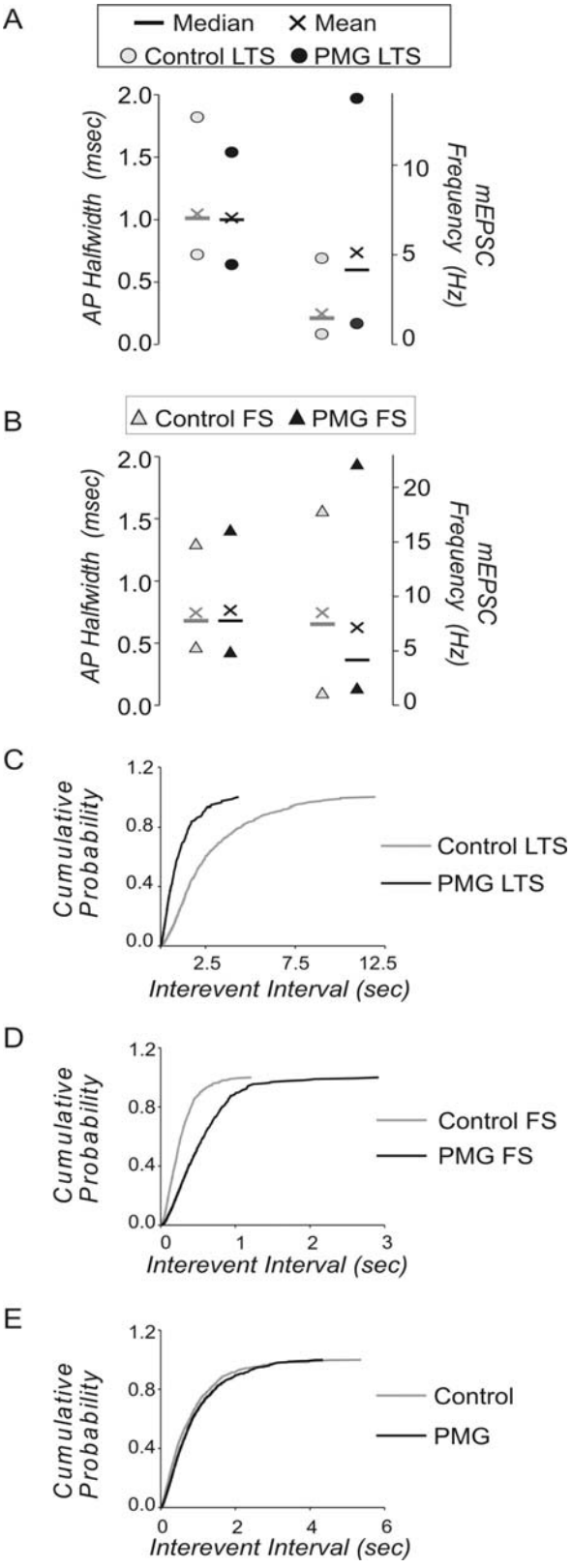

www.manaraa.com

Figure 3.6 Evoked postsynaptic currents. (A-B) Sample traces demonstrating the short-latency inward eEPSC recorded from interneurons following a series of five applied current intensities (1x, 2x, 4x, 8x, 16x threshold). **(A)** Graded responses in a representative LTS cell from control (1) and PMG (2) cortex. **(B)** Graded responses in a representative FS cell from (1) control and (2) PMG cortex. **(C)** eEPSC area and **(D)** time-to-peak for short latency inward EPSCs is shown for all five stimulus intensities in control (filled symbols, n = 22 for LTS, n = 22 for FS) and PMG (open symbols, n = 15 for LTS, n = 22 for FS). For the area measurement shown in **(C)**, both LTS populations (control and PMG) are different from both FS populations (control and PMG), repeated measures ANOVA, $p < 0.05$. For time-to-peak measurement shown in **(D)**, control and PMG LTS populations are not different from one another, control FS is different from all other cell populations, repeated measures ANOVA, $p < 0.05$. **(E-F)** Sample traces demonstrating the presence of variable-latency evoked activity in response to a low intensity stimulus (left, corresponding to 200 pA vertical measurement on scale bar) compared to a normal response to high intensity stimulation (right, corresponding to 400 pA vertical measurement on scale bar) in **(E)** a control FS cell and **(F)** a PMG FS cell. **(G)** eEPSC area for variable-latency activity is plotted against stimulus intensities for control (filled symbols, n = 22 for LTS, n = 22 for FS) and PMG (open symbols, n = 15 for LTS, n = 22 for FS) cells. For late activity, control FS, control LTS, and PMG LTS cells are not different from each other. PMG FS cells differ from both control and PMG LTS cells on this measure, repeated measures ANOVA, $p < 0.05$.

www.manaraa.com

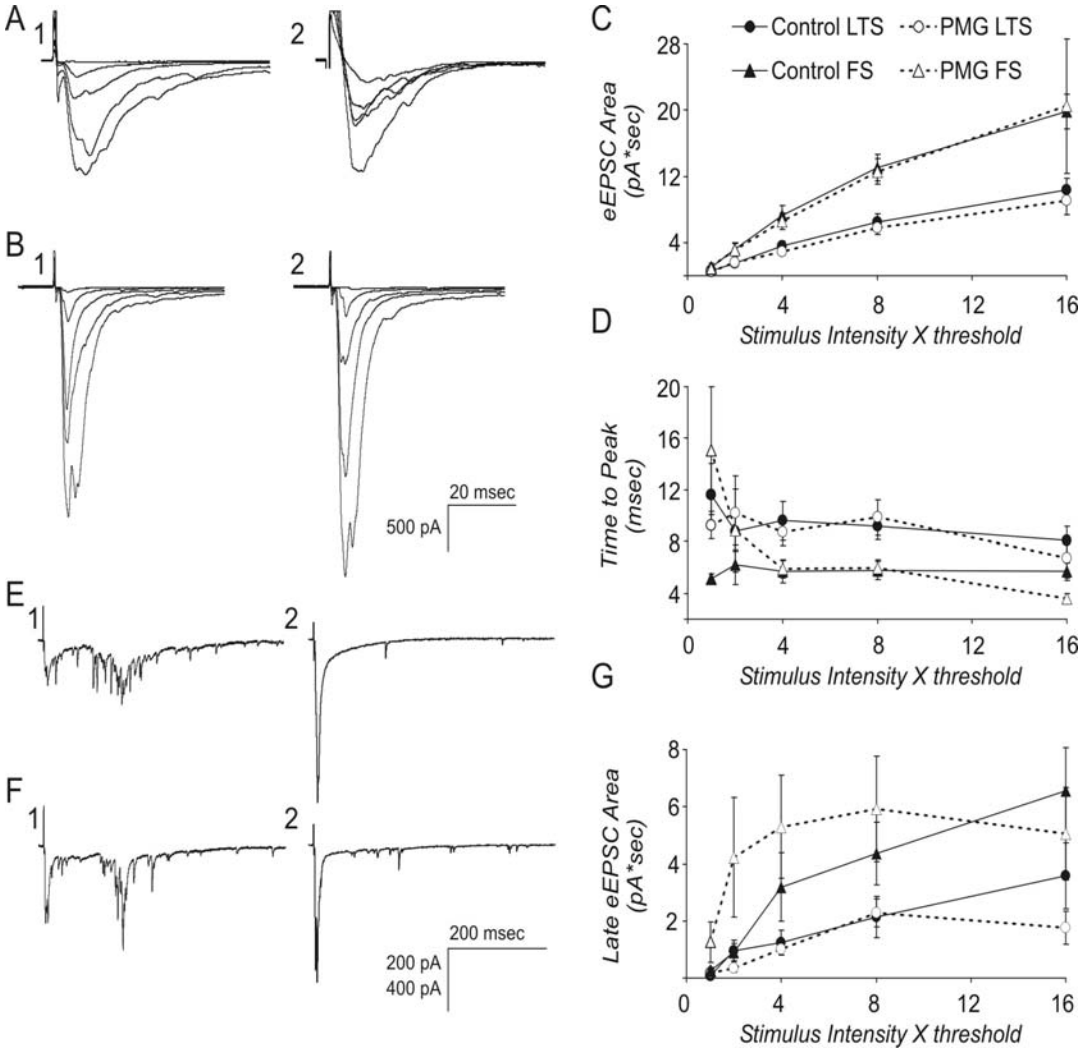

www.manaraa.com

Figure 3.7 Interneuron response to a 50Hz train of stimuli at maximal intensity (16x threshold). Sample eEPSC traces demonstrating **(A)** facilitation in control (1) and PMG (2) LTS interneurons and **(B)** depression in control (1) and PMG (2) FS interneurons. **(C)** Percent change for each eEPSC peak compared to the preceding peak (relative comparison) for FS interneurons, *t*-test, * $p < 0.05$. **(D)** Percent change for each eEPSC peak compared to the preceding peak for LTS interneurons, *t*-test, * $p < 0.05$. **(F)** Percent change in peak for each eEPSC, compared to the first eEPSC (absolute comparison) for LTS and FS interneurons from both control and PMG cortex, t-tests, all N.S. For all graphs, control LTS, filled circle, n = 21; PMG LTS, open circle, n = 15; control FS, filled triangle, n = 19; PMG FS, open triangle, n = 20.

www.manaraa.com

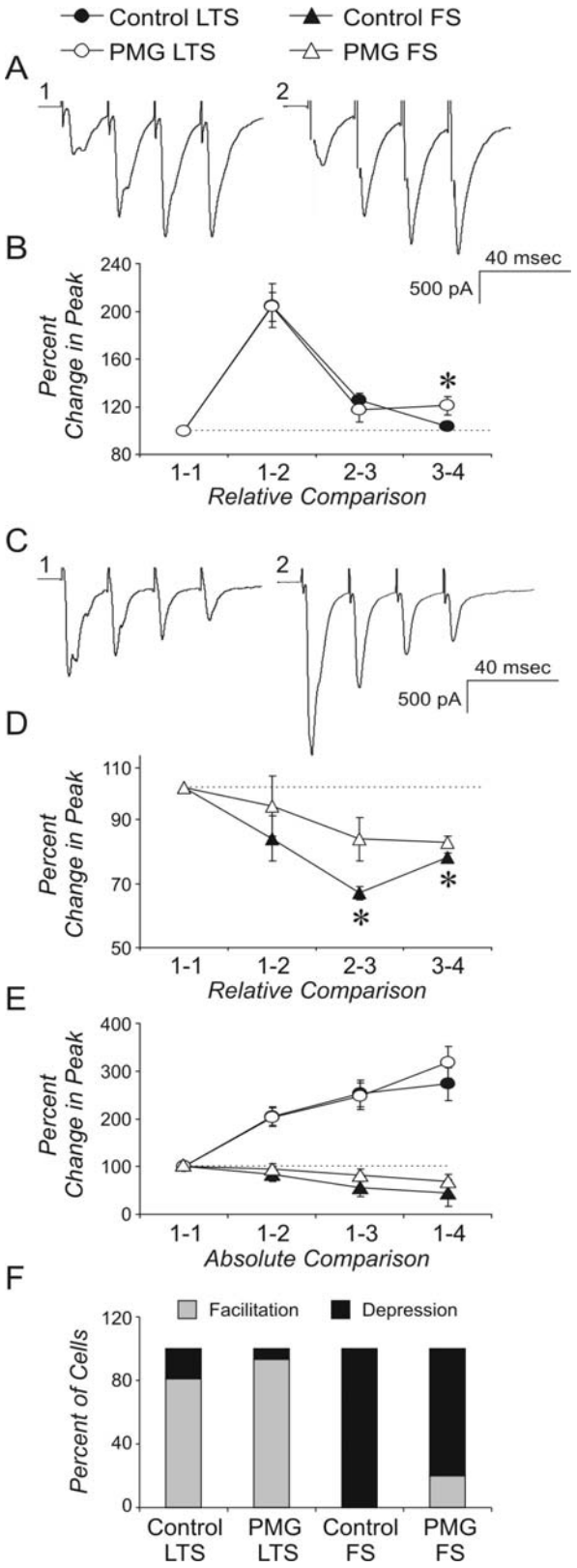

www.manaraa.com

Figure 3.8 Effect of altering aCSF Mg^{2+} and Ca^{2+} concentrations on sEPSC frequency. **(A)** Sample traces demonstrating typical sEPSCs in a control LTS interneuron, recorded in (1) normal aCSF and (2) modified (low Mg^{2+}/High Ca^{2+}) aCSF. **(B)** Typical sEPSCs recorded from a PMG LTS interneuron in (1) normal aCSF and (2) modified aCSF. **(C)** Mean percent change in sEPSC frequency for individual cells in control (gray, n = 8 for LTS, n = 6 for FS) and PMG (black, n = 5 for LTS, n = 5 for FS) populations. *t*-test, N.S.

www.manaraa.com

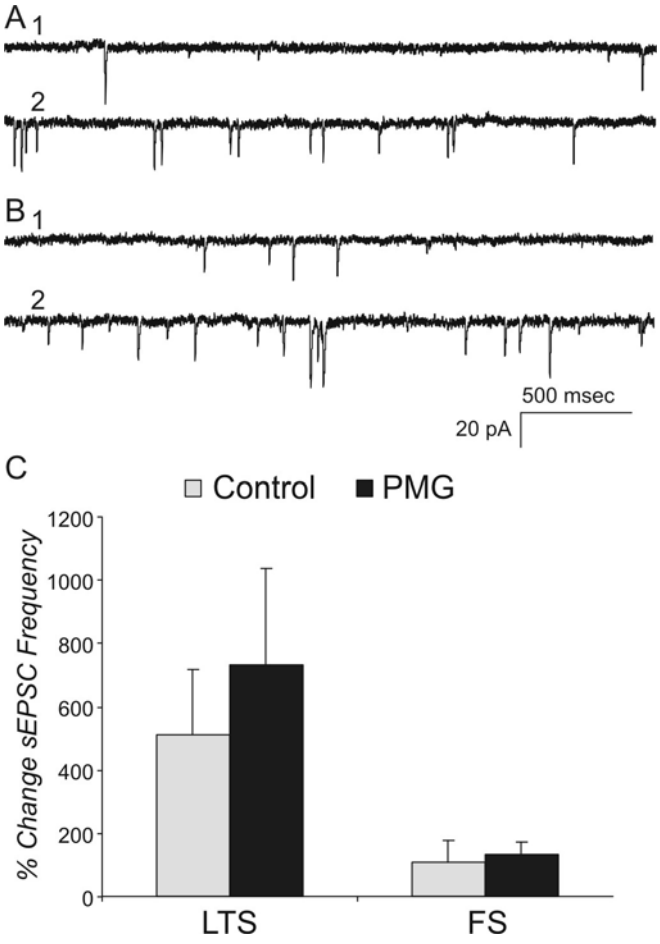

www.manaraa.com

Chapter 4

Introduction to metabotropic glutamate receptors

There are two main receptor types that mediate the cellular response to glutamate, the major excitatory neurotransmitter of the central nervous system. Fast excitatory transmission is mediated by ionotropic receptors that regulate the opening of cation-permeable channels in the neuronal membrane. The three main ionotropic receptor subtypes are: (1) the AMPA receptor, (2) the kainite receptor, and (3) the NMDA receptor. Functioning on a slower time scale, metabotropic glutamate receptors (mGluR) are coupled to G-proteins that initiate intracellular signaling cascades in response to glutamate (320). In contrast to ionotropic glutamate receptors, mGluRs are typically considered to have modulatory roles within the neocortex. As more is learned about these receptors and their physiological functions, it is increasingly possible to assign them potential roles in pathological processes, including epilepsy. The purpose of this chapter is to: (1) introduce the characteristics and developmental expression patterns of mGluRs, (2) establish the utility of mGluRs and their ligands for the pharmacological manipulation of specific interneuron subtypes, and (3) review their current and potential associations with disease states, including epilepsy.

www.manaraa.com

4.1 Classification and function of mGluRs

Eight different subtypes of mGluRs have been identified and segregated into three main groups based on amino acid sequence and mechanism of intracellular signal transduction. Group I contains mGluR1 and mGluR5, group II contains mGluR2 and mGluR3, and group III contains mGluR4, mGluR6, mGluR7 and mGluR8 (77; 261; 339). The majority of group I receptors are located postsynaptically (58; 204), while most of the group II and III receptors are located on the presynaptic membrane (58; 302). As group I mGluRs are of particular interest to the experiments described in the next chapter, the remainder of this introduction will focus on those receptors.

The signaling mechanism of group I mGluRs involves activation of phospholipase C and subsequent phosphoinositide hydrolysis, ultimately resulting in the production of diacylglycerol and release of calcium from intracellular stores (261). There are differences between the mGluR1 and mGluR5 subtypes with regard to calcium increase and oscillations. In transfected cell lines, glutamate application causes intracellular calcium oscillations following activation of mGluR5, but not mGluR1 (168). The distinction appears to be due to PKC phosphorylation of a threonine residue only found on the mGlu5 receptor (168). In immature rat neocortex, agonist application induces simple, non-oscillatory calcium responses from mGluR1 activation, but it causes oscillations through the mGlu5 receptor (113). However, in striatal cholinergic interneurons, which express both mGluR1 and mGluR5, only after blocking mGluR5 is oscillatory behavior observed (43). The mechanism for these oscillations appears to involve both tyrosine kinase and L-type Ca^{2+} channels (43). It appears that both subtypes

www.manaraa.com

of receptor are capable of inducing membrane oscillations, but this may depend on the cell type, source of calcium, and type of agonist used to elicit the response.

4.2 Ligands for mGluRs

4.2.1 Group I agonists

There are several known non-selective agonists to the group I mGluRs, such as quisqualate and, of course, glutamate (280). In the 1980s and early 1990s, the first selective agonist for mGluRs was identified. 1S,3R-1-aminocyclopentane-trans-1,3-dicarboxylic acid (ACPD) was determined to activate mGluRs at concentrations that do not affect the ionotropic receptors (EC_{50} in the range of 10-50 μM, 305). Since the discovery of ACPD, a number of compounds with increased selectivity have been identified or synthesized and are commonly used to distinguish the effects of mGluR subtypes.

The phenylglycine derivative (S)-3,5-dihydroxyphenylglycine (DHPG) is the first agent to demonstrate selective and potent group I mGluR agonist activity (154; 305; 310). DHPG does not affect the level of cAMP in neonatal or adult rat brain, even with DHPG at a concentration of 1 mM (304). This indicates that it lacks activity at mGluRs that make use of the cAMP second messenger system, namely group II and group III (304). In oocytes expressing mGluR1, the experimentally determined EC_{50} for DHPG (60μM) was lower than that of ACPD, but higher than that needed to activate group I mGluRs in rat brain tissue (154). In rat, the EC_{50} for DHPG ranges from 7 μM for

www.manaraa.com

neonatal brain slices to 28 μM in adults (304). DHPG is currently the drug of choice for studies in which selective activation of group I mGluRs is necessary. For the experiments in Chapter 5, DHPG was used at a concentration of 10 μM.

Currently, there is no specific agonist for mGluR1, but (RS)-2-Chloro-5-Hydroxyphenylglycine (CHPG), has recently been synthesized as a selective agonist for the mGlu5 receptor (95). As evidence of this, CHPG-induced CREB phosphorylation and its downstream effects were reversed by specific mGluR5 antagonism but were unaffected by antagonists to mGluR1 (208). CHPG has also been shown to activate mGluR5 *in vivo*, and again this response is selectively reduced by antagonists specific for mGluR5 but not mGluR1 (295). The hippocampal cellular response to CHPG activation of mGluR5 involves modulation of NMDA receptor- induced depolarization (95), but this is not reflected in the present study, as NMDA receptors were blocked. For the experiments in the following chapter, CHPG was used at a concentration equal to its EC_{50}, 750 μM (95).

4.2.2 Group I antagonists

There are a number of well-characterized and selective antagonists for the group I mGluRs. The mGluR1-specific antagonist used for the experiments described in the next chapter is 1-Aminoindan-1,5-dicarboxylic Acid (AIDA). AIDA is a potent, selective and competitive mGluR1α antagonist (254). In cells transfected with mGluR1α, AIDA was able to reduce glutamate-induced phosphoinositide synthesis, successfully inhibiting the activity of the mGlu1 receptor, while having a much smaller effect on the activity of

www.manaraa.com

mGluR5 (231). The range of EC_{50} values spans from 7 μM to 214 μM, though this is likely due to the variety of both the experimental conditions and the agonists used (231). At very high concentrations (1mM), weak agonist activity on the mGlu2 receptor and weak antagonism of the ACPD effect on mGlu5a receptors were observed (305). The concentration of AIDA needed to achieve these responses, however, was greater than three times the concentration used for the experiments in the following chapter. Of the other compounds that have been identified as mGluR1α-specific antagonists, many have activity at other receptors, depending on the concentrations used (305). Comparatively, AIDA must be applied at a concentration many-fold higher than its EC_{50} to promiscuously activate receptors besides mGluR1.

Finally, 2-methyl-6-(phenylethynyl)-pyridine (MPEP) is the selective mGluR5 antagonist used for these experiments (305). It is a non-competitive antagonist that binds at a novel allosteric site (127). MPEP has been shown to inhibit phosphoinositide hydrolysis in cells expressing the human mGluR5 (245), neonatal rat brain slices (127). It also reduces DHPG-induced excitation, recorded *in vivo* from adult rat hippocampus (127). In cells expressing rat mGluR5, MPEP also demonstrated inverse agonist activity (245). Specific residues in transmembrane domains III and VII are necessary for the selective binding of MPEP to mGluR5 (245). The proposed mechanism of action of MPEP is stabilization of the inactive conformation of the mGluR5 receptor within the membrane (191). Recently, electrophysiological effects of MPEP on ionotropic glutamate receptors have been reported (191). However, for the experiments discussed

www.manaraa.com

here, AMPA and NMDA receptors were pharmacologically blocked, allowing MPEP to effectively discriminate between mGluR1 and mGluR5.

4.3 Development and expression of group I mGluRs

The presence of group I mGluRs has been demonstrated in neocortex through *in situ* hybridization (314) and immunohistochemistry (198; 281). Both immunogold and immunohistochemical labeling indicate that the group I receptors are located primarily on postsynaptic elements (313; 315), but largely outside the synaptic specialization (24; 242). Various forms of mGluR1 are present in cell bodies throughout the layers of neocortex, sometimes with region-specific splice variant expression (107). Furthermore, in neocortex, mGluR1 immunostaining is present in interneurons only (256). Double-labeling studies indicate that mGluR1 colocalizes with SS and VIP, but not PV, demonstrating that expression of the mGlu1 receptor is restricted further to a specific interneuron subpopulation (24; 326). This is supported by an in-situ hybridization study that shows mGluR1 mRNA in interneurons that contain SS but not PV (177). Furthermore, mGluR5 mRNA was shown to be present in projection neurons and some interneurons but was almost completely absent from SS interneurons (177). It has also been demonstrated in striatum that the expression of mGluR5 mRNA is specifically absent from SS and cholinergic interneurons (343). This specificity is employed in the following chapter, as mGluR1 agonists are used to selectively activate the SS/LTS interneuron type.

www.manaraa.com

Each mGluR has a different, dynamic pattern of expression throughout development. In the rat, mGluR5 has its highest transcript expression in utero and during the first days of postnatal life, while mGluR1 mRNA gradually increases to adult levels over the first three postnatal weeks (59). In the adult, less than ten percent of all neuronal cells express mGluR1, and most are scattered in cortical layers IV-VI (314). This pattern of mGluR1 expression can be recognized as early as P7 (59) and is relatively established by P11 (314), although some increase still occurs until P21 (59). In a complementary immunohistochemical study, the prevalence of the mGluR1 protein increases postnatally, so that by P15, interneurons with bipolar or multipolar morphology express it in all layers of neocortex (198). Conversely, there is strong mGluR5 expression from P0 to P2. After one week, mGluR5 can be observed in the neuropil, particularly in layer IV barrel hollows until P21, when all layers approached the same level of neuropil labeling (198). The experiments in chapter 5 are performed during the third postnatal week, and both mGluR1 and mGluR5 should be approaching mature distributions at that time.

4.4 Potential role for group I mGluRs in pathological states

With regard to disease processes, activation of group I mGluRs tends to be detrimental to the nervous system, while activation of group II and III is considered to be neuroprotective (116; 163; 238; 333). Different studies have implicated the group I mGluRs in neurological injury and a variety of disease states, such as Alzheimer disease, Huntington disease, Parkinson disease, Down syndrome and epilepsy (11; 40; 45; 58; 234; 244). For epilepsy in particular, analyses of both human tissue samples and

www.manaraa.com

experimental models have demonstrated an alteration of mGluR expression (96). For example, in two animal models of epilepsy, as well as in human cases, there is a selective upregulation of mRNA and protein expression of the mGlu1 receptor subtype (40). Immunohistochemistry shows an upregulation of both mGluR1 and mGluR5 in patients with glioneuronal tumors and intractable epilepsy (11). Patients with Taylor-type focal cortical dysplasia (8) and temporal lobe epilepsy (40; 241) also show an upregulation of one or both group I mGluRs. Much attention has recently been placed on the mGlu5 receptor as a potential contributor to the pathophysiology of Fragile X syndrome, a condition that includes, among other symptoms, seizures and abnormal neuronal morphology (58). The ibotenate injection model, that produces a cortical injury similar to the freeze-lesion used for these studies, demonstrates a significant increase in mGluR5 expression in the contralateral hippocampus one week post-injection (233). Group I receptors are also increased in the uninjured CA1 and DG regions of the hippocampal formation in these animals (233). Furthermore, as activation of group I receptors has a proconvulsant effect (229), pharmacological agents that antagonize these receptors are being identified as potential treatment options for some of these conditions (247).

A number of studies that have investigated the role of group I mGluR activation with regard to epileptiform activity have done so in the presence of GABA antagonists, using disinhibition to induce hyperexcitability (221; 222; 298; 345). One advantage of this inhibitory blockade is that it facilitates the observation of mGluR-mediated pyramidal cell activation. The idea of using group I mGluR antagonists as anticonvulsants would, in this paradigm, depend on their ability to reduce the excitatory

www.manaraa.com

or bursting activity in the pyramidal cells (222). However, blocking GABA receptors also disallows evaluation of the potential mGluR-mediated interneuron contribution to epileptogenesis. It is necessary to address this possibility for several reasons. Firstly, the SS/LTS interneuron subtype that expresses mGluR1 receptors (177; 326) also receives extra excitatory input (Chapter 3) and has increased action potential firing capability (Chapter 2) in this model. This increased input has the potential to translate into enhanced output from this specific group of interneurons. This is important because, as discussed in chapter 1, LTS/SS cells have a vertical axon distribution that can span several cortical layers (173; 174) and they function within a coordinated network to generate synchronous activity in cortex (197). Enhanced cortical synchrony could then promote epileptiform activity. The following experiments employ the specific agonists and antagonists discussed in this chapter to selectively manipulate the activity of LTS/SS interneurons. The goal of this study, especially in light of the findings from chapters 2 and 3, is to determine whether the output of LTS/SS interneurons is augmented. This would provide a potential mechanism for columnar synchrony and the impetus for future studies on the network properties of these cells.

www.manaraa.com

Chapter 5

Enhanced Responsiveness of Interneurons to Group I Metabotropic Glutamate Receptors in Malformed Epileptogenic Cortex

Introduction

Epilepsy caused by developmental cortical malformations, such as polymicrogyria (52; 70; 88; 140), produces seizures that are difficult to treat (188; 246). In this study we employ a rat model that closely approximates the human condition with regard to both histopathology (99; 100) and hyperexcitability (156; 157). Previous work with this model has suggested that neurons adjacent to the malformed region are hyperinnervated by excitatory afferents (160; 375). Inhibitory as well as pyramidal neurons receive this increased synaptic input (160).

Interneurons are affected in this model, but inhibition does not show a clear decrease when measured as a whole (269). However, immunohistochemical studies in this model have demonstrated a differential effect on inhibitory interneurons, based on subtype. A down-regulation of parvalbumin (PV) staining has been demonstrated (288), but the number of calbindin (CB)-immunopositive interneurons has been shown to increase (308). These two markers co-localize, but the populations are not completely overlapping, and this appears to be specific to layer II/III (184). Furthermore, the CB cell population contains a separate overlap with the SS cells (174). The number of SS

www.manaraa.com

interneurons remains unchanged at the age of hyperexcitability onset (250). These results indicate that either the number of inhibitory cells is altered in this model, or the number of cells is the same but they have altered protein expression and enhanced or diminished functional capability.

With regard to function, the subset of SS interneurons is of particular interest for this study. SS interneurons are part of the class of bipolar, vertically-oriented, low-threshold-spiking (LTS) cells (60; 170; 172). They also express the mGlu1 receptor, a characteristic they share with at least one other subtype of bipolar interneurons, those staining for vasoactive intestinal peptide (326). Bipolar cells normally provide a relatively weak, modulatory inhibition. In contrast, the horizontally-oriented population of interneurons is made up of PV-immunopositive (170) fast-spiking (FS) cells (170; 172) that do not express mGluR1 (326). The basket cell morphology of FS cells permits them to provide powerful inhibition at the cell body or axon initial segment.

If one or more interneuron subtypes have diminished efficacy due to low cell number or activity, the observed maintenance of global inhibition could result from the compensatory over-functioning of another type. Here, we investigated whether the output of bipolar interneurons is enhanced in PMG cortex, specifically within layer V. These cells are orientated to have contacts within several layers of the same cortical column. Increased efficacy may give them the potential to create columnar synchrony, and thereby promote epileptogenesis. Selective activation of bipolar interneurons, including SS/LTS cells, by group I mGluR agonists has previously been shown (73; 373).

www.manaraa.com

Using various ligands for group I mGluRs, these studies evaluate group I mGluR-induced output by recording sIPSCs in layer V pyramidal cells.

Materials and Methods

Freeze lesion surgery

These experiments were done in accordance with the policies and guidelines of Virginia Commonwealth University regarding care and use of animals. Freeze lesions were made as previously described (375). Rat pups aged postnatal day (P)1 were anesthetized with hypothermia by placing them in ice for 4-5 minutes. Using an anterior-posterior incision, the skull was exposed, and a freeze probe consisting of a copper bar with a 2 by 5 mm rectangular tip cooled to -50° C was applied to the skull over the left somatosensory cortex for 5 seconds. The skin was sutured, the pup warmed and returned to the dam.

In vitro slice preparation

Lesioned animals and unoperated control rats aged P12-17 were anesthetized with isoflurane and decapitated. The brain was removed and immediately placed into cold (4°C) sucrose slicing solution containing (in mM): 2.5 KCl, 1.25 NaH_2PO_4, 10 $MgCl_2$, 0.5 $CaCl_2$, 26$NaHCO_3$, 11 glucose, and 234 sucrose. Slices 300 µm thick were cut on a vibratome and transferred to a holding chamber filled with 'normal' artificial cerebrospinal fluid (aCSF) containing (in mM): 126 NaCl, 5 KCl, 1.25 NaH_2PO_4, 2

www.manaraa.com

$MgCl_2$, 2 $CaCl_2$, 26 $NaHCO_3$, and 10 glucose, 285-290 mOsm. All solutions were infused with 95%O_2/5%CO_2, maintaining pH at 7.4. Sections were maintained at 34°C for 45 minutes and at room temperature thereafter. To isolate layer V interneurons and eliminate the influence of other cortical layers, horizontal slices were used for all recordings from pyramidal neurons in this study. Recordings from interneurons were made within layer V in coronal slices. In all cases, recordings were made at 30-32°C, in normal aCSF containing dinitroquinoxaline [(6,7)],2,3(1H,4H)-dione (DNQX, 20 μM) and D,L-2-amino-5-phosphonopentanoic acid (APV, 100 μM) to block AMPA and NMDA receptors, respectively.

Electrophysiology

Whole cell patch-clamp recordings from layer V pyramidal neurons (Fig 1) in somatosensory cortex were obtained using glass micropipettes (2-5 MΩ, Garner glass Co., Claremont, CA) filled with (in mM): 70 K-gluconate, 70KCl, 10 Hepes, 4 EGTA, 2 NaCl, 4 Na-ATP, 0.3 Na-GTP, 275-285 mOsm, E_{Cl^-} = -15 mV, pH 7.3. Recordings were made from an area of cortex 0.5-1.5 mm on either side of the lesion and from homotopic cortex in controls. Spontaneous inhibitory postsynaptic currents (sIPSCs) were recorded in isolation in voltage clamp mode at V_h = -70 mV (Fig. 1B). Current clamp recordings were made from interneurons using glass pipettes as described above, that contained (in mM): 130 K-gluconate, 10 Hepes, 11 EGTA, 2 MgCl2*6H2O, 2 CaCl2*2H2O, 4 Na-ATP, 0.2 Na-GTP, 275-285 mOsm.

www.manaraa.com

Recordings were made with a Multiclamp-700A amplifier (Axon Instruments), and only recordings with an access resistance less than 23 MΩ were accepted for analysis. Data was digitized online (20 kHz) using software from Axon Instruments. Data analysis for voltage clamp experiments was performed using MiniAnalysis (Synaptosoft). Amplitude measurements were made on 'Type I' events, which are isolated (no overlap with adjacent events) currents. Since the max decay time was ~20 msec, events having an interevent interval of 40 msec or more were identified as Type I. Some intrinsic parameters were measured using Clampfit (Axon Instruments). Measurements are reported as means ± SEM. Student's *t*-test with or without Bonferroni correction (as indicated), as well as one-way and two-way ANOVAs were used to test for significance, $p < 0.05$ was considered to be significant.

Pharmacological agents and application

Ligands for group I mGluRs were applied using a four-barrel local perfusion system. The first recording was made with normal aCSF flowing in the local perfusion line. A second data file was collected during which the local perfusion was switched to aCSF containing one or more drugs active at group I mGluRs. This recording was continued for ~1 minute after the drug application began, during which time the response stabilized (Fig 2A). After this period, separate data files were collected for analysis. The pharmacological agents used in the local perfusion system were as follows: S-3,5-dihydroxyphenylglycine hydrate (DHPG, group I mGluR agonist, 10 μM); 6-methyl-2-(phenylethynyl) pyridine hydrochloride (MPEP, mGluR5-specific antagonist, 10 μM); 1-

www.manaraa.com

amino-2,3-dihydro-1H-indene-1,5-dicarboxylic acid (AIDA, mGluR1-specific antagonist; 30 μM, 100 μM, 300 μM); (RS)-2-chloro-5-hydroxyphenylglycine (CHPG, mGluR5-specific agonist, 750 μM). For some experiments, MPEP and AIDA were applied in the bathing solution at concentrations specified above. For interneuron recordings, MPEP (10 μM) was included in the bathing solution and DHPG was applied at a variety of concentrations (1 μM, 10 μM, 100 μM, 200 μM).

Results

Recordings were made from a total of 93 control and 83 PMG pyramidal neurons. Overall health of the recorded neurons was consistent across both cell populations, based on intrinsic properties of resting membrane potential, input resistance, membrane time constant, and action potential amplitude (Table 5.1). All recordings were made at a holding potential of -70 mV in aCSF containing APV (100 μM) and DNQX (20 μM), limiting these measurements to monosynaptic IPSCs that could be abolished with application of the $GABA_A$ antagonist, bicuculline (10 μM, Fig. 5.1B).

DHPG application increases sIPSC frequency

The mean sIPSC frequency recorded in normal aCSF was not different between control (5.3 ±0.3 Hz) and PMG (4.9 ±0.7 Hz) populations, nor was there any difference in the amplitude of isolated (Type I) events (Fig. 5.2). To activate group I mGluRs, DHPG (10 μM) was applied with a local perfusion system that bathed ~300 μm around the recorded cell. As expected, this caused an increase in sIPSC frequency in both

www.manaraa.com

control and PMG neurons (Fig. 5.2). Although both control and PMG cells responded to DHPG, they did not respond equally. The mean percent increase in frequency, calculated in individual cells, was much greater in PMG compared to control cortex (354 ±71 versus 195 ±43% for PMG versus control cells, respectively, *t*-test, $p<0.05$, Fig. 5.2F). While most cells showed an increase in sIPSC frequency after DHPG application, a slight decrease in sIPSC frequency was observed in a small number of cells in both control (4 cells) and PMG (2 cells) cortex (Fig. 5.2G). Even when cells that did not respond to DHPG are excluded, there is still a clear difference in the median values for PMG compared to control (horizontal bars, Fig. 5.2G). The sIPSC mean amplitude (Type I events) was unaffected by drug application for both control and PMG groups (Fig. 5.2E). Here for DHPG and in all drug application cases, the sIPSC rise time and decay time were unaffected by the drug application (*t*-tests, N.S.). In control cells for aCSF versus DHPG, mean rise times were 2.3 ±0.05 versus 2.4 ±0.04 ms, and mean decay times were 15.5 ±0.3 versus 14.9 ±0.2 ms. In PMG cells for aCSF versus DHPG, mean rise times were 2.4 ±0.1 versus 2.4 ±0.1 ms, and mean decay times were 16.0 ±0.2 versus 14.5 ±0.3 ms. There was also no significant difference between control and PMG groups for these measures (*t*-test, N.S.).

Immunohistochemical studies indicate that mGlu1 receptors are located on SS-positive, LTS-type interneurons (326). For this reason we expected that the effect of DHPG was due to interneuron activation by mGluR1s. To confirm this, the mGluR1-specific antagonist AIDA was added to the local application of DHPG. At 300 μM,

www.manaraa.com

AIDA significantly reduced the DHPG effect in both control and PMG cortex (Fig. 5.2B-D).

Effect of DHPG with antagonists in the bath

To further examine whether DHPG was acting at mGluR1 or mGluR5, selective antagonists for each were applied in the bathing medium. It was reported previously that baseline glutamate levels can activate group I mGluRs in the same cell population we studied here (16). However, in the presence of APV and DNQX used for these experiments, sIPSC frequency and amplitude were not changed within the control or PMG groups when mGluR antagonists were applied (MPEP, 10μM, AIDA, 100 μM or 300 μM, Fig. 5.3). When control and PMG groups were compared under these conditions, only when MPEP was included in the bathing medium was there a difference. In this case, the sIPSC frequency was significantly less in PMG cells compared to control (Fig. 5.3C, *t*-test, $p<0.05$).

With the mGluR5 antagonist MPEP (10 μM) in the bathing medium, local DHPG application still increased sIPSC frequency in both control and PMG cells, as expected (Fig. 5.4). The percent increase in PMG cortex was not different from control (233 ±78 and 158 ±45% for 21 PMG and 21 control cells, respectively, *t*-test, N.S.). Under these conditions, adding AIDA (300 μM) to the local perfusion of DHPG returned the sIPSC frequency to near-baseline levels for both control and PMG cells (Fig. 5.4).

With the mGluR1 antagonist, AIDA (100 μM) in the bathing medium, control cells showed no change in sIPSC frequency during application of DHPG (Fig. 5.5A-C).

www.manaraa.com

Surprisingly, for PMG cells under the same conditions, DHPG still caused a large increase in sIPSC frequency (from 3.3 ±0.7 to 8.8 ±1.4 Hz, *t*-test, $p<0.05$, Fig. 5.5C,E). The sIPSC frequency was reduced nearly back to the baseline value by subsequent MPEP application (10 μM, Fig. 5.5C). This effect was even more convincing when 300 μM AIDA was included in the bathing medium (Fig. 5.5D,F). In both cases of 100 and 300 μM AIDA in the bath, the percent change in sIPSC frequency after addition of DHPG was significantly greater in PMG compared to control cells (Fig. 5.5E,F, *t*-tests, $p<0.05$).

CHPG: mGluR5 selective agonist

To confirm that mGlu5 receptors activate interneurons in PMG, but not control cortex, the mGluR5 specific agonist CHPG was applied through the local perfusion system, with normal aCSF bathing medium. In PMG cortex, CHPG (750 μM) caused a significant increase in sIPSC frequency that was reversed by MPEP (10 μM) application (Fig. 5.6A). CHPG did not affect sIPSC frequency in control cortex (Fig. 5.6B). Similar to the results for DHPG, sIPSC amplitude, rise time and decay time were also unaffected by CHPG application. In control cells for aCSF versus CHPG, mean amplitudes were 25.3 ±3.0 versus 20.8 ±1.3 pA, mean rise times were 2.3 ±0.03 versus 2.4 ±0.1 ms, and mean decay times were 14.0 ±1.1 versus 13.2 ±1.1 ms. In PMG cells for aCSF versus CHPG, mean amplitudes were 33.1 ±2.9 versus 36.85 ±11.3 pA, mean rise times were 2.2 ±0.1 versus 2.2 ±0.1 ms, and mean decay times were 14.6 ±0.7 versus 14.3 ±1.0 ms.

www.manaraa.com

DHPG activates LTS but not FS cells

Although previous studies have shown that group I mGluR agonists activate LTS but not FS cells (27), it was necessary to confirm that this selectivity is not altered in PMG cortex. To verify this, current clamp recordings were made from interneurons before and during DHPG application in control and PMG cortex. Interneurons were initially selected based on their appearance under DIC optics. Cells having an oval or elongated soma and appearing to have thick processes directed toward both the pia and the subcortical white matter were suspected LTS neurons. Cells having a small, round soma with multiple processes and/or a thin dendrite directed toward the pial surface were suspected FS neurons. Interneuron subtype was confirmed based on the action potential firing pattern. As previously described, FS interneurons had a brief action potential (<1 msec), and showed little adaptation during a 400 msec depolarizing current pulse injection (Fig. 5.7B). In contrast, LTS interneurons had longer action potentials and fired at high frequencies initially, with slowing frequency during a long current injection (Fig. 5.7A). These cells showed the same previously reported difference in the peak of the afterhyperpolarizations (AHP) for a long spike train, namely that the first AHP was more hyperpolarized than the rest (28). Cells identified as LTS in control cortex responded to DHPG application with abrupt depolarization, a noticeable increase in baseline noise and, in some cells, action potential firing (Fig. 5.7A, C). The same was true in PMG cortex (Fig. 5.7B). In contrast, FS cells in both control and PMG cortex demonstrated only slight depolarization, no increase in noise and no action potential firing in response to DHPG (Fig. 5.7B,C).

www.manaraa.com

Although these results suggest that the increased response of PMG cells to DHPG was due in part to mGluR5 receptors, it could also be caused by an increased sensitivity of mGluR1 receptors on PMG interneurons. To test this idea, the magnitude of the DHPG-elicited depolarization of interneurons was examined during application of varying concentrations of DHPG. We measured both the peak and the 'steady-state' (observed after >1 min of application) depolarization. LTS cells responded to increasing concentrations of DHPG with increasingly larger depolarizations, reaching the maximum response at 100 μM. In addition, membrane oscillations were induced in the majority of LTS interneurons in both control and PMG cortex, with concentrations of DHPG of 10μM and greater (80% of 15 control and 89% of 19 PMG cells). The dose-response curves of the peak and steady-state membrane potential change suggest that there was no change in the sensitivity of mGlu1 receptors in PMG cortex relative to control cortex, for either LTS or FS interneurons (Fig. 5.7D, E). A two-way ANOVA showed a significant difference for concentration in LTS cells, but no difference between control and PMG populations and no interaction between concentration and subject group ($p < 0.05$ was used for significance). For FS interneurons, the two-way ANOVA showed no significant differences for either concentration or subject group or for interaction between these two.

Discussion

These data show that group I mGluRs activate inhibitory cells with greater efficacy in PMG cortex than in control and that this increase is due to mGluR5 in addition to mGluR1. The mGluR5s are either not present or not functional on

www.manaraa.com

interneurons in control neocortex. The LTS but not FS interneurons mediate this response in both control and PMG cortex, with no change in mGluR1 sensitivity. This is the first demonstration of a change in mGluR in this model, although increased mGluR have been shown in dysplastic cortex from epilepsy patients (8; 11; 58).

The DHPG-induced increase in sIPSC frequency was nearly twice as large in PMG as in control cortex when ionotropic glutamate receptors were blocked. Based on current treatment strategies for epilepsy that involve augmentation of GABAergic activity in the cortex, we would expect increased inhibition to reduce seizure activity and counteract hyperexcitability. However, increased susceptibility to seizures seen in some animal strains has actually been associated with enhanced inhibition (183; 338). Furthermore, some antiepileptic drugs have even been shown to exacerbate seizure activity, one of them through activation of GABA receptors (196). In addition, interneurons do not contribute equally to inhibitory function, as varying morphologies, connectivity, and target domains dictate the type of influence interneurons have in the cortex (28; 131; 173; 174). Whether or not the functional alteration promotes seizure activity will likely depend on the type of interneuron that is affected (36; 183). Our data suggest that release of glutamate that reaches extrasynaptic receptors will cause a selective increase in LTS interneuron activation. Activation of LTS neurons through group I mGluR has previously been shown to cause synchronous oscillations in surrounding neocortical pyramidal neurons (27). Small changes in the level of mGluR activation can also significantly affect thalamocortical rhythms (102). We hypothesize that the increase in mGluR5 function in PMG cortex will increase synchronization of

www.manaraa.com

pyramidal neurons under conditions of high levels of excitatory activity and thereby actually promote epileptiform activity. Tests of this hypothesis are currently underway.

The degree of control of inhibitory neurons exerted by group I mGluRs will depend on the overall level of excitation in the neocortex. In this study, none of the group I mGluR antagonists decreased sIPSC frequency in the absence of applied agonists for control or PMG (Fig. 5.3), indicating that under these conditions ambient glutamate is not sufficient to activate group I mGluRs. This is most likely due to the fact that ionotropic glutamate receptors were blocked for this study, reducing overall levels of neuronal activity. Others have shown that group I mGluRs are active when ionotropic glutamate receptors are unblocked (16), suggesting that action potential-driven release of glutamate, plentiful in hyperexcitable cortex, is necessary to stimulate the mGluRs. Under normal slice conditions, IPSC frequency is decreased after addition of ionotropic glutamate blockers. It was previously shown that the decrease in sIPSC frequency is significantly greater in PMG than control cortex (158). It is possible that this is due to not only an increased excitatory drive onto the interneurons, but also the decreased activation of the extrasynaptic mGluRs. Anatomical studies have also suggested that excitatory afferents are increased in the PMG (158; 159; 286). Therefore, mGluRs are likely to be even more active *in vivo* in the malformed cortex. Interestingly, the sIPSC frequency is slightly but significantly lower in PMG compared to control neurons when MPEP is included in the bath. This difference, possibly due to an inverse agonist action of MPEP (205; 245), supports the assertion that the observed sIPSC frequency difference

www.manaraa.com

in PMG versus control is likely due to the atypical presence of mGluR5s on PMG interneurons.

The mGluR1 antagonist AIDA (300μM) reversed the effect of DHPG, both in control and PMG cortex. This occurred in normal aCSF and when MPEP was included in the bath solution, indicating that mGluR1 is sufficient to mediate the response to DHPG. These results are in agreement with previously reported data that show mGluR1 alone can mediate increased sIPSC frequency in CA1 pyramidal cells following DHPG application (207). Therefore, it is possible that an enhanced mGluR1 response could contribute to increased activity in PMG. However, with mGluR5 blocked, dose-response curves for DHPG showed no difference between the control and PMG LTS responses (Fig. 5.7). A left shift in the curve would have indicated increased sensitivity of the mGluR1 receptors, while a larger maximum response would have suggested an increased number of receptors. Neither was observed, so it seems unlikely that the higher level of activity is due to either of these factors. As appears to be the case here, mGluR1 and mGluR5 are sometimes expressed in the same cell types and even in the same individual cells (262; 355).

In many cases activation of mGluR1 and mGluR5 produce similar responses through a similar mechanism (260; 261; 303), suggesting that synergism of their dual activation may contribute to the overall effect (327). In fact, activation of both mGluR1 and mGluR5 is necessary to mediate DHPG-induced bursting behavior in hippocampus (327). Both mGluR1 and mGluR5 have roles in LTP in the hippocampus (236; 344), as well as in neocortical layer V (358). However, it has been shown that specific

www.manaraa.com

mechanisms of action may actually allow them different, if overlapping, roles (365). In CA1 pyramidal cells, mGluR1 mediates DHPG-induced depolarization, while mGluR5 contributes to increased excitability through decreased I_{AHP} and potentiation of the NMDA-R response (207). Also, mGluR5 has been shown to increase the excitability of layer V pyramidal cells, specifically by decreasing AHP duration (325). This is particularly relevant, as we have observed decreased AHP duration in PMG LTS interneurons (Chapter 2), perhaps caused by the same mechanism. In hippocampal interneurons expressing both receptor subtypes, it is mGluR5 that is responsible for acute enhancement of epileptiform bursts, while mGluR1 is necessary to maintain long term neuronal excitation (222). Furthermore, currents specific to each type of receptor show differing kinetics in hippocampal interneurons. Activation of mGluR1 have been shown to cause large, fast-rising calcium transients, most likely due to influx of extracellular calcium, while activation of mGluR5 caused small, slow-rising calcium transients abolished by depletion of internal calcium stores (350). There is also evidence for a G-protein-independent mechanism of mGluR1 signaling in hippocampal mossy fiber terminals (150). Both of these receptor types have been implicated in oscillatory membrane activity for hippocampus and neocortex (41; 362), but activation of mGluR5 specifically has been shown to recapitulate the oscillatory activity seen in immature tissue (113). Alternatively, in cholinergic basal ganglia neurons, DHPG application combined with mGluR5 blockade uncovered oscillatory activity, apparently driven by mGluR1 and dependent on both L-type Ca^{2+} channels and tyrosine kinase (43). The roles that each of

www.manaraa.com

these subtypes play in oscillations and epileptiform activity in PMG cortex will require further investigation.

Previous findings have demonstrated that LTS cells, but not FS cells, are the interneuron subtype activated by DHPG in control cortex (27). According to immunohistochemical analyses, one to five percent of the cells in neocortex contain mGluR1 (107), and the mGluR1 immunopositivity is observed in interneurons (256). Two separate immunohistochemical studies have shown that in neocortex, mGluR1 colocalizes with SS (24; 326), found in LTS cells (174), but not PV (326). Here we have shown that the selective functional expression of group I mGluR on LTS interneurons is maintained in PMG cortex (Fig. 5.6). This suggests that the expression of these receptors develops prior to or is simply impervious to the P1 lesion. In contrast to this is the persistence of mGluR5 expression, possibly representing the maintenance of an immature state. The mGlu5 receptors are expressed early in development and decline within layer V during the second postnatal week, ultimately reaching a low level in all layers in adult cortex (198). Previous work has characterized malformed cortex as having persistent immature qualities that last beyond their typical chronological endpoint (62; 158; 290; 331). Some intrinsic properties also lag behind, such as action potential half-width and firing frequency (201).

It is also possible that rather than maintaining a high state that the mGluR5 are specifically upregulated, perhaps as a compensatory response to high levels of activity. Recent studies have demonstrated that group I mGluRs are aberrantly expressed in tissue from individuals with epilepsy and in various epilepsy models. For example, in patients

www.manaraa.com

with intractable temporal lobe epilepsy, upregulation of mGluR5 immunoreactivity in hippocampus has been demonstrated (166). Conversely, following status epilepticus in the pilocarpine model of epilepsy, there is a downregulation of mGluR5 mRNA (182). In humans with Taylor-type focal cortical dysplasia, an increase in mGluR1 has been shown in heterotopic neurons and dysplastic cells, along with an increase in neuronal and glial mGluR5 expression (8). In the kindling model of epilepsy, mGluR1 but not mGluR5 transcript was increased in dentate gyrus (40). Additionally, in a rat model of spontaneous seizures, mGluR5 expression was increased in reactive glial cells (10). Studies mapping protein levels and functional activation of these receptors to changes in cortical activity will be necessary to elucidate whether abnormal mGluR5 function contributes to onset of or occurs in response to epileptiform activity.

Together, the observed increase in sIPSC frequency and the selective activation of LTS cells suggest that the effectiveness of vertically projecting interneurons following group I mGluR activation with DHPG will be enhanced when glutamate levels are high enough to reach extrasynaptic receptors. Zhou and Hablitz have argued that increased excitation, leading to increased glutamate release and mGluR activation, ultimately results in increased inhibitory feedback to pyramidal cells (373). With regard to the data presented here, the presence of mGluR5s on LTS interneurons could potentially focus the augmented inhibitory feedback into a selective increase in vertical inhibition. This represents a mechanism for promoting synchronous activity between layers and within cortical columns, and thereby enabling the initiation of epileptiform activity. It has already been demonstrated that activation of group I mGluRs results in pro-convulsant

www.manaraa.com

activity, while specific antagonists to both mGluR1 and mGluR5 have anti-convulsant activity in vivo (5; 96; see 229). Agonists of group I mGluR injected intracerebrally cause limbic seizures (347; 348) that can be blocked with mGluR1 antagonists (22; 181). DHPG applied in hippocampal slices produce long lasting epileptiform activity (167; 167; 221; 222). Antagonists of either mGluR1 or mGluR5 can block induction of this epileptiform activity (167).

Because clinical trials are currently underway to test mGluR5 antagonists in patients with Fragile X syndrome, it is likely that we will soon know whether these compounds are an effective antiepileptic drug for a neuro-developmental disorder. Our work suggests that they may also be an effective drug for malformation-associated epilepsies (69).

www.manaraa.com

Table 5.1 Intrinsic properties of layer V pyramidal cells.

Parameter	Control	PMG
Resting membrane potential, mV	-55.8 ±0.7 (93)	-52.4 ±0.8 (83)
Input resistance, MΩ	111.7 ±6.3 (93)	110.8 ±5.0 (83)
Time constant (τ), ms	1.8 ±0.05 (93)	1.9 ±0.06 (83)
Action potential amplitude, mV	101.9 ±0.6 (92)	102.1 ±0.5 (82)

All data are expressed as means ±SEM (n cells). There were no differences between control and PMG on any of these measures (*t*-test, $p<0.05$).

www.manaraa.com

Figure 5.1 **A.** Pyramidal cell in layer V of a horizontal slice, imaged using DIC optics. Image through two focal planes from dorsal (left) to ventral (right). Apical dendrite apparent in left image (arrow), basal dendrites apparent in right image (arrowheads). **B.** Sample traces demonstrating that recordings are isolated $GABA_A$ currents. **B1a.** Cell 1, recording of sIPSCs in APV and DNQX. **B1b.** Recording from the same cell as in 1a, during application of 10 μM bicuculline. The sIPSCs are abolished. **B2a.** Cell 2, recording of sIPSCs in APV and DNQX. **B2b.** Recording from the same cell as shown in 2a, following addition of DHPG. **B2c.** Recording from the same cell as shown in 2a and 2b, during application of 10 μM bicuculline. This demonstrates that sIPSCs induced by DHPG are abolished by the $GABA_A$ antagonist, bicuculline.

www.manaraa.com

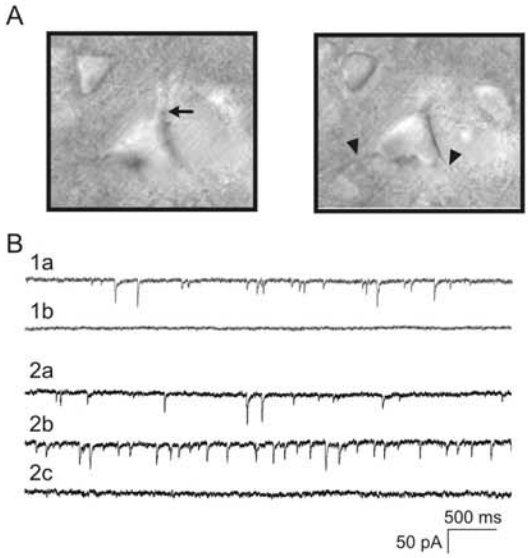

www.manaraa.com

Figure 5.2 Effect of DHPG (10 µM) and AIDA (300 µM) on sIPSC frequency and amplitude. A. Sample traces demonstrating that DHPG affected IPSC frequency within seconds of application in both control (1) and PMG (2). DHPG was applied at the beginning of the recording. Files showing onset were not used for further analysis. **B-C.** Typical traces from analyzed files for one control (B) and one PMG (C) cell. Traces shown are for the following conditions: normal aCSF (B1, C1); local application of DHPG (B2, C2); and local application of DHPG + AIDA (B3, C3). **D.** Mean sIPSC frequency before (aCSF) and during application of DHPG or DHPG and AIDA. For control (gray bars): $n_{aCSF} = 42$, $n_{DHPG} = 42$, $n_{AIDA} = 13$. For PMG (black bars): $n_{aCSF} = 31$, $n_{DHPG} = 31$, $n_{AIDA} = 11$. * = Student's *t*-test with Bonferroni correction, $p<0.05$. **E.** Amplitude of Type I events before and during application of DHPG (no significant differences). **F.** Percent change in sIPSC frequency after DHPG application, calculated within individual cells in control (gray bar, n = 42) and PMG (black bar, n = 31) cortex. * = Student's *t*-test, $p<0.05$. **G.** Percent change in sIPSC frequency after DHPG application for individual cells (gray symbols = control, n = 42; black symbols = PMG, n = 31). Circles indicate an increase in frequency, triangles indicate no change or decreased frequency. The "X" represents median for each group with all cells included, while the horizontal bar represents median for each group excluding cells indicated by triangles that fall below the dashed line. Even when cells that did not respond are not included, there is still a distinct difference in the medians for control and PMG cells.

www.manaraa.com

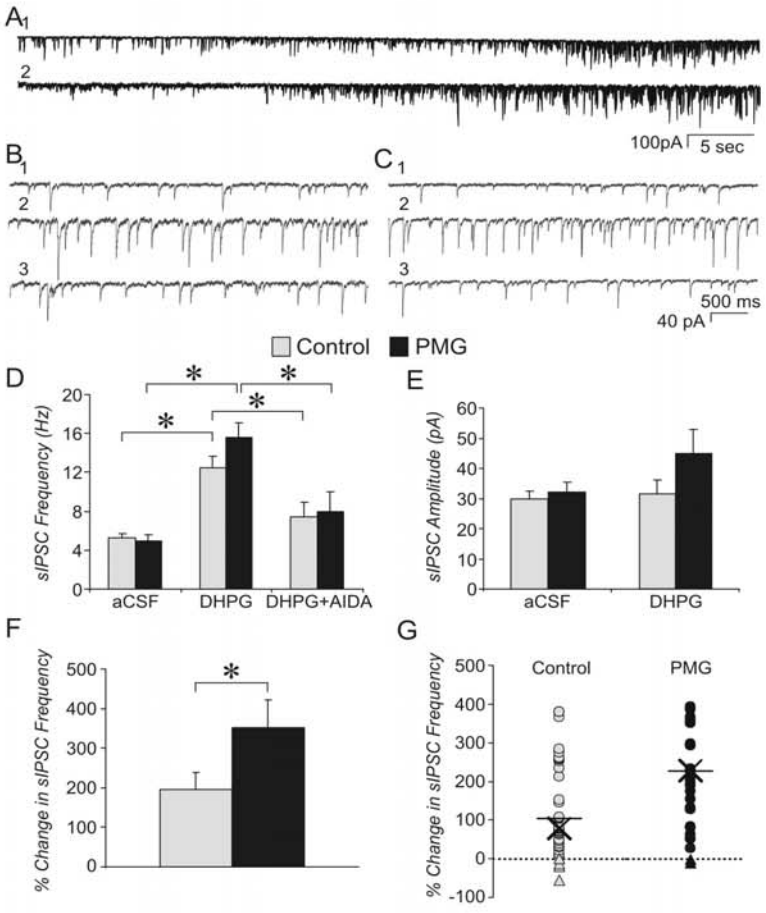
A1
2
100pA
5 sec
B1
2
3
C1
2
3
500 ms
40 pA
Control
PMG
D
sIPSC Frequency (Hz)
aCSF
DHPG
DHPG+AIDA
E
sIPSC Amplitude (pA)
aCSF
DHPG
F
% Change in sIPSC Frequency
G
% Change in sIPSC Frequency
Control
PMG

Figure 5.3 Effect of Group I mGluR antagonists in bathing solution. A-B. Example traces showing typical sIPSC recordings for control (A) and PMG (B) in aCSF (A1, B1), 100 μM AIDA (A2, B2), 300 μM AIDA (A3, B3) and 10 μM MPEP (A4, B4). **C-D.** Mean sIPSC frequency (C) and amplitude (D) recorded in control (left) and PMG (right) cells with either normal aCSF bathing medium, or with the addition of antagonists as shown in the bathing medium. Number of cells for conditions of normal aCSF, 100 μM AIDA, 300 μM AIDA, and 10 μM MPEP, respectively are: 42, 15, 10, 26 for control, and 31, 13, 21, 20 for PMG. One-way ANOVAs performed for each subject group (control, PMG) across bathing conditions, showed that adding antagonists to the bathing medium did not change the mean sIPSC frequency or amplitude. Student's *t*-test was performed to compare control vs. PMG for each bathing medium condition. MPEP showed a significant difference ($p < 0.05$), all others NS.

www.manaraa.com

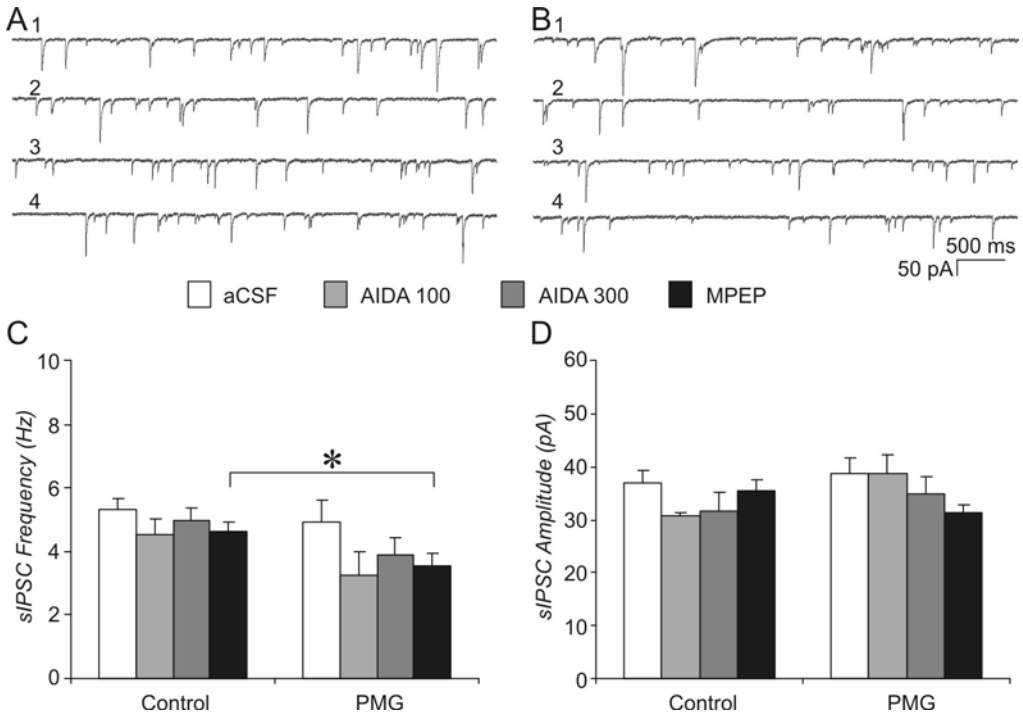

www.manaraa.com

Figure 5.4 Effect of DHPG on sIPSC frequency with MPEP (10 µM) in bath. A. Mean sIPSC frequency in aCSF with MPEP in the bath, during local application of 10 µM DHPG application and during addition of 300 µM AIDA to DHPG local application. * = *t*-test with Bonferroni correction, $p < 0.05$. **B.** Percent change in sIPSC frequency following addition of DHPG. There was no significant difference between control and PMG cells (*t*-test, NS). **C.** Distribution of individual cell responses for percent change in sIPSC frequency following DHPG application. Circles indicate an increase in frequency, triangles indicate no change or decreased frequency. The "X" represents median for each group with all cells included, while the horizontal bar represents median for each group excluding cells indicated by triangles that fall below the dashed line. There is little difference between control and PMG groups whether or not the possible technical failures (triangles) are excluded. In all cases, control data is shown in gray and PMG in black. Data shown is for 26, 22, and 10 control, and 21, 21, and 8 PMG cells, under conditions of aCSF, DHPG, and DHPG + AIDA, respectively.

www.manaraa.com

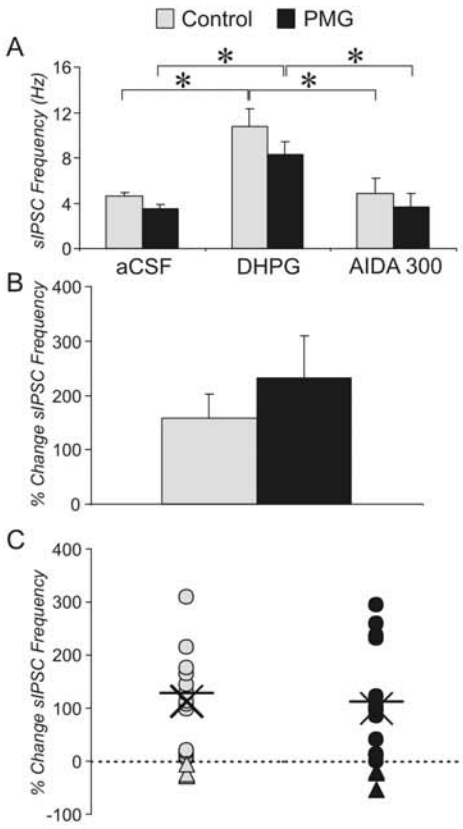

www.manaraa.com

Figure 5.5 Effect of DHPG on sIPSC frequency with AIDA (100 µM or 300 µM) in bath. **A-B.** Sample traces showing typical sIPSC characteristics for control (A) and PMG (B) under the following conditions: (1) aCSF with 100 µM AIDA in the bathing medium; (2) same as 1, but during local application of 10 µM DHPG; and (3) during addition of 10 µM MPEP to the local perfusate (DHPG also in local perfusate for 3). **C.** Mean sIPSC frequency for conditions described in 1-3 above (control, gray bars, PMG, black bars), with 100 µM AIDA in the bathing medium. Number of cells recorded for these three conditions was 15, 10, and 5 in control and 13, 10, and 7 in PMG cortex. * = *t*-test with Bonferroni correction, $p < 0.05$. **D.** Mean sIPSC frequency for conditions described in 1-3 above, with 300 µM AIDA in the bathing medium. Number of cells recorded for these three conditions was 10, 8, and 2 in control and 21, 17, and 13 in PMG cortex. * = *t*-test with Bonferroni correction, $p < 0.05$. **E-F.** Percent change in sIPSC frequency following addition of DHPG in bathing conditions of either 100 µM AIDA (E, control, n = 9; PMG, n = 10) or 300 µM AIDA (F, control, n = 7; PMG, n = 15). * = *t*-test, $p < 0.05$.

www.manaraa.com

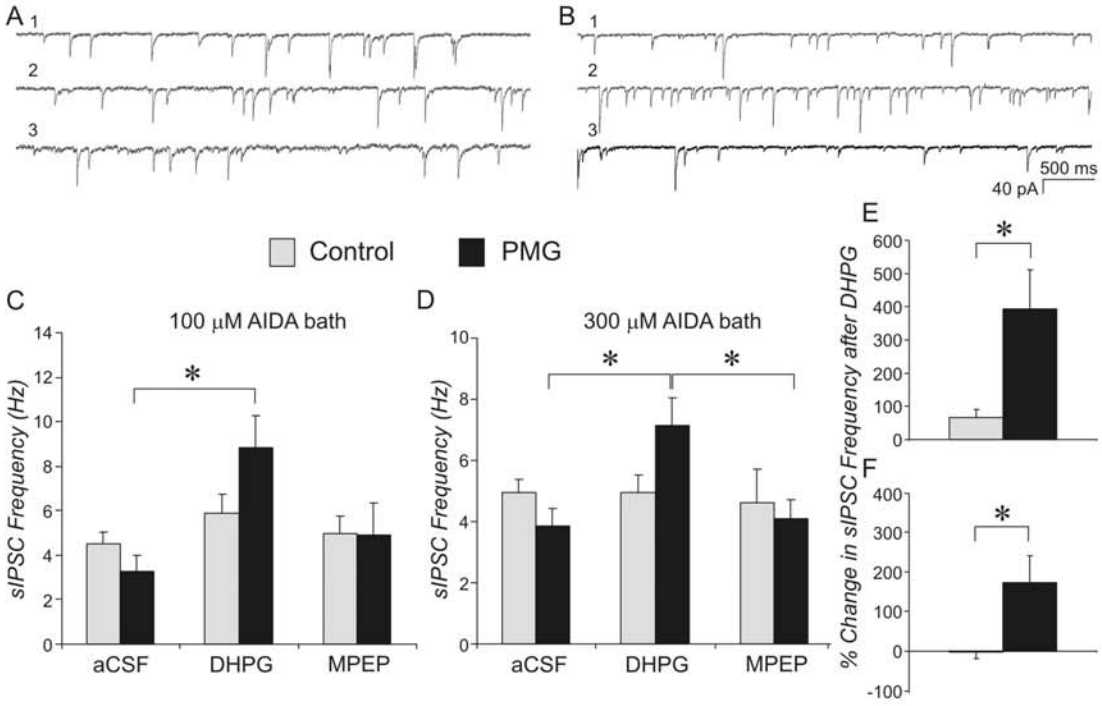
A
1
2
3
B
1
2
3
500 ms
40 pA
Control
PMG
C
100 μM AIDA bath
sIPSC Frequency (Hz)
aCSF
DHPG
MPEP
D
300 μM AIDA bath
sIPSC Frequency (Hz)
aCSF
DHPG
MPEP
E
F
% Change in sIPSC Frequency after DHPG

om

Figure 5.6 Effect of CHPG on sIPSC frequency. A. Change in sIPSC frequency following local application of 750 μM CHPG in PMG cortex. Results shown are for 6 PMG cells in conditions of normal aCSF, during CHPG application and during the addition of the MPEP to the CHPG application. **B.** Same as in A, but for control cells. MPEP was not applied here because there was no effect of CHPG. Results shown are for 5 control cells in conditions of normal aCSF and during CHPG application. * = *t*-test, $p < 0.05$.

www.manaraa.com

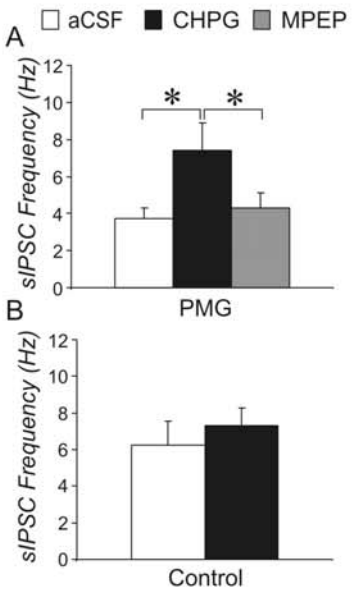
aCSF
CHPG
MPEP
A
sIPSC Frequency (Hz)
12
10
8
6
4
2
0
*
*
PMG
B
sIPSC Frequency (Hz)
12
10
8
6
4
2
0
Control

استشارات

Figure 5.7 Response of FS and LTS interneurons to DHPG application. A. Example LTS interneurons from control (A1) and PMG (A2) cortex. Firing pattern in response to an intracellular depolarizing current pulse (400 msec) is shown at left. Response to 10 μM DHPG (local application) shown at right. Cells depolarized within seconds of DHPG application (at beginning of trace). **B.** Example FS interneurons from control (B1) and PMG (B2) cortex. Response to DHPG was a slight membrane depolarization (right). **C.** Example LTS (C1) and FS (C2) cells demonstrating characteristic responses to 100 μM DHPG. The LTS cell depolarized within seconds and then fired action potentials following application of DHPG (beginning of trace). **D.** Maximal depolarization occurring after DHPG application. **E.** Steady-state depolarization observed after >1 min of DHPG application. There were no significant differences between control and PMG cells. **F.** Example of membrane oscillations induced in an LTS interneuron.

www.manaraa.com

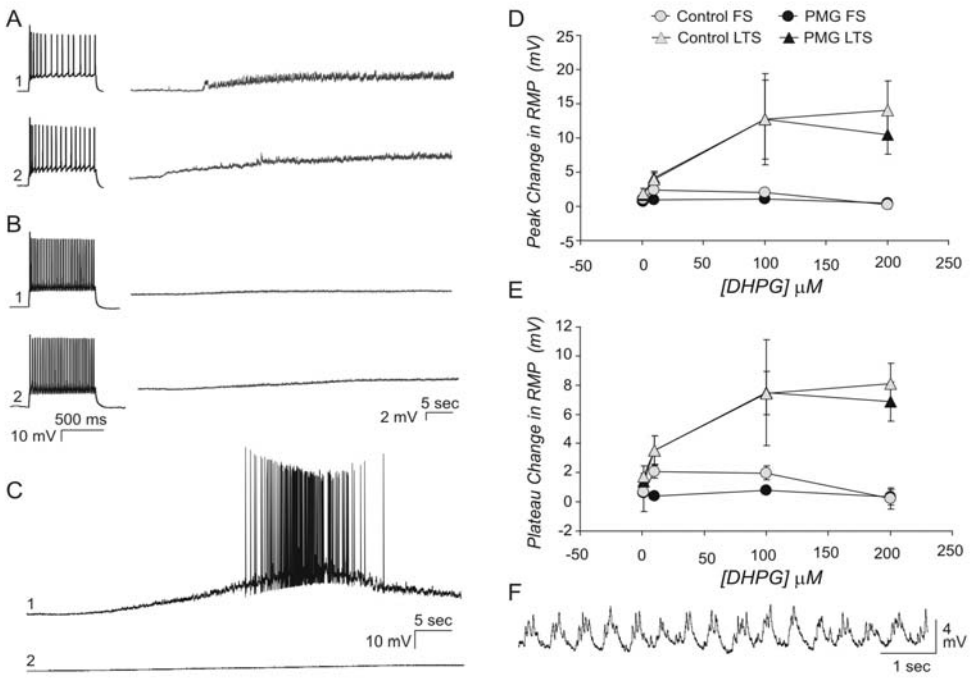

www.manaraa.com

Chapter 6

General Discussion

For decades, the dogma in epilepsy treatment and research has been that seizures are due to increased excitation or decreased inhibition. Within this framework, and despite advances in the diagnosis and treatment of epilepsy, modern medicine has not been able to counteract mechanisms of neocortical hyperexcitability for many patients. In order to successfully treat patients with intractable seizures, particularly those associated with malformations of cortical development, it is necessary to understand all the factors that contribute to abnormal cortical function. Past epilepsy research has investigated the role of increased pyramidal cell activity and bursting behavior in both hippocampal and neocortical models of epilepsy. Recent work from this lab has demonstrated that increased excitatory input to pyramidal cells occurs in the freeze-lesion model of cortical hyperexcitability used for the studies described here. Of particular relevance to the experiments described in this body of work is the fact that the observed increase occurs prior to the onset of epileptiform activity, indicating that there are other factors involved in controlling or "masking" it (375). The experiments described here focused on the role of neocortical interneurons in epileptogenesis, as several aspects of their development reach mature levels around the time epileptiform activity can be evoked in this model. In recent years, increased attention has been focused on the

www.manaraa.com

networks of inhibitory cells that are responsible for regulating excitation. This is because the pattern of excitatory output may be as important as the magnitude, with regard to abnormal synchrony and seizure activity. In fact, some studies have shown that excitation occurs in the presence of maintained, even enhanced, inhibitory function (206). The work presented in this dissertation was performed to increase our understanding of the seemingly paradoxical contribution of GABAergic inhibitory cells to neocortical hyperexcitability and epileptogenesis.

A number of the properties responsible for stereotypical characteristics of FS and LTS interneurons were evaluated in the preceding chapters. These two interneuron subpopulations form separate networks of electrically interconnected cells, and due to their distinct characteristics, it has been suggested that these networks also have separate functional roles in the cortex (131). In addition, morphology indicates that the network of vertically extended LTS cells is capable of providing intracolumnar inhibition, while horizontally oriented FS cells provide intralaminar inhibition. Alterations to either subtype could affect these specific roles, leading to the overall hypothesis that in PMG cortex, increased efficacy of LTS cells and decreased efficacy of FS cells create a synchrony-promoting imbalance of neocortical inhibition. The results presented in the preceding chapters suggest that interneuron subtypes are differentially altered in a manner that could cause abnormal synchrony in epileptogenic cortex. Specific findings that support this include: (1) increased firing frequency in PMG LTS cells and a parallel decrease in PMG FS cells, (2) increased excitatory input to PMG LTS cells, and (3) increased inhibitory output in PMG cortex when LTS cells are selectively activated.

www.manaraa.com

As demonstrated in chapter 2, interneuron subtypes can be clearly identified in PMG cortex. This was accomplished using the same classification criteria as in control, a critical point, as the significance of altered connectivity depends on the maintenance of properties that endow interneuron subtypes with their specific functions. Intrinsically altering these subtypes could change the function of individual cells, as well as the entire network to which they belong. This would make evidence of other types of changes difficult to interpret. Abnormal cell types have been demonstrated in animal models and in human cases of epilepsy (62), so defining these interneuron populations for the freeze-lesion model was necessary to validate these and future studies that intend to exploit the differences between them. In addition to this observation, the findings in chapter 3 demonstrate that LTS interneurons receive more excitatory input in PMG. This suggests that they may be depolarized to action potential threshold more frequently than their control counterparts. In combination with the fact that PMG LTS interneurons also have an increased firing frequency (Chapter 2), these data suggest that LTS interneurons are likely excited with greater frequency and to a greater extent in PMG cortex. As a result, the network of LTS cells may exert more powerful inhibition in PMG cortex than in control. In contrast, the input to FS cells does not appear to be altered. However, the results from chapter 2 show a lower action potential firing frequency for FS cells in PMG. This is interesting because decreased PV expression also suggests that there is a selective loss of FS cells in this model (288). The presence of fewer cells, combined with a lower firing frequency for the cells that remain, indicates that a decrease in the overall efficacy of FS cells is likely.

www.manaraa.com

The current working hypothesis based on these data is that (1) increased input and excitability enhance LTS output, increasing columnar synchrony, and (2) diminished excitability and cell number cause a decrease in FS output, permitting the spread of this synchrony to neighboring columns. Postsynaptically, this mechanism would result in more LTS-generated sIPSCs in pyramidal cells, but fewer FS-generated sIPSCs. Although it would likely involve complex analysis, the veracity of this hypothesis could be assessed on a cellular level by evaluating pyramidal cell sIPSCs. As has been discussed in chapter 1, vertically-oriented LTS cells synapse on the dendrites of their post-synaptic targets, while FS cells synapse on the soma. Somatic and dendritic IPSCs can be differentiated from each other with intracellular recordings (81). Unless the target domains of interneuron subtypes are also altered in this model, this would provide a means to compare input based on the inhibitory cell type. An increase in the frequency of dendritic events and a comparable decrease in the frequency of somatic events would simultaneously support this hypothesis and permit the overall frequency of IPSCs to remain unaffected. IPSC kinetics may be helpful in differentiating the source of IPSCs; however, this also reflects synapse location and is not necessarily specific to the presynaptic cell type. For example, increased dendritic inhibition could signify increased output from the typical dendrite-targeting cell population, or it may reflect a reorganization of inhibitory outputs that previously targeted the soma. However, were this observation to be made in conjunction with the data presented here, it would strongly support the presence of increased LTS output. In PMG cortex, if LTS inhibition is more readily activated, the very same inhibitory pattern that is seen in control could be applied

www.manaraa.com

to PMG pyramidal cells, only with greater strength. Following the cessation of this powerful inhibition, depolarizing glutamatergic inputs would simultaneously bring the previously hyperpolarized cells to threshold potential. Repetition and magnification of this cycle through feedback inhibition would allow this synchronous activity to persist.

In this study, to assess whether or not the output of LTS interneurons was enhanced in PMG cortex, this cell type was selectively activated with a group I mGluR agonist, and sIPSCs recorded from pyramidal cells were compared between control and PMG. Perhaps the most important finding discussed in chapter 5 is that the response to this activation was twice as large in the PMG cortex. Further investigation revealed that this could be attributed to increased agonist sensitivity, due to mGluR5 activation that does not occur in control. This increased inhibitory output is consistent with the increased LTS firing frequency and excitatory input described in chapters 2 and 3. Further, the release of extra glutamate in PMG cortex, due in part to an increased number of excitatory terminals, may activate mGlu5 receptors on PMG LTS cells. Although the experiments in chapter 5 indicate that the group I mGluRs are not active in response to spontaneous glutamate release when ionotropic receptors are blocked, mGluRs have demonstrated activity in response to ambient glutamate when the ionotropic receptors are not blocked (16). Interestingly, activation of mGluR5 has also been shown to increase firing frequency and decrease AHP duration (325), two effects also seen in PMG LTS cells (Chapter 2). While these data do not definitively establish a causal relationship between increased input to and output from LTS, together they makes a strong case for the increased efficacy of the LTS population

www.manaraa.com

Future experiments that may complement these findings

These studies reveal functional changes likely to promote epileptogenesis, but an even stronger argument for these underlying mechanisms could be made with accompanying structural evidence. Immunohistochemcal results suggest that the rearrangement of afferent fibers occurs in this model (159; 286). Additional studies using electron microscopy to look specifically at the number of excitatory synapses on interneurons would help clarify the organizational pattern. It is also possible that not all of the relevant changes are reflected anatomically. For example, if release probability is altered but not detected by the methods of this study, a significant increase in the number of synapses may not be observed, even at the ultrastructural level. Despite this, based on current immunohistochemical and physiological data, it is probable that this type of study would demonstrate an increase in the number of excitatory afferents to some interneurons and most pyramidal cells of layer V somatosensory cortex.

The findings from chapter 5 provide a convincing argument for the presence of functional mGluR5s on the PMG LTS interneurons, but several different approaches could be taken in order to visually confirm what the physiological data suggest. As has been performed in a number of other models and disease states, *in situ* hybridization could be used to demonstrate upregulation of mGluR5 mRNA. To establish an estimate of whether or not the protein is increased in PMG, a western blot could be used to compare levels in control and PMG. Development of a good mGluR5 antibody to be used for immunohistochemistry would also permit visible co-localization of these receptors with other LTS cellular markers in PMG. Visualizing these receptors is

www.manaraa.com

important, though, because the possibility remains that mGlu5 receptors are present but not functional in control. Alteration of a single subunit could provide the functionality that is exclusively demonstrated in PMG cortex. This type of information would direct future studies, differentiating between the utility of an mGluR5 knockout or a more subtle experimental designed to detect the presence of specific subunits.

To determine whether any or all of these observed changes contribute to cortical synchrony, it is necessary to perform experiments at a higher level of organization than the single cell. Field potential recordings are ongoing in the lab to assess whether the coordinated activity of LTS interneurons results in synchronous firing within cortical columns in the paramicrogyral region.

Translation and Therapeutic Relevance

Current anti-convulsive treatment for most patients with epilepsy involves the use of drugs with varied mechanisms of action, but all of them decrease excitatory cellular activity or increase inhibition. Phenobarbital and benzodiazepines, some of the first drugs used to treat seizures, bind the $GABA_A$ receptor to prolong or increase the frequency of channel opening, respectively. Several anti-seizure medications target specific membrane channels. For example, pregabalin binds a subunit of voltage-gated calcium channels and has effective anticonvulsant activity in electroshock, kindling and some chemically-induced seizures (31). Specific blockade of voltage sensitive sodium currents by lamotrigine prevents high-frequency firing, circumventing an excitatory overload (216). Zonisamaide also blocks sodium channels but has demonstrated activity

www.manaraa.com

on the T-type calcium current as well (193). Other mechanisms of anticonvulsant action include inhibition of GABA reuptake by tigabine (301) and reduction of IP_3-dependent calcium release by levetiracetam (57).

While these drugs have a fairly good success rate for treating some seizures, they fail for others. In addition, polypharmacy is often the only way to effectively limit seizure activity in some patients. When this fails, the only recourse for patients with intractable epilepsy may be invasive surgery. Even when the anti-epileptic drugs are effective, side effects may be prohibitive. Drug interactions may be especially problematic for AEDs, as their long-term use is often necessary for enduring remission of seizures. The possibility of using mGluR5 as a target for the development of new pharmacotherapy is attractive, because this receptor is not normally expressed at high levels in the developed brain. As a result, antagonism of mGluR5 may not cause the extensive side effect profile of some other anticonvulsants.

In vivo experiments have determined that mGluR5 antagonists have anticonvulsant properties. This may be due to a dampening effect on pyramidal cell activity, and therefore has the potential to be at least partially successful in a number of models. Based on the observations in this model, an mGluR5 antagonist may also be able to decrease activity in one subset of interneurons, potentially counteracting the development of synchronous activity. If this type of mechanism translates to the human condition, antagonism of mGluR5 could have a synergistic effect, potentially resulting in successful seizure control in this type of epilepsy.

www.manaraa.com

List of References

www.manaraa.com

List of References

1. *Cerebral Cortex: Cellular Components of the Cerebral Cortex; Vol 1*. New York: Plenum Publishing Corp., 1984.

2. Proposal for revised classification of epilepsies and epileptic syndromes. Commission on Classification and Terminology of the International League Against Epilepsy. *Epilepsia* 30: 389-399, 1989.

3. **Abuelo D**. Microcephaly syndromes. *Semin Pediatr Neurol* 14: 118-127, 2007.

4. **Alcantara S, Ferrer I and Soriano E**. Postnatal development of parvalbumin and calbindin D28K immunoreactivities in the cerebral cortex of the rat. *Anat Embryol (Berl)* 188: 63-73, 1993.

5. **Alexander GM and Godwin DW**. Metabotropic glutamate receptors as a strategic target for the treatment of epilepsy. *Epilepsy Res* 71: 1-22, 2006.

6. **Anderson SA, Marin O, Horn C, Jennings K and Rubenstein JL**. Distinct cortical migrations from the medial and lateral ganglionic eminences. *Development* 128: 353-363, 2001.

7. **Ang ES, Jr., Haydar TF, Gluncic V and Rakic P**. Four-dimensional migratory coordinates of GABAergic interneurons in the developing mouse cortex. *J Neurosci* 23: 5805-5815, 2003.

8. **Aronica E, Gorter JA, Jansen GH, van Veelen CW, van Rijen PC, Ramkema M and Troost D**. Expression and cell distribution of group I and group II metabotropic glutamate receptor subtypes in taylor-type focal cortical dysplasia. *Epilepsia* 44: 785-795, 2003.

www.manaraa.com

9. **Aronica E, Gorter JA, Redeker S, Ramkema M, Spliet WG, van Rijen PC, Leenstra S and Troost D**. Distribution, characterization and clinical significance of microglia in glioneuronal tumours from patients with chronic intractable epilepsy. *Neuropathol Appl Neurobiol* 31: 280-291, 2005.

10. **Aronica E, van Vliet EA, Mayboroda OA, Troost D, da Silva FH and Gorter JA**. Upregulation of metabotropic glutamate receptor subtype mGluR3 and mGluR5 in reactive astrocytes in a rat model of mesial temporal lobe epilepsy. *Eur J Neurosci* 12: 2333-2344, 2000.

11. **Aronica E, Yankaya B, Jansen GH, Leenstra S, van Veelen CW, Gorter JA and Troost D**. Ionotropic and metabotropic glutamate receptor protein expression in glioneuronal tumours from patients with intractable epilepsy. *Neuropathol Appl Neurobiol* 27: 223-237, 2001.

12. **Bacci A and Huguenard JR**. Enhancement of spike-timing precision by autaptic transmission in neocortical inhibitory interneurons. *Neuron* 49: 119-130, 2006.

13. **Bacci A, Huguenard JR and Prince DA**. Long-lasting self-inhibition of neocortical interneurons mediated by endocannabinoids. *Nature* 431: 312-316, 2004.

14. **Bacci A, Huguenard JR and Prince DA**. Modulation of neocortical interneurons: extrinsic influences and exercises in self-control. *Trends Neurosci* 28: 602-610, 2005.

15. **Bacci A, Rudolph U, Huguenard JR and Prince DA**. Major differences in inhibitory synaptic transmission onto two neocortical interneuron subclasses. *J Neurosci* 23: 9664-9674, 2003.

16. **Bandrowski AE, Huguenard JR and Prince DA**. Baseline glutamate levels affect group I and II mGluRs in layer V pyramidal neurons of rat sensorimotor cortex. *J Neurophysiol* 89: 1308-1316, 2003.

17. **Baraban SC and Schwartzkroin PA**. Electrophysiology of CA1 pyramidal neurons in an animal model of neuronal migration disorders: prenatal methylazoxymethanol treatment. *Epilepsy Res* 22: 145-156, 1995.

www.manaraa.com

18. **Barkovich AJ and Kjos BO**. Gray matter heterotopias: MR characteristics and correlation with developmental and neurologic manifestations. *Radiology* 182: 493-499, 1992.

19. **Barkovich AJ and Kjos BO**. Nonlissencephalic cortical dysplasias: correlation of imaging findings with clinical deficits. *AJNR Am J Neuroradiol* 13: 95-103, 1992.

20. **Barkovich AJ, Kuzniecky RI, Jackson GD, Guerrini R and Dobyns WB**. Classification system for malformations of cortical development: update 2001. *Neurology* 57: 2168-2178, 2001.

21. **Barkovich AJ and Lindan CE**. Congenital cytomegalovirus infection of the brain: imaging analysis and embryologic considerations. *AJNR Am J Neuroradiol* 15: 703-715, 1994.

22. **Barton ME and Shannon HE**. Behavioral and convulsant effects of the (S) enantiomer of the group I metabotropic glutamate receptor agonist 3,5-DHPG in mice. *Neuropharmacology* 48: 779-787, 2005.

23. **Battaglia G, Chiapparini L, Franceschetti S, Freri E, Tassi L, Bassanini S, Villani F, Spreafico R, D'Incerti L and Granata T**. Periventricular nodular heterotopia: classification, epileptic history, and genesis of epileptic discharges. *Epilepsia* 47: 86-97, 2006.

24. **Baude A, Nusser Z, Roberts JD, Mulvihill E, McIlhinney RA and Somogyi P**. The metabotropic glutamate receptor (mGluR1 alpha) is concentrated at perisynaptic membrane of neuronal subpopulations as detected by immunogold reaction. *Neuron* 11: 771-787, 1993.

25. **Beck H and Yaari Y**. Plasticity of intrinsic neuronal properties in CNS disorders. *Nat Rev Neurosci* 9: 357-369, 2008.

26. **Behr J, Gloveli T and Heinemann U**. Kindling induces a transient suppression of afterhyperpolarization in rat subicular neurons. *Brain Res* 867: 259-264, 2000.

www.manaraa.com

27. **Beierlein M, Gibson JR and Connors BW**. A network of electrically coupled interneurons drives synchronized inhibition in neocortex. *Nat Neurosci* 3: 904-910, 2000.

28. **Beierlein M, Gibson JR and Connors BW**. Two dynamically distinct inhibitory networks in layer 4 of the neocortex. *J Neurophysiol* 90: 2987-3000, 2003.

29. **Belluardo N, Mud inverted question mG, Trovato-Salinaro A, Le Gurun S, Charollais A, Serre-Beinier V, Amato G, Haefliger JA, Meda P and Condorelli DF**. Expression of connexin36 in the adult and developing rat brain. *Brain Res* 865: 121-138, 2000.

30. **Belluardo N, Trovato-Salinaro A, Mudo G, Hurd YL and Condorelli DF**. Structure, chromosomal localization, and brain expression of human Cx36 gene. *J Neurosci Res* 57: 740-752, 1999.

31. **Ben Menachem E**. Pregabalin pharmacology and its relevance to clinical practice. *Epilepsia* 45 Suppl 6:13-8.: 13-18, 2004.

32. **Benardete EA and Kriegstein AR**. Increased excitability and decreased sensitivity to GABA in an animal model of dysplastic cortex. *Epilepsia* 43: 970-982, 2002.

33. **Berger T and Luscher HR**. Timing and precision of spike initiation in layer V pyramidal cells of the rat somatosensory cortex. *Cereb Cortex* 13: 274-281, 2003.

34. **Berkovic SF, Mulley JC, Scheffer IE and Petrou S**. Human epilepsies: interaction of genetic and acquired factors. *Trends Neurosci* 29: 391-397, 2006.

35. **Bernard C, Anderson A, Becker A, Poolos NP, Beck H and Johnston D**. Acquired dendritic channelopathy in temporal lobe epilepsy. *Science* 305: 532-535, 2004.

36. **Bernard C, Cossart R, Hirsch JC, Esclapez M and Ben Ari Y**. What is GABAergic inhibition? How is it modified in epilepsy? *Epilepsia* 41 Suppl 6: S90-S95, 2000.

www.manaraa.com

37. **Best N, Mitchell J and Wheal HV**. Ultrastructure of parvalbumin-immunoreactive neurons in the CA1 area of the rat hippocampus following a kainic acid injection. *Acta Neuropathol (Berl)* 87: 187-195, 1994.

38. **Bikson M, Id BR, Vreugdenhil M, Kohling R, Fox JE and Jefferys JG**. Quinine suppresses extracellular potassium transients and ictal epileptiform activity without decreasing neuronal excitability in vitro. *Neuroscience* 115: 251-261, 2002.

39. **Bladin CF, Alexandrov AV, Bellavance A, Bornstein N, Chambers B, Cote R, Lebrun L, Pirisi A and Norris JW**. Seizures after stroke: a prospective multicenter study. *Arch Neurol* 57: 1617-1622, 2000.

40. **Blumcke I, Becker AJ, Klein C, Scheiwe C, Lie AA, Beck H, Waha A, Friedl MG, Kuhn R, Emson P, Elger C and Wiestler OD**. Temporal lobe epilepsy associated up-regulation of metabotropic glutamate receptors: correlated changes in mGluR1 mRNA and protein expression in experimental animals and human patients. *J Neuropathol Exp Neurol* 59: 1-10, 2000.

41. **Boddeke HW, Best R and Boeijinga PH**. Synchronous 20 Hz rhythmic activity in hippocampal networks induced by activation of metabotropic glutamate receptors in vitro. *Neuroscience* 76: 653-658, 1997.

42. **Boer K, Spliet WG, van Rijen PC, Redeker S, Troost D and Aronica E**. Evidence of activated microglia in focal cortical dysplasia. *J Neuroimmunol* 173: 188-195, 2006.

43. **Bonsi P, Cuomo D, De Persis C, Centonze D, Bernardi G, Calabresi P and Pisani A**. Modulatory action of metabotropic glutamate receptor (mGluR) 5 on mGluR1 function in striatal cholinergic interneurons. *Neuropharmacology* 49 Suppl 1: 104-113, 2005.

44. **Bordey A, Lyons SA, Hablitz JJ and Sontheimer H**. Electrophysiological characteristics of reactive astrocytes in experimental cortical dysplasia. *J Neurophysiol* 85: 1719-1731, 2001.

45. **Bordi F and Ugolini A**. Group I metabotropic glutamate receptors: implications for brain diseases. *Prog Neurobiol* 59: 55-79, 1999.

www.manaraa.com

46. **Bourdeau ML, Morin F, Laurent CE, Azzi M and Lacaille JC**. Kv4.3-mediated A-type K+ currents underlie rhythmic activity in hippocampal interneurons. *J Neurosci* 27: 1942-1953, 2007.

47. **Boyett JM and Buckmaster PS**. Somatostatin-immunoreactive interneurons contribute to lateral inhibitory circuits in the dentate gyrus of control and epileptic rats. *Hippocampus* 11: 418-422, 2001.

48. **Brunelli S, Faiella A, Capra V, Nigro V, Simeone A, Cama A and Boncinelli E**. Germline mutations in the homeobox gene EMX2 in patients with severe schizencephaly. *Nat Genet* 12: 94-96, 1996.

49. **Buckmaster PS and Dudek FE**. Neuron loss, granule cell axon reorganization, and functional changes in the dentate gyrus of epileptic kainate-treated rats. *J Comp Neurol* 385: 385-404, 1997.

50. **Buhl EH, Otis TS and Mody I**. Zinc-induced collapse of augmented inhibition by GABA in a temporal lobe epilepsy model. *Science* 271: 369-373, 1996.

51. **Buhl EH, Tamas G, Szilagyi T, Stricker C, Paulsen O and Somogyi P**. Effect, number and location of synapses made by single pyramidal cells onto aspiny interneurones of cat visual cortex. *J Physiol (Lond)* 500 (Pt 3): 689-713, 1997.

52. **Burneo JG, Kuzniecky RI, Bebin M and Knowlton RC**. Cortical reorganization in malformations of cortical development: a magnetoencephalographic study. *Neurology* 63: 1818-1824, 2004.

53. **Bush PC, Prince DA and Miller KD**. Increased Pyramidal Excitability and NMDA Conductance Can Explain Posttraumatic Epileptogenesis Without Disinhibition: A Model. *J Neurophysiol* 82: 1748-1758, 1999.

54. **Butt SJ, Fuccillo M, Nery S, Noctor S, Kriegstein A, Corbin JG and Fishell G**. The temporal and spatial origins of cortical interneurons predict their physiological subtype. *Neuron* 48: 591-604, 2005.

www.manaraa.com

55. **Calcagnotto ME, Paredes MF and Baraban SC**. Heterotopic neurons with altered inhibitory synaptic function in an animal model of malformation-associated epilepsy. *J Neurosci* 22: 7596-7605, 2002.

56. **Castro PA, Cooper EC, Lowenstein DH and Baraban SC**. Hippocampal heterotopia lack functional Kv4.2 potassium channels in the methylazoxymethanol model of cortical malformations and epilepsy. *J Neurosci* 21: 6626-6634, 2001.

57. **Cataldi M, Lariccia V, Secondo A, di Renzo G and Annunziato L**. The antiepileptic drug levetiracetam decreases the inositol 1,4,5-trisphosphate-dependent [Ca2+]I increase induced by ATP and bradykinin in PC12 cells. *J Pharmacol Exp Ther* 313: 720-730, 2005.

58. **Catania MV, D'Antoni S, Bonaccorso CM, Aronica E, Bear MF and Nicoletti F**. Group I metabotropic glutamate receptors: a role in neurodevelopmental disorders? *Mol Neurobiol* 35: 298-307, 2007.

59. **Catania MV, Landwehrmeyer GB, Testa CM, Standaert DG, Penney JB, Jr. and Young AB**. Metabotropic glutamate receptors are differentially regulated during development. *Neuroscience* 61: 481-495, 1994.

60. **Cauli B, Audinat E, Lambolez B, Angulo MC, Ropert N, Tsuzuki K, Hestrin S and Rossier J**. Molecular and physiological diversity of cortical nonpyramidal cells. *J Neurosci* 17: 3894-3906, 1997.

61. **Cauli B, Porter JT, Tsuzuki K, Lambolez B, Rossier J, Quenet B and Audinat E**. Classification of fusiform neocortical interneurons based on unsupervised clustering. *Proc Natl Acad Sci U S A* 97: 6144-6149, 2000.

62. **Cepeda C, Andre VM, Levine MS, Salamon N, Miyata H, Vinters HV and Mathern GW**. Epileptogenesis in pediatric cortical dysplasia: the dysmature cerebral developmental hypothesis. *Epilepsy Behav* 9: 219-235, 2006.

63. **Cepeda C, Andre VM, Vinters HV, Levine MS and Mathern GW**. Are cytomegalic neurons and balloon cells generators of epileptic activity in pediatric cortical dysplasia? *Epilepsia* 46 Suppl 5: 82-88, 2005.

www.manaraa.com

64. **Cepeda C, Hurst RS, Flores-Hernandez J, Hernandez-Echeagaray E, Klapstein GJ, Boylan MK, Calvert CR, Jocoy EL, Nguyen OK, Andre VM, Vinters HV, Ariano MA, Levine MS and Mathern GW**. Morphological and electrophysiological characterization of abnormal cell types in pediatric cortical dysplasia. *J Neurosci Res* 72: 472-486, 2003.

65. **Chagnac-Amitai Y and Connors BW**. Synchronized excitation and inhibition driven by intrinsically bursting neurons in neocortex. *J Neurophysiol* 62: 1149-1162, 1989.

66. **Chang BS, Piao X, Bodell A, Basel-Vanagaite L, Straussberg R, Dobyns WB, Qasrawi B, Winter RM, Innes AM, Voit T, Grant PE, Barkovich AJ and Walsh CA**. Bilateral frontoparietal polymicrogyria: clinical and radiological features in 10 families with linkage to chromosome 16. *Ann Neurol* 53: 596-606, 2003.

67. **Chang BS, Piao X, Giannini C, Cascino GD, Scheffer I, Woods CG, Topcu M, Tezcan K, Bodell A, Leventer RJ, Barkovich AJ, Grant PE and Walsh CA**. Bilateral generalized polymicrogyria (BGP): a distinct syndrome of cortical malformation. *Neurology* 62: 1722-1728, 2004.

68. **Chang SY, Zagha E, Kwon ES, Ozaita A, Bobik M, Martone ME, Ellisman MH, Heintz N and Rudy B**. Distribution of Kv3.3 potassium channel subunits in distinct neuronal populations of mouse brain. *J Comp Neurol* 502: 953-972, 2007.

69. **Chapman AG, Nanan K, Williams M and Meldrum BS**. Anticonvulsant activity of two metabotropic glutamate group I antagonists selective for the mGlu5 receptor: 2-methyl-6-(phenylethynyl)-pyridine (MPEP), and (E)-6-methyl-2-styryl-pyridine (SIB 1893). *Neuropharmacology* 39: 1567-1574, 2000.

70. **Chassoux F, Landre E, Rodrigo S, Beuvon F, Turak B, Semah F and Devaux B**. Intralesional recordings and epileptogenic zone in focal polymicrogyria. *Epilepsia* 49: 51-64, 2008.

71. **Chen K, Aradi I, Thon N, Eghbal-Ahmadi M, Baram TZ and Soltesz I**. Persistently modified h-channels after complex febrile seizures convert the seizure-induced enhancement of inhibition to hyperexcitability. *Nat Med* 7: 331-337, 2001.

www.manaraa.com

72. **Chow A, Erisir A, Farb C, Nadal MS, Ozaita A, Lau D, Welker E and Rudy B**. K(+) channel expression distinguishes subpopulations of parvalbumin- and somatostatin-containing neocortical interneurons. *J Neurosci* 19: 9332-9345, 1999.

73. **Chu Z and Hablitz JJ**. Activation of group I mGluRs increases spontaneous IPSC frequency in rat frontal cortex. *J Neurophysiol* 80: 621-627, 1998.

74. **Cobb SR, Buhl EH, Halasy K, Paulsen O and Somogyi P**. Synchronization of neuronal activity in hippocampus by individual GABAergic interneurons. *Nature* 378: 75-78, 1995.

75. **Colmers WF and El Bahh B**. Neuropeptide Y and Epilepsy. *Epilepsy Curr* 3: 53-58, 2003.

76. **Condorelli DF, Belluardo N, Trovato-Salinaro A and Mudo G**. Expression of Cx36 in mammalian neurons. *Brain Res Brain Res Rev* 32: 72-85, 2000.

77. **Conn PJ and Pin JP**. Pharmacology and functions of metabotropic glutamate receptors. *Annu Rev Pharmacol Toxicol* 37: 205-237, 1997.

78. **Connors BW, Benardo LS and Prince DA**. Coupling between neurons of the developing rat neocortex. *J Neurosci* 3: 773-782, 1983.

79. **Connors BW and Long MA**. Electrical synapses in the mammalian brain. *Annu Rev Neurosci* 27: 393-418, 2004.

80. **Cossart R, Dinocourt C, Hirsch JC, Merchan-Perez A, De Felipe J, Esclapez M, Bernard C and Ben Ari Y**. Dendritic but not somatic GABAergic inhibition is decreased in experimental epilepsy. *Nat Neurosci* 4: 52-62, 2001.

81. **Cossart R, Hirsch JC, Cannon RC, Dinoncourt C, Wheal HV, Ben Ari Y, Esclapez M and Bernard C**. Distribution of spontaneous currents along the somato-dendritic axis of rat hippocampal CA1 pyramidal neurons. *Neuroscience* 99: 593-603, 2000.

www.manaraa.com

82. **Crome L**. Microgyria. *J Path Bact* 64: 479-495, 1952.

83. **Cruikshank SJ, Landisman CE, Mancilla JG and Connors BW**. Connexon connexions in the thalamocortical system. *Prog Brain Res* 149: 41-57, 2005.

84. **Cui C, Sakata-Haga H, Ohta K, Nishida M, Yashiki M, Sawada K and Fukui Y**. Histological brain alterations following prenatal methamphetamine exposure in rats. *Congenit Anom (Kyoto)* 46: 180-187, 2006.

85. **de Leon GA**. Observations on cerebral and cerebellar microgyria. *Acta Neuropathol (Berl)* 20: 278-287, 1972.

86. **De Simoni MG, Perego C, Ravizza T, Moneta D, Conti M, Marchesi F, De Luigi A, Garattini S and Vezzani A**. Inflammatory cytokines and related genes are induced in the rat hippocampus by limbic status epilepticus. *Eur J Neurosci* 12: 2623-2633, 2000.

87. **Deans MR, Gibson JR, Sellitto C, Connors BW and Paul DL**. Synchronous activity of inhibitory networks in neocortex requires electrical synapses containing connexin36. *Neuron* 31: 477-485, 2001.

88. **Deblaere K and Achten E**. Structural magnetic resonance imaging in epilepsy. *Eur Radiol* 18: 119-129, 2008.

89. **Defazio RA and Hablitz JJ**. Reduction of Zolpidem Sensitivity in a Freeze Lesion Model of Neocortical Dysgenesis. *J Neurophysiol* 81: 404-407, 1999.

90. **Defazio RA and Hablitz JJ**. Alterations in NMDA receptors in a rat model of cortical dysplasia. *J Neurophysiol* 83: 315-321, 2000.

91. **DeFelipe J, Garcia SR, Marco P, del RM, Pulido P and Ramon**. Selective changes in the microorganization of the human epileptogenic neocortex revealed by parvalbumin immunoreactivity. *Cereb Cortex* 3: 39-48, 1993.

www.manaraa.com

92. **Di Rocco F, Giannetti S, Gaglini P, Di Rocco C and Granato A**. Dendritic architecture of corticothalamic neurons in a rat model of microgyria. *Childs Nerv Syst* 18: 690-693, 2002.

93. **Dinocourt C, Petanjek Z, Freund TF, Ben Ari Y and Esclapez M**. Loss of interneurons innervating pyramidal cell dendrites and axon initial segments in the CA1 region of the hippocampus following pilocarpine-induced seizures. *J Comp Neurol* 459: 407-425, 2003.

94. **Dobyns WB, Elias ER, Newlin AC, Pagon RA and Ledbetter DH**. Causal heterogeneity in isolated lissencephaly. *Neurology* 42: 1375-1388, 1992.

95. **Doherty AJ, Palmer MJ, Henley JM, Collingridge GL and Jane DE**. (RS)-2-chloro-5-hydroxyphenylglycine (CHPG) activates mGlu5, but no mGlu1, receptors expressed in CHO cells and potentiates NMDA responses in the hippocampus. *Neuropharmacology* 36: 265-267, 1997.

96. **Doherty J and Dingledine R**. The roles of metabotropic glutamate receptors in seizures and epilepsy. *Curr Drug Targets CNS Neurol Disord* 1: 251-260, 2002.

97. **Du T, Xu Q, Ocbina PJ and Anderson SA**. NKX2.1 specifies cortical interneuron fate by activating Lhx6. *Development* 135: 1559-1567, 2008.

98. **Dubeau F, Tampieri D, Lee N, Andermann E, Carpenter S, Leblanc R, Olivier A, Radtke R, Villemure JG and Andermann F**. Periventricular and subcortical nodular heterotopia. A study of 33 patients. *Brain* 118 (Pt 5): 1273-1287, 1995.

99. **Dvorak K and Feit J**. Migration of neuroblasts through partial necrosis of the cerebral cortex in newborn rats. Contribution to the problems of morphological development and developmental period of cerebral microgyria. *Acta Neuropathol* 38: 203-212, 1977.

100. **Dvorak K, Feit J and Jurankova Z**. Experimentally induced focal microgyria and status verrucosus deformis in rats. Pathogenesis and interrelation histological and autoradiographical study. *Acta Neuropathol* 44: 121-129, 1978.

www.manaraa.com

101. **Eadie MJ and Bladin PF**. *A Disease Once Sacred, A History of the Medical Understanding of Epilepsy*. England: John Libbey and Co., LTD, 2001.

102. **Emri Z, Antal K and Crunelli V**. The impact of corticothalamic feedback on the output dynamics of a thalamocortical neurone model: the role of synapse location and metabotropic glutamate receptors. *Neuroscience* 117: 229-239, 2003.

103. **Eriksson SH, Thom M, Heffernan J, Lin WR, Harding BN, Squier MV and Sisodiya SM**. Persistent reelin-expressing Cajal-Retzius cells in polymicrogyria. *Brain* 124: 1350-1361, 2001.

104. **Erisir A, Lau D, Rudy B and Leonard CS**. Function of specific K(+) channels in sustained high-frequency firing of fast-spiking neocortical interneurons. *J Neurophysiol* 82: 2476-2489, 1999.

105. **Fairen A, DeFelipe J and Regidor J**. Nonpyramidal Neurons: general account. In: Cerebral Cortex, edited by Jones EG and Peters A. New York: Plenum, 1984, p. 201-245.

106. **Ferezou I, Cauli B, Hill EL, Rossier J, Hamel E and Lambolez B**. 5-HT3 receptors mediate serotonergic fast synaptic excitation of neocortical vasoactive intestinal peptide/cholecystokinin interneurons. *J Neurosci* 22: 7389-7397, 2002.

107. **Ferraguti F, Conquet F, Corti C, Grandes P, Kuhn R and Knopfel T**. Immunohistochemical localization of the mGluR1beta metabotropic glutamate receptor in the adult rodent forebrain: evidence for a differential distribution of mGluR1 splice variants. *J Comp Neurol* 400: 391-407, 1998.

108. **Ferrer I**. A Golgi analysis of unlayered polymicrogyria. *Acta Neuropathol* 65: 69-76, 1984.

109. **Ferrer I, Alcantara S, Catala I and Zujar MJ**. Experimentally induced laminar necrosis, status verrucosus, focal cortical dysplasia reminiscent of microgyria, and porencephaly in the rat. *Exp Brain Res* 94: 261-269, 1993.

110. **Finardi A, Gardoni F, Bassanini S, Lasio G, Cossu M, Tassi L, Caccia C, Taroni F, LoRusso G, Di Luca M and Battaglia G**. NMDA receptor

www.manaraa.com

composition differs among anatomically diverse malformations of cortical development. *J Neuropathol Exp Neurol* 65: 883-893, 2006.

111. **Fitch RH, Brown CP, Tallal P and Rosen GD**. Effects of sex and MK-801 on auditory-processing deficits associated with developmental microgyric lesions in rats. *Behav Neurosci* 111: 404-412, 1997.

112. **Flames N and Marin O**. Developmental mechanisms underlying the generation of cortical interneuron diversity. *Neuron* 46: 377-381, 2005.

113. **Flint AC, Dammerman RS and Kriegstein AR**. Endogenous activation of metabotropic glutamate receptors in neocortical development causes neuronal calcium oscillations. *Proc Natl Acad Sci U S A* 96: 12144-12149, 1999.

114. **Flint AC and Kriegstein AR**. Mechanisms underlying neuronal migration disorders and epilepsy. *Curr Opin Neurol* 10: 92-97, 1997.

115. **Fogli A, Guerrini R, Moro F, Fernandez-Alvarez E, Livet MO, Renieri A, Cioni M, Pilz DT, Veggiotti P, Rossi E, Ballabio A and Carrozzo R**. Intracellular levels of the LIS1 protein correlate with clinical and neuroradiological findings in patients with classical lissencephaly. *Ann Neurol* 45: 154-161, 1999.

116. **Folbergrova J, Druga R, Haugvicova R, Mares P and Otahal J**. Anticonvulsant and neuroprotective effect of (S)-3,4-dicarboxyphenylglycine against seizures induced in immature rats by homocysteic acid. *Neuropharmacology* 54: 665-675, 2008.

117. **Fox JW, Lamperti ED, Eksioglu YZ, Hong SE, Feng Y, Graham DA, Scheffer IE, Dobyns WB, Hirsch BA, Radtke RA, Berkovic SF, Huttenlocher PR and Walsh CA**. Mutations in filamin 1 prevent migration of cerebral cortical neurons in human periventricular heterotopia. *Neuron* 21: 1315-1325, 1998.

118. **Franceschetti S, Sancini G, Panzica F, Radici C and Avanzini G**. Postnatal differentiation of firing properties and morphological characteristics in layer V pyramidal neurons of the sensorimotor cortex. *Neuroscience* 83: 1013-1024, 1998.

www.manaraa.com

119. **Freund TF, Ylinen A, Miettinen R, Pitkanen A, Lahtinen H, Baimbridge KG and Riekkinen PJ**. Pattern of neuronal death in the rat hippocampus after status epilepticus. Relationship to calcium binding protein content and ischemic vulnerability. *Brain Res Bull* 28: 27-38, 1992.

120. **Frey LC**. Epidemiology of posttraumatic epilepsy: a critical review. *Epilepsia* 44 Suppl 10: 11-17, 2003.

121. **Fricker D and Miles R**. Interneurons, spike timing, and perception. *Neuron* 32: 771-774, 2001.

122. **Fukuda T and Kosaka T**. Ultrastructural study of gap junctions between dendrites of parvalbumin-containing GABAergic neurons in various neocortical areas of the adult rat. *Neuroscience* 120: 5-20, 2003.

123. **Galaburda AM, Sherman GF, Rosen GD, Aboitiz F and Geschwind N**. Developmental dyslexia: four consecutive patients with cortical anomalies. *Ann Neurol* 18: 222-233, 1985.

124. **Galarreta M and Hestrin S**. A network of fast-spiking cells in the neocortex connected by electrical synapses. *Nature* 402: 72-75, 1999.

125. **Galarreta M and Hestrin S**. Electrical synapses between GABA-releasing interneurons. *Nat Rev Neurosci* 2: 425-433, 2001.

126. **Gao WJ and Goldman-Rakic PS**. Selective modulation of excitatory and inhibitory microcircuits by dopamine. *Proc Natl Acad Sci U S A* 100: 2836-2841, 2003.

127. **Gasparini F, Lingenhohl K, Stoehr N, Flor PJ, Heinrich M, Vranesic I, Biollaz M, Allgeier H, Heckendorn R, Urwyler S, Varney MA, Johnson EC, Hess SD, Rao SP, Sacaan AI, Santori EM, Velicelebi G and Kuhn R**. 2-Methyl-6-(phenylethynyl)-pyridine (MPEP), a potent, selective and systemically active mGlu5 receptor antagonist. *Neuropharmacology* 38: 1493-1503, 1999.

www.manaraa.com

128. **Geiger JR, Lubke J, Roth A, Frotscher M and Jonas P**. Submillisecond AMPA receptor-mediated signaling at a principal neuron-interneuron synapse. *Neuron* 18: 1009-1023, 1997.

129. **Giannetti S, Gaglini P, Di Rocco F, Di Rocco C and Granato A**. Organization of cortico-cortical associative projections in a rat model of microgyria. *Neuroreport* 11: 2185-2189, 2000.

130. **Giannetti S, Gaglini P, Granato A and Di Rocco C**. Organization of callosal connections in rats with experimentally induced microgyria. *Childs Nerv Syst* 15: 444-448, 1999.

131. **Gibson JR, Beierlein M and Connors BW**. Two networks of electrically coupled inhibitory neurons in neocortex. *Nature* 402: 75-79, 1999.

132. **Golden JA**. Cell migration and cerebral cortical development. *Neuropathol Appl Neurobiol* 27: 22-28, 2001.

133. **Gressens P, Marret S and Evrard P**. Developmental spectrum of the excitotoxic cascade induced by ibotenate: a model of hypoxic insults in fetuses and neonates. *Neuropathol Appl Neurobiol* 22: 498-502, 1996.

134. **Gropman AL, Barkovich AJ, Vezina LG, Conry JA, Dubovsky EC and Packer RJ**. Pediatric congenital bilateral perisylvian syndrome: clinical and MRI features in 12 patients. *Neuropediatrics* 28: 198-203, 1997.

135. **Guerrini R, Barkovich AJ, Sztriha L and Dobyns WB**. Bilateral frontal polymicrogyria: a newly recognized brain malformation syndrome. *Neurology* 54: 909-913, 2000.

136. **Guerrini R and Carrozzo R**. Epilepsy and genetic malformations of the cerebral cortex. *Am J Med Genet* 106: 160-173, 2001.

137. **Guerrini R, Dobyns WB and Barkovich AJ**. Abnormal development of the human cerebral cortex: genetics, functional consequences and treatment options. *Trends Neurosci* 31: 154-162, 2008.

www.manaraa.com

138. **Guerrini R and Filippi T**. Neuronal migration disorders, genetics, and epileptogenesis. *J Child Neurol* 20: 287-299, 2005.

139. **Guerrini R, Genton P, Bureau M, Parmeggiani A, Salas-Puig X, Santucci M, Bonanni P, Ambrosetto G and Dravet C**. Multilobar polymicrogyria, intractable drop attack seizures, and sleep-related electrical status epilepticus. *Neurology* 51: 504-512, 1998.

140. **Guerrini R, Sicca F and Parmeggiani L**. Epilepsy and malformations of the cerebral cortex. *Epileptic Disord* 5 Suppl 2: S9-26, 2003.

141. **Gupta A, Wang Y and Markram H**. Organizing principles for a diversity of GABAergic interneurons and synapses in the neocortex. *Science* 287: 273-278, 2000.

142. **Hablitz JJ and Defazio RA**. Altered receptor subunit expression in rat neocortical malformations. *Epilepsia* 41 Suppl 6: S82-S85, 2000.

143. **Hammond V, So E, Gunnersen J, Valcanis H, Kalloniatis M and Tan SS**. Layer positioning of late-born cortical interneurons is dependent on Reelin but not p35 signaling. *J Neurosci* 26: 1646-1655, 2006.

144. **Hauser WA**. *Epilepsy, A Comprehensive Textbook*. Philadelphia: Lippincott-Raven, 1998.

145. **Hauser WA, Annegers JF and Rocca WA**. Descriptive epidemiology of epilepsy: contributions of population-based studies from Rochester, Minnesota. *Mayo Clin Proc* 71: 576-586, 1996.

146. **Hayashi N, Tsutsumi Y and Barkovich AJ**. Polymicrogyria without porencephaly/schizencephaly. MRI analysis of the spectrum and the prevalence of macroscopic findings in the clinical population. *Neuroradiology* 44: 647-655, 2002.

147. **Helbig I, Scheffer IE, Mulley JC and Berkovic SF**. Navigating the channels and beyond: unravelling the genetics of the epilepsies. *Lancet Neurol* 7: 231-245, 2008.

www.manaraa.com

148. **Herman AE, Galaburda AM, Fitch RH, Carter AR and Rosen GD**. Cerebral microgyria, thalamic cell size and auditory temporal processing in male and female rats. *Cereb Cortex* 7: 453-464, 1997.

149. **Hestrin S**. Different glutamate receptor channels mediate fast excitatory synaptic currents in inhibitory and excitatory cortical neurons. *Neuron* 11: 1083-1091, 1993.

150. **Heuss C, Scanziani M, Gahwiler BH and Gerber U**. G-protein-independent signaling mediated by metabotropic glutamate receptors. *Nat Neurosci* 2: 1070-1077, 1999.

151. **Hirotsune S, Fleck MW, Gambello MJ, Bix GJ, Chen A, Clark GD, Ledbetter DH, McBain CJ and Wynshaw-Boris A**. Graded reduction of Pafah1b1 (Lis1) activity results in neuronal migration defects and early embryonic lethality [see comments]. *Nat Genet* 19: 333-339, 1998.

152. **Hof PR, Glezer II, Condé F, Flagg RA, Rubin MB, Nimchinsky EA and Vogt W**. Cellular distribution of the calcium-binding proteins parvalbumin, calbindin, and calretinin in the neocortex of mammals: phylogenetic and developmental patterns. *J Chem Neuroanat* 16: 77-116, 1999.

153. **Houser CR, Hendry SH, Jones EG and Vaughn JE**. Morphological diversity of immunocytochemically identified GABA neurons in the monkey sensory-motor cortex. *J Neurocytol* 12: 617-638, 1983.

154. **Ito I, Kohda A, Tanabe S, Hirose E, Hayashi M, Mitsunaga S and Sugiyama H**. 3,5-Dihydroxyphenyl-glycine: a potent agonist of metabotropic glutamate receptors. *Neuroreport* 3: 1013-1016, 1992.

155. **Jacobs KM, Graber KD, Kharazia VN, Parada I and Prince DA**. Postlesional epilepsy: the ultimate brain plasticity. *Epilepsia* 41 Suppl 6: S153-S161, 2000.

156. **Jacobs KM, Gutnick MJ and Prince DA**. Hyperexcitability in a model of cortical maldevelopment. *Cereb Cortex* 6: 514-523, 1996.

www.manaraa.com

157. **Jacobs KM, Hwang BJ and Prince DA**. Focal epileptogenesis in a rat model of polymicrogyria. *J Neurophysiol* 81: 159-173, 1999.

158. **Jacobs KM, Kharazia VN and Prince DA**. Mechanisms underlying epileptogenesis in cortical malformations. *Epilepsy Res* 36: 165-188, 1999.

159. **Jacobs KM, Mogensen M, Warren L and Prince DA**. Experimental microgyri disrupt the barrel field pattern in rat somatosensory cortex. *Cerebral Cortex* 9: 733-744, 1999.

160. **Jacobs KM and Prince DA**. Excitatory and inhibitory postsynaptic currents in a rat model of epileptogenic microgyria. *J Neurophysiol* 93: 687-696, 2005.

161. **Jallon P, Loiseau P and Loiseau J**. Newly diagnosed unprovoked epileptic seizures: presentation at diagnosis in CAROLE study. Coordination Active du Reseau Observatoire Longitudinal de l' Epilepsie. *Epilepsia* 42: 464-475, 2001.

162. **Jansen LA, Uhlmann EJ, Crino PB, Gutmann DH and Wong M**. Epileptogenesis and reduced inward rectifier potassium current in tuberous sclerosis complex-1-deficient astrocytes. *Epilepsia* 46: 1871-1880, 2005.

163. **Jesse CR, Savegnago L, Rocha JB and Nogueira CW**. Neuroprotective effect caused by MPEP, an antagonist of metabotropic glutamate receptor mGluR5, on seizures induced by pilocarpine in 21-day-old rats. *Brain Res* 1198: 197-203, 2008.

164. **Jung HY, Staff NP and Spruston N**. Action potential bursting in subicular pyramidal neurons is driven by a calcium tail current. *J Neurosci* 21: 3312-3321, 2001.

165. **Jung S, Jones TD, Lugo JN, Jr., Sheerin AH, Miller JW, D'Ambrosio R, Anderson AE and Poolos NP**. Progressive dendritic HCN channelopathy during epileptogenesis in the rat pilocarpine model of epilepsy. *J Neurosci* 27: 13012-13021, 2007.

www.manaraa.com

166. **Kamal A, Notenboom RG, De Graan PN and Ramakers GM**. Persistent changes in action potential broadening and the slow afterhyperpolarization in rat CA1 pyramidal cells after febrile seizures. *Eur J Neurosci* 23: 2230-2234, 2006.

167. **Karr L and Rutecki PA**. Activity-dependent induction and maintenance of epileptiform activity produced by group I metabotropic glutamate receptors in the rat hippocampal slice. *Epilepsy Res* 2008.

168. **Kawabata S, Tsutsumi R, Kohara A, Yamaguchi T, Nakanishi S and Okada M**. Control of calcium oscillations by phosphorylation of metabotropic glutamate receptors. *Nature* 383: 89-92, 1996.

169. **Kawaguchi Y**. Groupings of nonpyramidal and pyramidal cells with specific physiological and morphological characteristics in rat frontal cortex. *J Neurophysiol* 69: 416-431, 1993.

170. **Kawaguchi Y**. Physiological subgroups of nonpyramidal cells with specific morphological characteristics in layer II/III of rat frontal cortex. *J Neurosci* 15: 2638-2655, 1995.

171. **Kawaguchi Y**. Selective cholinergic modulation of cortical GABAergic cell subtypes. *J Neurophysiol* 78: 1743-1747, 1997.

172. **Kawaguchi Y and Kondo S**. Parvalbumin, somatostatin and cholecystokinin as chemical markers for specific GABAergic interneuron types in the rat frontal cortex. *J Neurocytol* 31: 277-287, 2002.

173. **Kawaguchi Y and Kubota Y**. Correlation of physiological subgroupings of nonpyramidal cells with parvalbumin- and calbindinD28k-immunoreactive neurons in layer V of rat frontal cortex. *J Neurophysiol* 70: 387-396, 1993.

174. **Kawaguchi Y and Kubota Y**. Physiological and morphological identification of somatostatin- or vasoactive intestinal polypeptide-containing cells among GABAergic cell subtypes in rat frontal cortex. *J Neurosci* 16: 2701-2715, 1996.

175. **Kawaguchi Y and Kubota Y**. GABAergic cell subtypes and their synaptic connections in rat frontal cortex. *Cereb Cortex* 7: 476-486, 1997.

www.manaraa.com

176. **Kellinghaus C, Moddel G, Shigeto H, Ying Z, Jacobsson B, Gonzalez-Martinez J, Burrier C, Janigro D and Najm IM**. Dissociation between in vitro and in vivo epileptogenicity in a rat model of cortical dysplasia. *Epileptic Disord* 9: 11-19, 2007.

177. **Kerner JA, Standaert DG, Penney JB, Jr., Young AB and Landwehrmeyer GB**. Expression of group one metabotropic glutamate receptor subunit mRNAs in neurochemically identified neurons in the rat neostriatum, neocortex, and hippocampus. *Brain Res Mol Brain Res* 48: 259-269, 1997.

178. **Kim HG, Beierlein M and Connors BW**. Inhibitory control of excitable dendrites in neocortex. *J Neurophysiol* 74: 1810-1814, 1995.

179. **Kim J, Jung SC, Clemens AM, Petralia RS and Hoffman DA**. Regulation of dendritic excitability by activity-dependent trafficking of the A-type K+ channel subunit Kv4.2 in hippocampal neurons. *Neuron* 54: 933-947, 2007.

180. **Kim J, Wei DS and Hoffman DA**. Kv4 potassium channel subunits control action potential repolarization and frequency-dependent broadening in rat hippocampal CA1 pyramidal neurones. *J Physiol* 569: 41-57, 2005.

181. **Kingston AE, Griffey K, Johnson MP, Chamberlain MJ, Kelly G, Tomlinson R, Wright RA, Johnson BG, Schoepp DD, Harris JR, Clark BP, Baker RS and Tizzano JT**. Inhibition of group I metabotropic glutamate receptor responses in vivo in rats by a new generation of carboxyphenylglycine-like amino acid antagonists. *Neurosci Lett* %20;330: 127-130, 2002.

182. **Kirschstein T, Bauer M, Muller L, Ruschenschmidt C, Reitze M, Becker AJ, Schoch S and Beck H**. Loss of metabotropic glutamate receptor-dependent long-term depression via downregulation of mGluR5 after status epilepticus. *J Neurosci* 27: 7696-7704, 2007.

183. **Klaassen A, Glykys J, Maguire J, Labarca C, Mody I and Boulter J**. Seizures and enhanced cortical GABAergic inhibition in two mouse models of human autosomal dominant nocturnal frontal lobe epilepsy. *Proc Natl Acad Sci U S A* 103: 19152-19157, 2006.

www.manaraa.com

184. **Kubota Y, Hattori R and Yui Y**. Three distinct subpopulations of GABAergic neurons in rat frontal agranular cortex. *Brain Res* 649: 159-173, 1994.

185. **Kubota Y and Kawaguchi Y**. Dependence of GABAergic synaptic areas on the interneuron type and target size. *J Neurosci* 20: 375-386, 2000.

186. **Kuzniecky R, Andermann F and Guerrini R**. The epileptic spectrum in the congenital bilateral perisylvian syndrome. CBPS Multicenter Collaborative Study. *Neurology* 44: 379-385, 1994.

187. **Kwan P and Brodie MJ**. Effectiveness of first antiepileptic drug. *Epilepsia* 42: 1255-1260, 2001.

188. **Lagae L**. Cortical malformations: a frequent cause of epilepsy in children. *Eur J Pediatr* 159: 555-562, 2000.

189. **Lau D, Vega-Saenz de Miera EC, Contreras D, Ozaita A, Harvey M, Chow A, Noebels JL, Paylor R, Morgan JI, Leonard CS and Rudy B**. Impaired fast-spiking, suppressed cortical inhibition, and increased susceptibility to seizures in mice lacking Kv3.2 K+ channel proteins. *J Neurosci* 20: 9071-9085, 2000.

190. **Laurie DJ, Wisden W and Seeburg PH**. The distribution of thirteen GABAA receptor subunit mRNAs in the rat brain. III. Embryonic and postnatal development. *J Neurosci* 12: 4151-4172, 1992.

191. **Lea PM and Faden AI**. Metabotropic glutamate receptor subtype 5 antagonists MPEP and MTEP. *CNS Drug Rev* 12: 149-166, 2006.

192. **Lee KS, Schottler F, Collins JL, Lanzino G, Couture D, Rao A, Hiramatsu K, Goto Y, Hong SC, Caner H, Yamamoto H, Chen ZF, Bertram E, Berr S, Omary R, Scrable H, Jackson T, Goble J and Eisenman L**. A genetic animal model of human neocortical heterotopia associated with seizures. *J Neurosci* 17: 6236-6242, 1997.

193. **Leppik IE**. Zonisamide. *Epilepsia* 40 Suppl 5:S23-9.: S23-S29, 1999.

www.manaraa.com

194. **Leventer RJ, Guerrini R and Dobyns WB**. Malformations of cortical development and epilepsy. *Dialogues Clin Neurosci* 10: 47-62, 2008.

195. **Lim CC, Yin H, Loh NK, Chua VG, Hui F and Barkovich AJ**. Malformations of cortical development: high-resolution MR and diffusion tensor imaging of fiber tracts at 3T. *AJNR Am J Neuroradiol* 26: 61-64, 2005.

196. **Liu L, Zheng T, Morris MJ, Wallengren C, Clarke AL, Reid CA, Petrou S and O'Brien TJ**. The mechanism of carbamazepine aggravation of absence seizures. *J Pharmacol Exp Ther* 319: 790-798, 2006.

197. **Long MA, Cruikshank SJ, Jutras MJ and Connors BW**. Abrupt maturation of a spike-synchronizing mechanism in neocortex. *J Neurosci* 25: 7309-7316, 2005.

198. **Lopez-Bendito G, Shigemoto R, Fairen A and Lujan R**. Differential distribution of group I metabotropic glutamate receptors during rat cortical development. *Cereb Cortex* 12: 625-638, 2002.

199. **Luders H and Schuele SU**. Epilepsy surgery in patients with malformations of cortical development. *Curr Opin Neurol* 19: 169-174, 2006.

200. **Luhmann HJ, Huston JP and Hasenohrl RU**. Contralateral increase in thigmotactic scanning following unilateral barrel-cortex lesion in mice. *Behav Brain Res* 157: 39-43, 2005.

201. **Luhmann HJ, Karpuk N, Qu M and Zilles K**. Characterization of neuronal migration disorders in neocortical structures. II. Intracellular in vitro recordings. *J Neurophysiol* 80: 92-102, 1998.

202. **Luhmann HJ and Raabe K**. Characterization of neuronal migration disorders in neocortical structures: I. Expression of epileptiform activity in an animal model. *Epilepsy Res* 26: 67-74, 1996.

203. **Luhmann HJ, Raabe K, Qu M and Zilles K**. Characterization of neuronal migration disorders in neocortical structures: extracellular in vitro recordings. *Eur J Neurosci* 10: 3085-3094, 1998.

www.manaraa.com

204. **Lujan R, Roberts JD, Shigemoto R, Ohishi H and Somogyi P**. Differential plasma membrane distribution of metabotropic glutamate receptors mGluR1 alpha, mGluR2 and mGluR5, relative to neurotransmitter release sites. *J Chem Neuroanat* 13: 219-241, 1997.

205. **Malherbe P, Kratochwil N, Muhlemann A, Zenner MT, Fischer C, Stahl M, Gerber PR, Jaeschke G and Porter RH**. Comparison of the binding pockets of two chemically unrelated allosteric antagonists of the mGlu5 receptor and identification of crucial residues involved in the inverse agonism of MPEP. *J Neurochem* 98: 601-615, 2006.

206. **Mann EO and Mody I**. The multifaceted role of inhibition in epilepsy: seizure-genesis through excessive GABAergic inhibition in autosomal dominant nocturnal frontal lobe epilepsy. *Curr Opin Neurol* 21: 155-160, 2008.

207. **Mannaioni G, Marino MJ, Valenti O, Traynelis SF and Conn PJ**. Metabotropic glutamate receptors 1 and 5 differentially regulate CA1 pyramidal cell function. *J Neurosci* 21: 5925-5934, 2001.

208. **Mao L and Wang JQ**. Phosphorylation of cAMP response element-binding protein in cultured striatal neurons by metabotropic glutamate receptor subtype 5. *J Neurochem* 84: 233-243, 2003.

209. **Markram H, Toledo-Rodriguez M, Wang Y, Gupta A, Silberberg G and Wu C**. Interneurons of the neocortical inhibitory system. *Nat Rev Neurosci* 5: 793-807, 2004.

210. **Markram H, Wang Y and Tsodyks M**. Differential signaling via the same axon of neocortical pyramidal neurons. *Proc Natl Acad Sci U S A* 95: 5323-5328, 1998.

211. **Marret S, Mukendi R, Gadisseux JF, Gressens P and Evrard P**. Effect of ibotenate on brain development: an excitotoxic mouse model of microgyria and posthypoxic-like lesions. *J Neuropathol Exp Neurol* 54: 358-370, 1995.

212. **Martina M, Schultz JH, Ehmke H, Monyer H and Jonas P**. Functional and molecular differences between voltage-gated K+ channels of fast-spiking interneurons and pyramidal neurons of rat hippocampus. *J Neurosci* 18: 8111-8125, 1998.

www.manaraa.com

213. **Marty S and Onteniente B**. The expression pattern of somatostatin and calretinin by postnatal hippocampal interneurons is regulated by activity-dependent and -independent determinants. *Neuroscience* 80: 79-88, 1997.

214. **Massengill JL, Smith MA, Son DI and O'Dowd DK**. Differential expression of K4-AP currents and Kv3.1 potassium channel transcripts in cortical neurons that develop distinct firing phenotypes. *J Neurosci* 17: 3136-3147, 1997.

215. **Mathern GW, Cepeda C, Hurst RS, Flores-Hernandez J, Mendoza D and Levine MS**. Neurons recorded from pediatric epilepsy surgery patients with cortical dysplasia. *Epilepsia* 41 Suppl 6: S162-S167, 2000.

216. **Matsuo F**. Lamotrigine. *Epilepsia* 40 Suppl 5:S30-6.: S30-S36, 1999.

217. **McBain CJ and Fisahn A**. Interneurons unbound. *Nat Rev Neurosci* 2: 11-23, 2001.

218. **McBain CJ and Mayer ML**. N-methyl-D-aspartic acid receptor structure and function. *Physiol Rev* 74: 723-760, 1994.

219. **McCormick DA, Connors BW, Lighthall JW and Prince DA**. Comparative electrophysiology of pyramidal and sparsely spiny stellate neurons of the neocortex. *J Neurophysiol* 54: 782-806, 1985.

220. **McCormick DA and Prince DA**. Post-natal development of electrophysiological properties of rat cerebral cortical pyramidal neurones. *J Physiol (Lond)* 393: 743-762, 1987.

221. **Merlin LR**. Group I mGluR-mediated silent induction of long-lasting epileptiform discharges. *J Neurophysiol* 82: 1078-1081, 1999.

222. **Merlin LR**. Differential roles for mGluR1 and mGluR5 in the persistent prolongation of epileptiform bursts. *J Neurophysiol* 87: 621-625, 2002.

www.manaraa.com

223. **Metin C, Baudoin JP, Rakic S and Parnavelas JG**. Cell and molecular mechanisms involved in the migration of cortical interneurons. *Eur J Neurosci* 23: 894-900, 2006.

224. **Michelson HB and Wong RK**. Synchronization of inhibitory neurones in the guinea-pig hippocampus in vitro. *J Physiol (Lond)* 477 (Pt 1): 35-45, 1994.

225. **Miles R and Poncer JC**. Metabotropic glutamate receptors mediate a post-tetanic excitation of guinea-pig hippocampal inhibitory neurones. *J Physiol (Lond)* 463: 461-473, 1993.

226. **Mione MC, Danevic C, Boardman P, Harris B and Parnavelas JG**. Lineage analysis reveals neurotransmitter (GABA or glutamate) but not calcium-binding protein homogeneity in clonally related cortical neurons. *J Neurosci* 14: 107-123, 1994.

227. **Mirski MA and Varelas PN**. Seizures and status epilepticus in the critically ill. *Crit Care Clin* 24: 115-47, ix, 2008.

228. **Misonou H, Mohapatra DP, Park EW, Leung V, Zhen D, Misonou K, Anderson AE and Trimmer JS**. Regulation of ion channel localization and phosphorylation by neuronal activity. *Nat Neurosci* 7: 711-718, 2004.

229. **Moldrich RX, Chapman AG, De Sarro G and Meldrum BS**. Glutamate metabotropic receptors as targets for drug therapy in epilepsy. *Eur J Pharmacol* 476: 3-16, 2003.

230. **Momiyama T and Zaborszky L**. Somatostatin presynaptically inhibits both GABA and glutamate release onto rat basal forebrain cholinergic neurons. *J Neurophysiol* 96: 686-694, 2006.

231. **Moroni F, Lombardi G, Thomsen C, Leonardi P, Attucci S, Peruginelli F, Torregrossa SA, Pellegrini-Giampietro DE, Luneia R and Pellicciari R**. Pharmacological characterization of 1-aminoindan-1,5-dicarboxylic acid, a potent mGluR1 antagonist. *J Pharmacol Exp Ther* 281: 721-729, 1997.

www.manaraa.com

232. **Moroni RF, Inverardi F, Regondi MC, Panzica F, Spreafico R and Frassoni C**. Altered spatial distribution of PV-cortical cells and dysmorphic neurons in the somatosensory cortex of BCNU-treated rat model of cortical dysplasia. *Epilepsia* 49: 872-887, 2008.

233. **Mudo G, Trovato-Salinaro A, Caniglia G, Cheng Q and Condorelli DF**. Cellular localization of mGluR3 and mGluR5 mRNAs in normal and injured rat brain. *Brain Res* 1149: 1-13, 2007.

234. **Mukhin A, Fan L and Faden AI**. Activation of metabotropic glutamate receptor subtype mGluR1 contributes to post-traumatic neuronal injury. *J Neurosci* 16: 6012-6020, 1996.

235. **Nadarajah B, Alifragis P, Wong RO and Parnavelas JG**. Ventricle-directed migration in the developing cerebral cortex. *Nat Neurosci* 5: 218-224, 2002.

236. **Naie K and Manahan-Vaughan D**. Regulation by metabotropic glutamate receptor 5 of LTP in the dentate gyrus of freely moving rats: relevance for learning and memory formation. *Cereb Cortex* 14: 189-198, 2004.

237. **Nery S, Fishell G and Corbin JG**. The caudal ganglionic eminence is a source of distinct cortical and subcortical cell populations. *Nat Neurosci* 5: 1279-1287, 2002.

238. **Nicoletti F, Bruno V, Copani A, Casabona G and Knopfel T**. Metabotropic glutamate receptors: a new target for the therapy of neurodegenerative disorders? *Trends Neurosci* 19: 267-271, 1996.

239. **Nitsch R, Leranth C and Frotscher M**. Most somatostatin-immunoreactive neurons in the rat fascia dentata do not contain the calcium-binding protein parvalbumin. *Brain Res* 528: 327-329, 1990.

240. **Noctor SC, Palmer SL, Hasling T and Juliano SL**. Interference with the development of early generated neocortex results in disruption of radial glia and abnormal formation of neocortical layers. *Cereb Cortex* 9: 121-136, 1999.

www.manaraa.com

241. **Notenboom RG, Hampson DR, Jansen GH, van Rijen PC, van Veelen CW, van Nieuwenhuizen O and De Graan PN**. Up-regulation of hippocampal metabotropic glutamate receptor 5 in temporal lobe epilepsy patients. *Brain* 129: 96-107, 2006.

242. **Nusser Z, Mulvihill E, Streit P and Somogyi P**. Subsynaptic segregation of metabotropic and ionotropic glutamate receptors as revealed by immunogold localization. *Neuroscience* 61: 421-427, 1994.

243. **O'Rourke NA, Chenn A and McConnell SK**. Postmitotic neurons migrate tangentially in the cortical ventricular zone. *Development* 124: 997-1005, 1997.

244. **Oka A and Takashima S**. The up-regulation of metabotropic glutamate receptor 5 (mGluR5) in Down's syndrome brains. *Acta Neuropathol* 97: 275-278, 1999.

245. **Pagano A, Ruegg D, Litschig S, Stoehr N, Stierlin C, Heinrich M, Floersheim P, Prezeau L, Carroll F, Pin JP, Cambria A, Vranesic I, Flor PJ, Gasparini F and Kuhn R**. The non-competitive antagonists 2-methyl-6-(phenylethynyl)pyridine and 7-hydroxyiminocyclopropan[b]chromen-1a-carboxylic acid ethyl ester interact with overlapping binding pockets in the transmembrane region of group I metabotropic glutamate receptors. *J Biol Chem* 275: 33750-33758, 2000.

246. **Palmini A, Andermann F, Olivier A, Tampieri D, Robitaille Y, Andermann E and Wright G**. Focal neuronal migration disorders and intractable partial epilepsy: a study of 30 patients. *Ann Neurol* 30: 741-749, 1991.

247. **Palucha A and Pilc A**. Metabotropic glutamate receptor ligands as possible anxiolytic and antidepressant drugs. *Pharmacol Ther* 115: 116-147, 2007.

248. **Pang T, Atefy R and Sheen V**. Malformations of cortical development. *Neurologist* 14: 181-191, 2008.

249. **Paspalas CD and Papadopoulos GC**. Serotoninergic afferents preferentially innervate distinct subclasses of peptidergic interneurons in the rat visual cortex. *Brain Res* 891: 158-167, 2001.

www.manaraa.com

250. **Patrick SL, Connors BW and Landisman CE**. Developmental changes in somatostatin-positive interneurons in a freeze-lesion model of epilepsy. *Epilepsy Res* Epub ahead of print: 2006.

251. **Patz S, Grabert J, Gorba T, Wirth MJ and Wahle P**. Parvalbumin expression in visual cortical interneurons depends on neuronal activity and TrkB ligands during an Early period of postnatal development. *Cereb Cortex* 14: 342-351, 2004.

252. **Peiffer AM, Rosen GD and Fitch RH**. Sex differences in rapid auditory processing deficits in microgyric rats. *Brain Res Dev Brain Res* 148: 53-57, 2004.

253. **Peinado A, Yuste R and Katz LC**. Extensive dye coupling between rat neocortical neurons during the period of circuit formation. *Neuron* 10: 103-114, 1993.

254. **Pellicciari R, Luneia R, Costantino G, Marinozzi M, Natalini B, Jakobsen P, Kanstrup A, Lombardi G, Moroni F and Thomsen C**. 1-Aminoindan-1,5-dicarboxylic acid: a novel antagonist at phospholipase C-linked metabotropic glutamate receptors. *J Med Chem* 38: 3717-3719, 1995.

255. **Peters O, Redecker C, Hagemann G, Bruehl C, Luhmann HJ and Witte OW**. Impaired synaptic plasticity in the surround of perinatally acquired [correction of aquired] dysplasia in rat cerebral cortex. *Cereb Cortex* 14: 1081-1087, 2004.

256. **Petralia RS, Wang YX, Singh S, Wu C, Shi L, Wei J and Wenthold RJ**. A monoclonal antibody shows discrete cellular and subcellular localizations of mGluR1 alpha metabotropic glutamate receptors. *J Chem Neuroanat* 13: 77-93, 1997.

257. **Piao X, Basel-Vanagaite L, Straussberg R, Grant PE, Pugh EW, Doheny K, Doan B, Hong SE, Shugart YY and Walsh CA**. An autosomal recessive form of bilateral frontoparietal polymicrogyria maps to chromosome 16q12.2-21. *Am J Hum Genet* 70: 1028-1033, 2002.

258. **Piao X, Chang BS, Bodell A, Woods K, Benzeev B, Topcu M, Guerrini R, Goldberg-Stern H, Sztriha L, Dobyns WB, Barkovich AJ and Walsh CA**.

www.manaraa.com

Genotype-phenotype analysis of human frontoparietal polymicrogyria syndromes. *Ann Neurol* 58: 680-687, 2005.

259. **Piao X, Hill RS, Bodell A, Chang BS, Basel-Vanagaite L, Straussberg R, Dobyns WB, Qasrawi B, Winter RM, Innes AM, Voit T, Ross ME, Michaud JL, Descarie JC, Barkovich AJ and Walsh CA**. G protein-coupled receptor-dependent development of human frontal cortex. *Science* 303: 2033-2036, 2004.

260. **Pin JP and Acher F**. The metabotropic glutamate receptors: structure, activation mechanism and pharmacology. *Curr Drug Targets CNS Neurol Disord* 1: 297-317, 2002.

261. **Pin JP and Duvoisin R**. The metabotropic glutamate receptors: structure and functions. *Neuropharmacology* 34: 1-26, 1995.

262. **Pisani A, Bonsi P, Centonze D, Bernardi G and Calabresi P**. Functional coexpression of excitatory mGluR1 and mGluR5 on striatal cholinergic interneurons. *Neuropharmacology* 40: 460-463, 2001.

263. **Porter BE, Judkins AR, Clancy RR, Duhaime A, Dlugos DJ and Golden JA**. Dysplasia: a common finding in intractable pediatric temporal lobe epilepsy. *Neurology* 61: 365-368, 2003.

264. **Porter LL, Rizzo E and Hornung JP**. Dopamine affects parvalbumin expression during cortical development in vitro. *J Neurosci* 19: 8990-9003, 1999.

265. **Porter LL and White EL**. Afferent and efferent pathways of the vibrissal region of primary motor cortex in the mouse. *J Comp Neurol* 214: 279-289, 1983.

266. **Powell EM, Campbell DB, Stanwood GD, Davis C, Noebels JL and Levitt P**. Genetic disruption of cortical interneuron development causes region- and GABA cell type-specific deficits, epilepsy, and behavioral dysfunction. *J Neurosci* 23: 622-631, 2003.

267. **Prince DA**. Physiological mechanisms of focal epileptogenesis. *Epilepsia* 26 Suppl 1: S3-14, 1985.

www.manaraa.com

268. **Prince DA and Jacobs K**. Inhibitory function in two models of chronic epileptogenesis. *Epilepsy Res* 32: 83-92, 1998.

269. **Prince DA, Jacobs KM, Salin PA, Hoffman S and Parada I**. Chronic focal neocortical epileptogenesis: does disinhibition play a role? *Can J Physiol Pharmacol* 75: 500-507, 1997.

270. **Prince DA and Tseng GF**. Epileptogenesis in chronically injured cortex: in vitro studies. *J Neurophysiol* 69: 1276-1291, 1993.

271. **Ramon y Cajal S**. General Organization of the Cortex. In: Histology of the Nervous System of Man and Vertebrates, Vol II, New York: Oxford University Press, 1995, p. 429-485.

272. **Rash JE, Staines WA, Yasumura T, Patel D, Furman CS, Stelmack GL and Nagy JI**. Immunogold evidence that neuronal gap junctions in adult rat brain and spinal cord contain connexin-36 but not connexin-32 or connexin-43. *Proc Natl Acad Sci U S A* 97: 7573-7578, 2000.

273. **Redecker C, Luhmann HJ, Hagemann G, Fritschy JM and Witte OW**. Differential downregulation of GABAA receptor subunits in widespread brain regions in the freeze-lesion model of focal cortical malformations. *J Neurosci* 20: 5045-5053, 2000.

274. **Redecker C, Lutzenburg M, Gressens P, Evrard P, Witte OW and Hagemann G**. Excitability changes and glucose metabolism in experimentally induced focal cortical dysplasias. *Cereb Cortex* 8: 623-634, 1998.

275. **Reiner O, Carrozzo R, Shen Y, Wehnert M, Faustinella F, Dobyns WB, Caskey CT and Ledbetter DH**. Isolation of a Miller-Dieker lissencephaly gene containing G protein beta-subunit-like repeats. *Nature* 364: 717-721, 1993.

276. **Reyes A, Lujan R, Rozov A, Burnashev N, Somogyi P and Sakmann B**. Target-cell-specific facilitation and depression in neocortical circuits. *Nat Neurosci* 1: 279-285, 1998.

www.manaraa.com

277. **Ringstedt T, Linnarsson S, Wagner J, Lendahl U, Kokaia Z, Arenas E, Ernfors P and Ibanez CF**. BDNF regulates reelin expression and Cajal-Retzius cell development in the cerebral cortex. *Neuron* 21: 305-315, 1998.

278. **Rivera C, Voipio J, Payne JA, Ruusuvuori E, Lahtinen H, Lamsa K, Pirvola U, Saarma M and Kaila K**. The K+/Cl- co-transporter KCC2 renders GABA hyperpolarizing during neuronal maturation [see comments]. *Nature* 397: 251-255, 1999.

279. **Robbins RJ, Brines ML, Kim JH, Adrian T, de Lanerolle N, Welsh S and Spencer DD**. A selective loss of somatostatin in the hippocampus of patients with temporal lobe epilepsy. *Ann Neurol* 29: 325-332, 1991.

280. **Roberts PJ**. Pharmacological tools for the investigation of metabotropic glutamate receptors (mGluRs): phenylglycine derivatives and other selective antagonists--an update. *Neuropharmacology* 34: 813-819, 1995.

281. **Romano C, Sesma MA, McDonald CT, O'Malley K, van den Pol AN and Olney JW**. Distribution of metabotropic glutamate receptor mGluR5 immunoreactivity in rat brain. *J Comp Neurol* 355: 455-469, 1995.

282. **Roper SN**. In utero irradiation of rats as a model of human cerebrocortical dysgenesis: a review. *Epilepsy Res* 32: 63-74, 1998.

283. **Roper SN, Abraham LA and Streit WJ**. Exposure to in utero irradiation produces disruption of radial glia in rats. *Dev Neurosci* 19: 521-528, 1997.

284. **Roper SN, Eisenschenk S and King MA**. Reduced density of parvalbumin- and calbindin D28-immunoreactive neurons in experimental cortical dysplasia [In Process Citation]. *Epilepsy Res* 37: 63-71, 1999.

285. **Rosen GD, Bai J, Wang Y, Fiondella CG, Threlkeld SW, LoTurco JJ and Galaburda AM**. Disruption of neuronal migration by RNAi of Dyx1c1 results in neocortical and hippocampal malformations. *Cereb Cortex* 17: 2562-2572, 2007.

www.manaraa.com

286. **Rosen GD, Burstein D and Galaburda AM**. Changes in efferent and afferent connectivity in rats with induced cerebrocortical microgyria. *J Comp Neurol* 418: 423-440, 2000.

287. **Rosen GD, Herman AE and Galaburda AM**. Sex differences in the effects of early neocortical injury on neuronal size distribution of the medial geniculate nucleus in the rat are mediated by perinatal gonadal steroids. *Cereb Cortex* 9: 27-34, 1999.

288. **Rosen GD, Jacobs KM and Prince DA**. Effects of neonatal freeze lesions on expression of parvalbumin in rat neocortex. *Cereb Cortex* 8: 753-761, 1998.

289. **Rosen GD, Mesples B, Hendriks M and Galaburda AM**. Histometric changes and cell death in the thalamus after neonatal neocortical injury in the rat. *Neuroscience* Epub ahead of print: 2006.

290. **Rosen GD, Press DM, Sherman GF and Galaburda AM**. The development of induced cerebrocortical microgyria in the rat. *J Neuropathol Exp Neurol* 51: 601-611, 1992.

291. **Rosen GD, Sherman GF and Galaburda AM**. Birthdates of neurons in induced microgyria. *Brain Res* 727: 71-78, 1996.

292. **Ross NR and Porter LL**. Effects of dopamine and estrogen upon cortical neurons that express parvalbumin in vitro. *Brain Res Dev Brain Res* 137: 23-34, 2002.

293. **Rutecki PA, Lebeda FJ and Johnston D**. 4-Aminopyridine produces epileptiform activity in hippocampus and enhances synaptic excitation and inhibition. *J Neurophysiol* 57: 1911-1924, 1987.

294. **Salin P, Tseng GF, Hoffman S, Parada I and Prince DA**. Axonal sprouting in layer V pyramidal neurons of chronically injured cerebral cortex. *J Neurosci* 15: 8234-8245, 1995.

295. **Salt TE, Binns KE, Turner JP, Gasparini F and Kuhn R**. Antagonism of the mGlu5 agonist 2-chloro-5-hydroxyphenylglycine by the novel selective mGlu5

www.manaraa.com

antagonist 6-methyl-2-(phenylethynyl)-pyridine (MPEP) in the thalamus. *Br J Pharmacol* 127: 1057-1059, 1999.

296. **Sanabria ER, Su H and Yaari Y**. Initiation of network bursts by Ca2+-dependent intrinsic bursting in the rat pilocarpine model of temporal lobe epilepsy. *J Physiol* 532: 205-216, 2001.

297. **Sancini G, Franceschetti S, Battaglia G, Colacitti C, Di Luca M, Spreafico R and Avanzini G**. Dysplastic neocortex and subcortical heterotopias in methylazoxymethanol-treated rats: an intracellular study of identified pyramidal neurones. *Neurosci Lett* 246: 181-185, 1998.

298. **Sayin U and Rutecki PA**. Group I metabotropic glutamate receptor activation produces prolonged epileptiform neuronal synchronization and alters evoked population responses in the hippocampus. *Epilepsy Res* 53: 186-195, 2003.

299. **Scantlebury MH, Gibbs SA, Foadjo B, Lema P, Psarropoulou C and Carmant L**. Febrile seizures in the predisposed brain: a new model of temporal lobe epilepsy. *Ann Neurol* 58: 41-49, 2005.

300. **Scantlebury MH, Ouellet PL, Psarropoulou C and Carmant L**. Freeze lesion-induced focal cortical dysplasia predisposes to atypical hyperthermic seizures in the immature rat. *Epilepsia* 45: 592-600, 2004.

301. **Schachter SC**. Tiagabine. *Epilepsia* 40 Suppl 5:S17-22.: S17-S22, 1999.

302. **Schoepp DD**. Unveiling the functions of presynaptic metabotropic glutamate receptors in the central nervous system. *J Pharmacol Exp Ther* 299: 12-20, 2001.

303. **Schoepp DD and Conn PJ**. Metabotropic glutamate receptors in brain function and pathology. *Trends Pharmacol Sci* 14: 13-20, 1993.

304. **Schoepp DD, Goldsworthy J, Johnson BG, Salhoff CR and Baker SR**. 3,5-dihydroxyphenylglycine is a highly selective agonist for phosphoinositide-linked metabotropic glutamate receptors in the rat hippocampus. *J Neurochem* 63: 769-772, 1994.

www.manaraa.com

305. **Schoepp DD, Jane DE and Monn JA**. Pharmacological agents acting at subtypes of metabotropic glutamate receptors. *Neuropharmacology* 38: 1431-1476, 1999.

306. **Schuele SU and Luders HO**. Intractable epilepsy: management and therapeutic alternatives. *Lancet Neurol* 7: 514-524, 2008.

307. **Schwartzkroin PA and Walsh CA**. Cortical malformations and epilepsy. *Ment Retard Dev Disabil Res Rev* 6: 268-280, 2000.

308. **Schwarz P, Stichel CC and Luhmann HJ**. Characterization of neuronal migration disorders in neocortical structures: loss or preservation of inhibitory interneurons? *Epilepsia* 41: 781-787, 2000.

309. **Sedel F, Gourfinkel-An I, Lyon-Caen O, Baulac M, Saudubray JM and Navarro V**. Epilepsy and inborn errors of metabolism in adults: a diagnostic approach. *J Inherit Metab Dis* 30: 846-854, 2007.

310. **Sekiyama N, Hayashi Y, Nakanishi S, Jane DE, Tse HW, Birse EF and Watkins JC**. Structure-activity relationships of new agonists and antagonists of different metabotropic glutamate receptor subtypes. *Br J Pharmacol* 117: 1493-1503, 1996.

311. **Selke K, Muller A, Kukley M, Schramm J and Dietrich D**. Firing pattern and calbindin-D28k content of human epileptic granule cells. *Brain Res* 1120: 191-201, 2006.

312. **Shah MM, Anderson AE, Leung V, Lin X and Johnston D**. Seizure-induced plasticity of h channels in entorhinal cortical layer III pyramidal neurons. *Neuron* 44: 495-508, 2004.

313. **Shigemoto R, Kinoshita A, Wada E, Nomura S, Ohishi H, Takada M, Flor PJ, Neki A, Abe T, Nakanishi S and Mizuno N**. Differential presynaptic localization of metabotropic glutamate receptor subtypes in the rat hippocampus. *J Neurosci* 17: 7503-7522, 1997.

www.manaraa.com

314. **Shigemoto R, Nakanishi S and Mizuno N**. Distribution of the mRNA for a metabotropic glutamate receptor (mGluR1) in the central nervous system: an in situ hybridization study in adult and developing rat. *J Comp Neurol* 322: 121-135, 1992.

315. **Shigemoto R, Nomura S, Ohishi H, Sugihara H, Nakanishi S and Mizuno N**. Immunohistochemical localization of a metabotropic glutamate receptor, mGluR5, in the rat brain. *Neurosci Lett* 163: 53-57, 1993.

316. **Shimizu-Okabe C, Okabe A, Kilb W, Sato K, Luhmann HJ and Fukuda A**. Changes in the expression of cation-Cl- cotransporters, NKCC1 and KCC2, during cortical malformation induced by neonatal freeze-lesion. *Neurosci Res* 59: 288-295, 2007.

317. **Sicca F, Kelemen A, Genton P, Das S, Mei D, Moro F, Dobyns WB and Guerrini R**. Mosaic mutations of the LIS1 gene cause subcortical band heterotopia. *Neurology* 61: 1042-1046, 2003.

318. **Sinclair DB, Aronyk K, Snyder T, McKean JD, Wheatley M, Gross D, Bastos A, Ahmed SN, Hao C and Colmers W**. Extratemporal resection for childhood epilepsy. *Pediatr Neurol* 30: 177-185, 2004.

319. **Singer W**. Neuronal synchrony: a versatile code for the definition of relations? *Neuron* 24: 49-25, 1999.

320. **Sladeczek F, Recasens M and Bockaert J**. A new mechanism for glutamate receptor action: phosphoinositide hydrolysis. *Trends Neurosci* 11: 545-549, 1988.

321. **Sloviter RS**. Decreased hippocampal inhibition and a selective loss of interneurons in experimental epilepsy. *Science* 235: 73-76, 1987.

322. **Solbach S and Celio MR**. Ontogeny of the calcium binding protein parvalbumin in the rat nervous system. *Anat Embryol (Berl)* 184: 103-124, 1991.

323. **Somogyi P**. A specific 'axo-axonal' interneuron in the visual cortex of the rat. *Brain Res* 136: 345-350, 1977.

www.manaraa.com

324. **Somogyi P, Tamas G, Lujan R and Buhl EH**. Salient features of synaptic organisation in the cerebral cortex. *Brain Res Brain Res Rev* 26: 113-135, 1998.

325. **Sourdet V, Russier M, Daoudal G, Ankri N and Debanne D**. Long-term enhancement of neuronal excitability and temporal fidelity mediated by metabotropic glutamate receptor subtype 5. *J Neurosci* 23: 10238-10248, 2003.

326. **Stinehelfer S, Vruwink M and Burette A**. Immunolocalization of mGluR1alpha in specific populations of local circuit neurons in the cerebral cortex. *Brain Res* 861: 37-44, 2000.

327. **Stoop R, Conquet F and Pralong E**. Determination of group I metabotropic glutamate receptor subtypes involved in the frequency of epileptiform activity in vitro using mGluR1 and mGluR5 mutant mice. *Neuropharmacology* 44: 157-162, 2003.

328. **Sun C, Mtchedlishvili Z, Bertram EH, Erisir A and Kapur J**. Selective loss of dentate hilar interneurons contributes to reduced synaptic inhibition of granule cells in an electrical stimulation-based animal model of temporal lobe epilepsy. *J Comp Neurol* 500: 876-893, 2007.

329. **Sun QQ, Huguenard JR and Prince DA**. REORGANIZATION OF BARREL CIRCUITS LEADS TO THALAMICALLY-EVOKED CORTICAL EPILEPTIFORM ACTIVITY. *Thalamus Relat Syst* 3: 261-273, 2005.

330. **Sun QQ, Huguenard JR and Prince DA**. Barrel cortex microcircuits: thalamocortical feedforward inhibition in spiny stellate cells is mediated by a small number of fast-spiking interneurons. *J Neurosci* 26: 1219-1230, 2006.

331. **Super H, Perez SP and Soriano E**. Survival of Cajal-Retzius cells after cortical lesions in newborn mice: a possible role for Cajal-Retzius cells in brain repair. *Brain Res Dev Brain Res* 98: 9-14, 1997.

332. **Sussel L, Marin O, Kimura S and Rubenstein JL**. Loss of Nkx2.1 homeobox gene function results in a ventral to dorsal molecular respecification within the basal telencephalon: evidence for a transformation of the pallidum into the striatum. *Development* 126: 3359-3370, 1999.

www.manaraa.com

333. **Szydlowska K, Kaminska B, Baude A, Parsons CG and Danysz W**. Neuroprotective activity of selective mGlu1 and mGlu5 antagonists in vitro and in vivo. *Eur J Pharmacol* 554: 18-29, 2007.

334. **Takanashi J, Oba H, Barkovich AJ, Tada H, Tanabe Y, Yamanouchi H, Fujimoto S, Kato M, Kawatani M, Sudo A, Ozawa H, Okanishi T, Ishitobi M, Maegaki Y and Koyasu Y**. Diffusion MRI abnormalities after prolonged febrile seizures with encephalopathy. *Neurology* 66: 1304-1309, 2006.

335. **Takase K, Shigeto H, Suzuki SO, Kikuchi H, Ohyagi Y and Kira J**. Prenatal freeze lesioning produces epileptogenic focal cortical dysplasia. *Epilepsia* 49: 997-1010, 2008.

336. **Tamas G, Buhl EH and Somogyi P**. Massive autaptic self-innervation of GABAergic neurons in cat visual cortex. *J Neurosci* 17: 6352-6364, 1997.

337. **Tamas G, Somogyi P and Buhl EH**. Differentially interconnected networks of GABAergic interneurons in the visual cortex of the cat. *J Neurosci* 18: 4255-4270, 1998.

338. **Tan HO, Reid CA, Chiu C, Jones MV and Petrou S**. Increased thalamic inhibition in the absence seizure prone DBA/2J mouse. *Epilepsia* 49: 921-925, 2008.

339. **Tanabe Y, Masu M, Ishii T, Shigemoto R and Nakanishi S**. A family of metabotropic glutamate receptors. *Neuron* 8: 169-179, 1992.

340. **Teixeira KC, Montenegro MA, Cendes F, Guimaraes CA, Guerreiro CA and Guerreiro MM**. Clinical and electroencephalographic features of patients with polymicrogyria. *J Clin Neurophysiol* 24: 244-251, 2007.

341. **Telfeian AE and Connors BW**. Layer-specific pathways for the horizontal propagation of epileptiform discharges in neocortex. *Epilepsia* 39: 700-708, 1998.

342. **Telfeian AE and Connors BW**. Epileptiform propagation patterns mediated by NMDA and non-NMDA receptors in rat neocortex. *Epilepsia* 40: 1499-1506, 1999.

www.manaraa.com

343. **Testa CM, Standaert DG, Landwehrmeyer GB, Penney JB, Jr. and Young AB**. Differential expression of mGluR5 metabotropic glutamate receptor mRNA by rat striatal neurons. *J Comp Neurol* 354: 241-252, 1995.

344. **Thompson KJ, Mata ML, Orfila JE, Barea-Rodriguez EJ and Martinez JL, Jr.** Metabotropic glutamate receptor antagonist AIDA blocks induction of mossy fiber-CA3 LTP in vivo. *J Neurophysiol* 93: 2668-2673, 2005.

345. **Thomsen C and Dalby NO**. Roles of metabotropic glutamate receptor subtypes in modulation of pentylenetetrazole-induced seizure activity in mice. *Neuropharmacology* 37: 1465-1473, 1998.

346. **Threlkeld SW, Rosen GD and Fitch RH**. Age at developmental cortical injury differentially alters corpus callosum volume in the rat. *BMC Neurosci* 8: 94, 2007.

347. **Tizzano JP, Griffey KI, Johnson JA, Fix AS, Helton DR and Schoepp DD**. Intracerebral 1S,3R-1-aminocyclopentane-1,3-dicarboxylic acid (1S,3R-ACPD) produces limbic seizures that are not blocked by ionotropic glutamate receptor antagonists. *Neurosci Lett* 162: 12-16, 1993.

348. **Tizzano JP, Griffey KI and Schoepp DD**. Induction or protection of limbic seizures in mice by mGluR subtype selective agonists. *Neuropharmacology* 34: 1063-1067, 1995.

349. **Toledo-Rodriguez M, Blumenfeld B, Wu C, Luo J, Attali B, Goodman P and Markram H**. Correlation maps allow neuronal electrical properties to be predicted from single-cell gene expression profiles in rat neocortex. *Cereb Cortex* 14: 1310-1327, 2004.

350. **Topolnik L, Azzi M, Morin F, Kougioumoutzakis A and Lacaille JC**. mGluR1/5 subtype-specific calcium signalling and induction of long-term potentiation in rat hippocampal oriens/alveus interneurones. *J Physiol* 575: 115-131, 2006.

351. **Towers SK and Hestrin S**. D1-like dopamine receptor activation modulates GABAergic inhibition but not electrical coupling between neocortical fast-spiking interneurons. *J Neurosci* 28: 2633-2641, 2008.

www.manaraa.com

352. **Trotter SA, Kapur J, Anzivino MJ and Lee KS**. GABAergic synaptic inhibition is reduced before seizure onset in a genetic model of cortical malformation. *J Neurosci* 26: 10756-10767, 2006.

353. **Ulyings**.In: The Cerebral Cortex of the Rat, edited by Kolb B and Tees R. Cambridge, Mass: MIT Press, 1990.

354. **Valcanis H and Tan SS**. Layer specification of transplanted interneurons in developing mouse neocortex. *J Neurosci* 23: 5113-5122, 2003.

355. **van Hooft JA, Giuffrida R, Blatow M and Monyer H**. Differential expression of group I metabotropic glutamate receptors in functionally distinct hippocampal interneurons. *J Neurosci* 20: 3544-3551, 2000.

356. **Vezzani A, Conti M, De Luigi A, Ravizza T, Moneta D, Marchesi F and De Simoni MG**. Interleukin-1beta immunoreactivity and microglia are enhanced in the rat hippocampus by focal kainate application: functional evidence for enhancement of electrographic seizures. *J Neurosci* 19: 5054-5065, 1999.

357. **Vezzani A, Moneta D, Richichi C, Aliprandi M, Burrows SJ, Ravizza T, Perego C and De Simoni MG**. Functional role of inflammatory cytokines and antiinflammatory molecules in seizures and epileptogenesis. *Epilepsia* 43 Suppl 5: 30-35, 2002.

358. **Vickery RM, Morris SH and Bindman LJ**. Metabotropic glutamate receptors are involved in long-term potentiation in isolated slices of rat medial frontal cortex. *J Neurophysiol* 78: 3039-3046, 1997.

359. **Wahle P, Gorba T, Wirth MJ and Obst-Pernberg K**. Specification of neuropeptide Y phenotype in visual cortical neurons by leukemia inhibitory factor. *Development* 127: 1943-1951, 2000.

360. **Wang Y, Gupta A, Toledo-Rodriguez M, Wu CZ and Markram H**. Anatomical, physiological, molecular and circuit properties of nest basket cells in the developing somatosensory cortex. *Cereb Cortex* 12: 395-410, 2002.

www.manaraa.com

361. **Wellmer J, Su H, Beck H and Yaari Y**. Long-lasting modification of intrinsic discharge properties in subicular neurons following status epilepticus. *Eur J Neurosci* 16: 259-266, 2002.

362. **Whittington MA, Traub RD and Jefferys JG**. Synchronized oscillations in interneuron networks driven by metabotropic glutamate receptor activation [see comments]. *Nature* 373: 612-615, 1995.

363. **Wichterle H, Turnbull DH, Nery S, Fishell G and Alvarez-Buylla A**. In utero fate mapping reveals distinct migratory pathways and fates of neurons born in the mammalian basal forebrain. *Development* 128: 3759-3771, 2001.

364. **Wonders CP, Taylor L, Welagen J, Mbata IC, Xiang JZ and Anderson SA**. A spatial bias for the origins of interneuron subgroups within the medial ganglionic eminence. *Dev Biol* 314: 127-136, 2008.

365. **Wong RK, Bianchi R, Chuang SC and Merlin LR**. Group I mGluR-induced epileptogenesis: distinct and overlapping roles of mGluR1 and mGluR5 and implications for antiepileptic drug design. *Epilepsy Curr* 5: 63-68, 2005.

366. **Wyllie E**. Surgical treatment of epilepsy in pediatric patients. *Can J Neurol Sci* 27: 106-110, 2000.

367. **Xiang H, Chen HX, Yu XX, King MA and Roper SN**. Reduced excitatory drive in interneurons in an animal model of cortical dysplasia. *J Neurophysiol* 96: 569-578, 2006.

368. **Xiang Z, Huguenard JR and Prince DA**. Cholinergic switching within neocortical inhibitory networks. *Science* 281: 985-988, 1998.

369. **Xiang Z, Huguenard JR and Prince DA**. Synaptic inhibition of pyramidal cells evoked by different interneuronal subtypes in layer v of rat visual cortex. *J Neurophysiol* 88: 740-750, 2002.

370. **Xu Q, Cobos I, de la CE, Rubenstein JL and Anderson SA**. Origins of cortical interneuron subtypes. *J Neurosci* 24: 2612-2622, 2004.

www.manaraa.com

371. **Yoshimura Y, Dantzker JL and Callaway EM**. Excitatory cortical neurons form fine-scale functional networks. *Nature* 433: 868-873, 2005.

372. **Yue C and Yaari Y**. KCNQ/M channels control spike afterdepolarization and burst generation in hippocampal neurons. *J Neurosci* 24: 4614-4624, 2004.

373. **Zhou FM and Hablitz JJ**. Metabotropic glutamate receptor enhancement of spontaneous IPSCs in neocortical interneurons. *J Neurophysiol* 78: 2287-2295, 1997.

374. **Zilles K, Qu M, Schleicher A and Luhmann HJ**. Characterization of neuronal migration disorders in neocortical structures: quantitative receptor autoradiography of ionotropic glutamate, GABA(A) and GABA(B) receptors. *Eur J Neurosci* 10: 3095-3106, 1998.

375. **Zsombok A and Jacobs KM**. Postsynaptic Currents Prior to Onset of Epileptiform Activity in Rat Microgyria. *J Neurophysiol* 98: 178-186, 2007.

www.manaraa.com

Vita

Amanda Lynn George was born on December 29, 1979, in Virginia Beach, Virginia. She graduated from Frank W. Cox High School in 1997. She received her Bachelor of Arts in Spanish from Duke University, Durham, North Carolina in 2001 and subsequently worked at Duke University Health Systems for one year. In 2003 she entered the M.D./Ph.D. program at Virginia Commonwealth University.

www.manaraa.com